ESTEC CONTRACT 1121/70 AA

"DEVELOPMENT OF AN ANALYTICAL MODEL OP HYDRAZINE DECOMPOSITION MOTORS"

Carlos Sánchez Tarifa
J.L. Urrutia
A. Liñán
A. Crespo
E. Fraga

Madrid, July 1975

Instituto Nacional de Tecnica Aeroespacial "Esteban Terradas"
(Spain)

I N M E M O R I A M

To the late Professor José Luis Urrutia, who initiated and directed this research programme until his untimely death in 24th February 1973.

Madrid, July 1975

Carlos Sánchez Tarifa
and co-authors.

INTRODUCTION AND LITERATURE REVIEW

The purpose of this section is to present a survey of the existing literature on the subject and simultaneously provide an unified introduction to the different chapters forming this work.

The present work has been divided in four parts that more or less cover all the different aspects of the development of the hydrazine catalytic decomposition thrusters.

The first Part studies the processes occurring inside the catalyst particles during the ignition period corresponding to cold starts of the thrusters.

In a second Part a model is presented for the homogeneous gas phase decomposition of highly diluted hydrazine, using singular perturbation methods, that gives the overall reaction rate and stoichiometry for 1000°K initial temperature.

In the third Part an analysis is made of the heat and mass transfer to porous catalyst particles with either endothermic or exothermic reactions under steady state conditions.

In the fourth Part of this Report the steady state behaviour of a thruster is studied. In the thruster both catalytic and thermal decomposition processes are considered, so that the results of the second and third Parts of this Report are needed to perform this analysis. Evenmore, the ammonia resulting from

hydrazine decomposition also decomposes catalytically, this is the reason why in the third part the analysis has been carried out both for endothermic and exothermic reactions.

Before going into the details of the four parts of this Report, we are going to make a brief historical resumee of the way in wich hydrazine came up into the field of the satellite propulsion systems.

The propulsion systems for satellites that were flown before 1963 were required only for boosting from the earth and to supply the impulse necessary to achieve the desired flight path and there was no need for controlling neither the orbit nor the attitude of the satellite. In early 1963 the first geosynchronous satellite was launched marking the beginning of a new era in spacecraft control systems that were now required to perform orbit acquisition, station keeping, and attitude control. This first geosynchronous satellite used a monopropellant hydrogen peroxide system. During the years 1963 to 1968 most of the reaction control systems used the catalytic decomposition of hydrogen peroxide. Although the hydrogen peroxide systems performed their assigned functions, there were some basic limitations among which the most important were the relatively low specific impulse and unstability during the storage. The transition from the use of hydrogen peroxide to that of hydrazine was due to the development of the Shell 405 catalyst. Before the development

of the Shell 405 there were some catalysts for hydrazine decomposition that only worked at very high temperatures and did not have the simplicity and reliability of that catalyst.

In 1967 NASA launched the ATS-3 in which one of the hydrogen peroxide systems was modified to utilize hydrazine. The ATS-4 launched in 1968 utilized hydrazine in all propulsion systems, this propellant has become since then widely used in high performance satellite programs.

The history and most important aspects of the hydrazine monopropellant thrusters are presented in several survey papers (References 1-7).

Ignition Delay During Cold Starts

One of the most important problem areas in the field of hydrazine catalytic decomposition is the catalyst attrition originated by the large overpressures created inside the particles during long ignition delays. It has been found that the catalyst bed life is strongly related to the number of ignitions at ambient temperature (cold start). Low initial temperatures of the catalyst bed lead to long ignition delays that are accompanied by large over-pressures (References 8, 9). Sangiovanni and Kesten (Ref.10) postulated a model in which the liquid hydrazine will wet the porous catalyst particles, wiking into the pores, and consequently generating a large internal pres-

sure that will rupture the catalyst particle. This behaviour has been checked qualitatively in reference 13. A computer program manual for this study has been developed by Jasch (Ref.11). More recently Kesten (Ref.12) suggests that the catalyst breakup may be due to nonuniform wetting of the particles which create large pressure gradients. Sangiovanni and Kesten (Ref.10) assume that the transport of the different gaseous products obeys to a diffusion mechanism, hovewer, they also show that there appear large pressure gradients in the particle. In the work done in this Report the mass-flux of gaseous hydrazine in its decomposition region is adscribed to a diffusion mechanism, however, the mass flux of the decomposition products is due to the convective motion that appears as a result of the pressure gradients.

Rice and Williams have carried out a program directed to find an improved, long life multiple cold start catalyst (Ref. 14).

The Homogeneous Gas Phase Decomposition of Hydrazine

The thermal decomposition of hydrazine has been studied in the past (Ref 15-21) and its decomposition mechanism is well understood after Eberstein and Glassman (Ref.22).

Ref.15 gi account of the reactions involved in the decompos razine as they were known in 1951,

In Refs. 16 to 19 laminar flame studies are made in which the dependence of flame speed is used to obtain an activation energy for the reaction. More recent studies on the thermal homogeneous decomposition kinetics of hydrazine have been published at X Symposium International on Combustion (Refs. 20, 21 and 22) for different ranges of temperature and pressure and different degrees of dilution.

In Part II of this Report the overall reaction rate and stoichiometry for hydrazine thermal decomposition are obtained for highly diluted hydrazine concentration and 1000°K initial temperature.

Steady Heat and Mass Transfer in Porous Catalyst Particles.

In catalytic packed bed reactors the reaction chamber is filled with porous particles where chemical reactions take place. Due to the differences in concentrations of reacting species within the catalytic particles and on the surface, the species diffuse to the interior. Similarly, the reactive species diffuse from the interstitial fluid to the particles. If the reaction is exothermic, the heat evolved in the reaction will, under steady state conditions, leave the interior of the particle by heat conduction to increase the thermal energy of the interstitial fluid (References 23-25).

In Part III of this report the mathematical problem that

is solved is that of diffusion type of equations with chemical production terms and appropriate boundary conditions expressing that the temperature and concentrations are known at its surface. An early treatment of this problem was made by Thiele (Ref.26) which defined an effectiveness factor named after him and whose meaning can be found in the text. More recently this mathematical problem has been extensively treated in the literature (Refs. 23, 25, 27 and 28). This type of equation also appears in other physical problems related to combustion, see for example Frank-Kamenetskii (Ref.29). A numerical solution of this problem has been given by Weisz and Hicks (Ref. 30). The uniqueness and existence of the solution of the equation has been investigated in Refs. 31-34 among others. Catalyst particles are not always spherical and the temperature and concentrations are not uniform along its surface as it is assumed in most of the above-mentioned literature and in the present work; corrections due to these effects have been investigated in Refs. 35 to 38 among others.

In this report the problem has been solved using asymptotic methods to calculate temperature and concentration distributions along the particle radius under steady state conditions both for endothermic and exothermic reactions and for a wide variety of particle and propellant conditions.

When analyzing packed bed chemical reactors what is real-

ly known are the conditions of the interstitial fluid surrounding the catalyst particles that are different from the conditions at the particle surface because of external resistence effects. Since these conditions were assumed to be known as boundary conditions of the problem, some modifications are needed to take into account those effects; this analysis is done in Appendix C of Part III. This external resistence effect has been considered in the analysis carried out in references 39 to 44.

Steady State Analysis of Hydrazine Monopropellant Thrusters.

The steady-state performance of a hydrazine catalytic thruster depends on both the temperature and the composition of the fluid leaving the catalytic chamber.

There exist several theoretical studies of this problem, mainly those of Kesten, Smith E.J. and Smith D.B. (Refs. 45-49) who considered both steady and unsteady regimes. They obtained extensive numerical results for particular conditions and provided computer programs to allow the obtainment of data for further conditions. Nonetheless, the usefulness of their results for the design of an optimal thruster is limited for some applications, since correlation of numerical data, in order to attain significant design parameters, is always difficult.

In this part of the present Report an analytic study of steady-state performances is carried out. The main result of

the work is a description of the overall behaviour of the thruster in terms of three nondimensional parameters. Actually for all practical cases, only one parameter (J) is relevant, the dependence on the other two parameters being negligible, particularly for low values of J. Comparison of the results of the present theory with the experimental data of Ref.50 shows good agreement. Also some experiments on steady state performance of hydrazine catalytic thrusters have been carried out at INTA and a comparison have been made with the theory presented.

We want to complete this introductory study with a review of the different existing types of catalysts and the problem areas associated with their chemical kinetics.

Types of Catalysts and Associated Problem Areas

Much work has been dedicated to the study of the kinetic mechanisms occurring during the catalytic decomposition of hydrazine (Refs. 51-57) not only because of its relevance to the theoretical and experimental studies of the thruster performance but also because of the interest in knowing the causes of the decay in performance (poisoning) of the iridium catalyst (Refs. 57-61). This decay has been associated to the "poisoning" from the hydrazine itself, or to the construction materials employed in the feed lines of the thruster that cause an accumulation of

foreign metal surface impurities on the catalyst. Another type of catalyst degradation is due to its attrition originated by internal overpressures created during cold starts, this problem has already been examined is this section when introducing the work of part I of this Report.

Different types of catalysts have been used for hydrazine decomposition; the first one of relevance for space applications was the Shell 405 of the "Shell Development Company" (Ref.62) that consists of a large surface area alumina substrate on which iridium is deposited in a finely dispersed state. Another very important catalyst is the CNESRO-1 developed at the Centre National d'Etudes Spatiales (CNES) under financial support from ESRO, a detailed information on its manufacturing process can be found in Ref.63, and comparative studies of its characteristics are presented in Refs. 64 to 67. In Germany the "Kalichemie AG" has developed the catalysts KC-12, KC-23 and K -25 (Refs. 68 to 70), and in Britain the Rocket Propulsion Establishment has developed the RPE 72/1 (Ref.66).

In this Report we have examined some different technological problems arising when designing a catalytic hydrazine decomposition thruster to be integrated in a satellite, there are many other important aspects that should also be taken into ac-

count among them are the stability studies (Refs. 71 and 72). It is needless to say that for direct application all these problems have to be examined together and experimentation of the whole system is required (Refs. 50, 73-79). Examples of how these thrusters have been integrated in particular satellites are given in Refs. 65 and 80 to 85.

- - - - - - - -

R E F E R E N C E S

1. SUTHERLAND, G.S. and MAES, M.E. : A review of microrocket Technology: 10^{-6} to 1 lbf Thrust. J.S. and R. Vol 3 N° 8 pp 1153-65-1966.

2. SUTHERLAND, G.S. et al. : "Monopropellant Hydrazine Reaction Control Systems - A Five Year Status Report" Annual Aviation and Space Division Conference ASME - 1968.

3. PRICE, T.W. and EVANS, D.D. : The Status of Monopropellant Hydrazine Technology - J.P.L. Technical Report 32-1227 - 1968.

4. EGGERS, R.F. Microthrust monopropellant hydrazine propulsion system technology - AIAA Paper 68-556 - 1968.

5. HALCOMB, L.B. and LEE, D.H. : "Survey of Auxiliary Propulsion Systems for Communication Satellites" AIAA Paper N° 72-515 - 1972.

6. RUSSI, M.J. : A survey of monopropellant hydrazine thrusters technology - AIAA Paper 73-1263 - 1973.

7. ELLION, M.E. et al. : Hydrazine thrusters. Present Limitations and Possible Solutions. AIAA Paper 73-1265 - 1973.

8. GREER, H. et al. : Experimental evaluation of catalysts for monopropellant hydrazine propulsion. J.S. and R. Vol 8 pp 105-110 - 1971.

9. CARLSON, R.A. et al. : Space environment operation of experimental hydrazine reactors - TRW Report N° 47153.68-27 - 1968.

10. SANGIOVANNI,J.J. and KESTEN, A.S. : Study of hydrazine reactor vacuum start characteristics.- UARL Report - H-910758. Contract NAS 7-696-1969.

11. JASCH, P.M. et al. : Study of hydrazine reactor vacuum start characteristics. UARL Report-H-910761. Contract NAS 7-696 - 1969.

12. KESTEN, A.S. : A conceptual model of hydrazine catalytic reactor washout caused by decomposition product poisoning and pressure buildup. JANNAF Propulsion Meeting 1972.

13. SANGIOVANI, J and KESTEN, A.S. : Motion picture studies of the stastup characteristics of liquid hydrazine catalytic reactors. AIAA Paper N° 71-702-1971.

14. RICE, P.R. and WILLIAMS, P. : Hydrazine catalyst improvement. AIAA Paper 71-704. June 1971.

15. ANDRIETH, L.F. and ACKERSON, B. : "The Chemistry of Hydrazine" John Wiley and Sons N.Y. 1951.

16. ADAMS, G.K. and STOCKS, S.W. : "The Combustion of Hydrazine" IV Symposium (International) on Combustion pp 239-247 Williams & Wilkins (1953)

17. GRAY, P. and al. : "The Propagation and Stability of the Decomposition Flame of Hydrazine" VI Symposium International on Combustion pp 255-263 Reinhold (1957)

18. GILBERT, M. : "Kinetics of Hydrazine Decomposition in a Laminar Non-isothermal Flow" Combustion and Flame Vol 2 pp 149-156 June 1958.

19. GRAY, P. and LEE, J.C. : "Recent Studies of Oxidation and Decomposition Flames of Hydrazine" VII Symposium International on Combustion p 61. The Combustion Institute (1959).

20. MICHEL, K.W. and WAGNER, H.GG. : "The Pyrolysis and Oxidation of Hydrazine behind Shock Waves" X Symposium International on Combustion p 353. The Combustion Institute (1965).

21. Mc HALE, E.T. et al. : "Determination of the Decomposition Kinetics of Hydrazine Using a Single-pulse Shock Tube" X Symposium (International) on Combustion pp 341-351. The Combustion Institute (1965).

22. EBERSTEIN, I.J. and GLASSMAN, I. : "The Gas-phase Decomposition of Hydrazine and its Methyl Derivatives" X Symposium (International) on Combustion pp 365-374. The Combustion Institute (1965).

23. PETERSEN, E.E. : "Chemical Reaction Analysis" Prentice-Hall 1965.

24. ARIS, R. : "Introduction to the Analysis of Chemical Reactors" Prentice-Hall 1965.

25. ARIS, R. : "Elementary Chemical Reaction Analyses" Prentice - Hall 1969.

26. THIELE, E.W. : "Relation between Catalytic Activity and size Particle" Ind. Engng. Chem. p 31 (1939).

27. SATTERFIELD, C.N.: and SHERWOOD,T.K. "The Role of Diffusion in Catalysis" Adison-Wesley 1963.

28. SATTERFIELD, C.N.: "Mass Transfer in Heterogeneous Catalysis" M.I.T. Press, Cambridge Mass. 1970.

29. FRANK-KAMENETSKII, D.A. : "Diffusion and Heat Transfer in Chemical Kinetics" Plenum Press 1969.

30. WEISZ, P.B. and HICKS, J.S. : "The Behaviour of Porous Catalyst Particles in View of Internal Mass and Heat Diffusion Effects" Chem. Engng. Sci 17, 265-75, 1962.

31. CAPELOWITZ, I. and ARIS, R. : "Communication on the Theory of Diffusion and Reaction. V Findings and Conjectures Concerning the Multiplicity of Solutions" Chem. Engng. Sci 25, 906-09, 1970.

32. GAVALAS, G.R. : "Nonlinear Differential Equations of Chemically Reacting Systems" Springer - Verlag 1969.

33. HLAVACEK, V., MAREK, M. and KUBICEK, M : "Modelling of Chemical Reactors - X Multiple Solutions of Enthalpy and Mass Balances for a Catalytic Reaction within a Porous Catalyst Particle" Chem. Engng Sci 23, 1083-097, 1968.

34. LUSS, D. : "On the Uniqueness of a Large Distributed Parameter System with Chemical Reaction and Heat and Mass Diffusion" Chem. Engng. Sci. 24, 879-83, 1969.

35. BISCHOFF, K.B. : "Effectiveness Factors and Temperature Distributions for Catalyst Particles in Non-uniform Environments" Chem. Engng. Sci 23, 451-56, 1968.

36. VOLKMAN, Y. and KEHAT, E. : "Computation of Effectiveness Factors" Chem. Engng. Sci 24, 1531-32, 1969.

37. RESTER, S. and : "Communications on the Theory of Diffusion and Reaction - II The Effect of Shape on

ARIS, R — the Effectiveness factor"
Chem. Engng. Sci. 24, 793-95, 1969.

38. HLAVACEK, V. and KUBICEK, M. : "Modelling of Chemical Reactors - XX Heat and Mass Transfer in Porous Catalyst. The Particle in a Non-uniform External Field"
Chem. Engng. Sci. 25, 1527-36, 1970.

39. HLAVACEK, V. and MAREK, M. : "Modelling of Chemical Reactors - IX Non-isothermal Zero-order Reaction within a Porous Catalyst Particle"
Chem. Engng. Sci. 23, 1083-97, 1968.

40. KESTEN, A.S. : "An Integral Method for Evaluating the Effects of Film and Pore Diffusion of Heat and Mass on Reaction Rates in Porous Catalyst Particles"
AICHE Journal 15, 128-131, 1969.

41. CRESWELL, D.L. : "On the Uniqueness of the Steady State of a Catalytic Pellet Involving both Interphase and Interphase Transport"
Chem. Engng. Sci. 25, 267-75, 1970.

42. HATFIELD, B. and ARIS, R. : "Communications of the Theory of Diffusion Reaction - IV Combined Effects of Internal and External Diffusion in the Non-isothermal Case"
Chem.Engng.Sci. 24, 1213-222, 1969.

43. Mc GREAVY, C. and CRESWELL, D.L. : "Non-isothermal Effectiveness Factors"
Chem. Engng. Sci. 24, 608-11, 1969.

44. KEHOE, J.P.G. and BUTT, J.B. : "Boundary Layer Effects in Isothermal Catalysts"
Ind. Engng. Chem. 53, 663, 1970.

45. KESTEN, A.S. : "Analytical Study of Catalytic Reactors for Hydrazine Decomposition" U.A.R.L. Report-F-910461-12 Contract NAS 7-458 - 1967.

46. KESTEN, A.S. : "Analytical Study of Catalytic Reactors for Hydrazine Decomposition" U.A.R.L. Report G-910461-24 Contract NAS 7-458 - 1968.

47. SMITH, E.J. et al. : "Analytical Study of Catalytic Reactors for Hydrazine Decomposition" U.A.R.L. Report-G-910461-30 Contract NAS 7-458 - 1968.

48. KESTEN, A.S. : "Analytical Study of Catalytic Reactors for Hydrazine Decomposition" U.A.R.L. Report-H-910461-38 Contract NAS 7-458 - 1969.

49. SMITH, D.B. et al. : "Analytical Study of Catalytic Reactors for Hydrazine Decomposition" U.A.R.L. Report-H-910461-37 Contract NAS 7-458 - 1969.

50. Rocket Research Corporation: Development of Design and Scaling Criteria for Monopropellant Hydrazine Reactors Employing Shell 405 Spontaneous Catalyst. RRC-N 67-19123 - 1967.

51. CONTOUR, J.P. : "Sur la Decomposition Catalytique de L'hydrazine" Thèse de doctorat d'état présentée a la Faculté des Sciences de Paris - 1970.

52. SAYER, C.F. : "The Decomposition of Hydrazine on the Shell 405 Catalyst" AIAA Paper N° 70-606 - 1970.

53. KARSCHUNKE, H.E. : "The Catalytic Decomposition of Hydrazine over Various Precious Metals" Third International Conference of Space Technology Rome 1971.

54. SMITH, O.I. et al. : "Kinetics of Hydrazine Decomposition on Iridium and Alumina Supported Iridium Catalyst" AFRPL - TR-73-50 - 1973.

55. BROUSSELY, M. et GOUDEAU, J.G. : "Contribution à l'Etude de la Dècomposition Catalytique de L'Hydrazine en Phase Liquide sur Catalyseur Iridium-Alumine" Colloque International "Propriétés de L'Hydrazine" p 59. Poitiers - 1974 (C.N.E.S. Toulouse).

56. FOUCH, S. CARREAU, J.L. et GOUDEAU, J.C. : "Etude Cinétique de la Décomposition Catalytique de L'Hydrazine Liquide", Colloque International "Propriétés de L'Hydrazine" p 71. Poitiers - 1974 (C.N.E.S. Toulouse).

57. BENSON, S.W. and al. : "Homogeneous and Heterogeneous Hydrazine Decomposition for Monopropellant Propulsion Systems". AFOSR Contractors Meeting on Rocket Combustion Dynamics and Electric Propulsion Meeting. Lancaster (July 1975) California.

58. BALDER, J.R. and PETERSEN, E.E. : "Poisoning in a Single Pellet Reactor" Chemical Engineering Science Vol 23 pp 1287-1291 - 1968.

59. BUT, J.B. and ROHAN, Deunis M. : "Analysis of Nonselective Poisoning and his Influence on Reactor Behavior" Chemical E.S. Vol 23 pp 489-501 - 1968.

60. DOUGHARTY, N.A. : "Self - Poisoning Reactions in the Single-Pellet Catalytic Reactor" Chemical Engineering Science Vol 25 pp 489-494 - 1970.

61. FORBES, F.S. : "Effects of Contaminants on Hydrazine Monopropellant Catalysts" Colloque International "Propriétés de L'Hydrazine" p 127 - Poitiers - 1974 (C.N.E.S. Toulouse).

62. VOGE, H.H. et al. : "Development of Catalyst for Monopropellant Decomposition of Hydrazine" Final Report 3-13947 Shell Development Company Calif. 1964.

63. LECOQ M., LECLERE C. MICHEL, J.M. : "Le Catalyseur CNESRO: Industralisation et Performances" Colloque International "Propriétés de L'Hydrazine" p.139 - Poitiers - 1974 (C.N.E.S. Toulouse)

64. PANNETIER, G. : "Application de la Décomposition Catalytique de L'Hydrazine à la Micropropulsión Spatiale: Mise au point du Catalyseur" Colloque International "Propriétés de L'Hydrazine" p.451 - Poitiers - 1974 (C.N.E.S. Toulouse).

65. PFEFFER, H.A. : "The ESRO Activities in the Field of Hydrazine Monopropellant Technology for Satellite" Colloque International "Propriétés de L'Hydrazine" p.3 - Poitiers - 1974 (C.N.E.S. Toulouse).

66. SAYER, C.F. and SOUTHERN, G.R. : "The Comparative Testing of the Shell 405 CNESRO-1 and RPE 72/1 Hydrazine Decomposition Catalyst" AIAA Paper N°73-1266 - 1973.

67. MUTIN, J. : "L'Action du C.N.E.S. en Propulsion à Hydrazine" Colloque International "Propriétés de L'Hydrazine" p.19 - Poitiers - 1974 (C.N.E.S. Toulouse).

68. SELZER, H. : "Some New Contributions to the Understanding of the Catalytic Hydrazine Decomposition"
Colloque International "Propriétes de L'Hydrazine" p.85 - Poitiers - 1974 (C.N.E.S. Toulouse).

69. HARTUNG, W. : "Evaluation Tests of New German Catalysts for the Spontaneous Decomposition of Hydrazine"
Colloque International "Propriétés de L'Hydrazine" p.109 - Poitiers. 1974 (C.N.E.S. Toulouse).

70. GENTHE, A. : "Dévelopments en République Fédérale D'Allemagne en Matière de Technology d'Hydrazine pour Applications Spatiales"
Colloque International "Propriétés de L'Hydrazine" p.11 - Poitiers - 1974 (C.N.E.S. Toulouse).

71. BARRERE, M. : "Fonction de Transfert et Stabilité d'un Propulseur a Décomposition Catalytique d'Hydrazine"
Colloque International "Propriétés de L'Hydrazine" p.291 - Poitiers - 1974 (C.N.E.S. Toulouse).

72. OWENS, W.L. : "A Combustion Stability for Catalytic Monopropellant Thruster"
J.S. and Rokets Vol 9 N° 3 p.152 - 1972.

73. NUNZ, G.J. : "Experimental Evaluation of a Miniature Catalytic Hydrazine Thruster"
AIAA Paper N° 71-706 - 1971.

74. PRICE, T.W. : "Experimental Evaluation of High-Thrust Throttleable Monopropellant Hydrazine Reactors"
AIAA Paper N° 71-705 - 1971.

75. KUSAK, L. et al. : "Long-Life Firings of a Catalytic Reactor for Monopropellant Hydrazine" AIAA Paper N° 72-1045 - 1972.

76. MOYNIAHN, P.I. and BJORKLUND, R.A. : "Performance Characterization Test of Three 0'44-N (0,1-1bf) Hydrazine Catalytic Thrusters" J.P.L. Technical Report 32-1584 - 1973.

77. BALZER, D.L. and BELSLEY, A.C. : "Ascent Phase Guidance and Orbital Correction Propulsion Module" AIAA Paper 93-1276 - 1973.

78. BELSLEY, A.C. et al. : "Scalling Factor Verification of a High Performance Hydrazine Thruster Design" AIAA Paper N° 74-1138 - 1974.

79. LONGUET, M. : "Les Systèmes Propulsifs Spatiaux à Hydrazine" Colloque International "Propriétés de L'Hydrazine" p.185 - Poitiers - 1974 C.N.E.S. Toulouse).

80. MOSELEY, V.A. et al. : "Development of Monopropellant Hydrazine Propulsion System for INTELSAT III" TRW Systems, 1969.

81. MOYNIHAN, P.I. : "Attitude Propulsion Technology for TOPS" J.P.L. Technical Report 32-1560 - 1972.

82. ELLION, M.E. and DONATELLY, P.A. : "Development of a Long Life Hydrazine Thruster for the Intelsat IVA Satellite" AIAA Paper 74-1136 - 1973.

83. EMMONS, D.L. et al. : "Investigation of a Catalytic Gas Generator for the Space Shuttle APU" AIAA Paper N° 74-1107 - 1974.

84. SCHMITZ, H.D. : "Monopropellant Hydrazine Propulsion Technology for European Spacecraft Applications"
Colloque International "Propriétés de L'Hydrazine" p.161 - Poitiers - 1974 (C.N.E.S. Toulouse).

85. MARSILI, P.
MAZZUCA, A. : "Le Système de Contrôle d'Attitude et Orbitale à Hydrazine de Satellite SIRIO"
Colloque International "Propriétés de L'Hydrazine" p.171 - Poitiers - 1974 (C.N.E.S. Toulouse).

P A R T I

IGNITION DELAY OF HYDRAZINE MONOPROPELLANT THRUSTERS

Authors J.L. Urrutia
A. Liñán
A. Crespo
E. Fraga

LIST OF SYMBOLS

a_o = radius of the catalyst particle

a_i = radial location of the interphace

A = defined in formula (42)

C = nondimensional density

D = diffusion coefficient

J = mass flux

k_s = heterogeneous decomposition rate per unit mass

M = mean molecular mass of the gas

p = pressure of the gas phase

p_c = capillary pressure

r = radial location of the fluid element

r' = heterogenous decomposition rate

R = characteristic radius of the macropores

R_u = universal gas constant

t = time

T = temperature

V_m = mean velocity of products

x = nondimensional radial location

y = pore length

γ_v = void fraction

δ = tortuosity factor

ε = nondimensional parameter

η = nondimensional distance

θ = contact angle

μ_g = viscosity coefficient of the gaseous products

μ_l = viscosity coefficient of the liquid hydrazine

ξ = nondimensional distance

χ = nondimensional distance

ρ_g = mean density of the gas phase

$(\rho_A)_{vp}$ = density of gaseous hydrazine in equilibrium with the liquid phase

σ = surface tension

τ = nondimensional time

ϕ = nondimensional pressure.

Subscripts

A = hydrazine
i = interphace
ign = ignition
l = liquid
max = maximum

Superscripts

* = reference values.

IGNITION DELAY OF HYDRAZINE MONOPROPELLANT THRUSTERS

- - - - - - -

I. *INTRODUCTION*

The ignition mechanism of hydrazine monopropellant thrusters has been adscribed[1] to the transient processes occurrying in the interior of the catalyst particles filling the decomposition chamber of these thrusters.

These catalyst particles are manufactured by depositing an active material - iridium for the Shell 405 catalyst - on a porous base structure, usually alumina, this base structure consists of an inmense tangle of capillary tubes whose diameters range from a few to some hundreds of Amstrong.

When liquid hydrazine is injected in the decomposition chamber of a thruster, it flows through the interstices between the catalyst particles, and, at the same time, penetrates in the interior of the particles by capillary action. Hydrazine vaporizes at the interphace, that is formed in the interior of the particles, and then decomposes when the molecules, in the gaseous phase, contact the active sites in the walls of the pores, to give ammonia, hydrogen and nitrogen. These gaseous products are retained inside the particles by the blocking action of the liquid filling the outer shell of the particle.

Besides, and due to the large value of the capillary pressure in those small capillary tubes, the gas liquid interphase will

advance towards the interior of the particle while the decomposition of hydrazine proceeds; both mechanisms, the continuous source of gaseous products at the walls of the pores and the decreasing of the available volume for these products brought up by the advancing interphase, will contribute to a pressure build up in the interior of the particle.

When the internal pressure equalizes the value of the capillary pressure, the interphase will cease in its progression towards the center of the particle. Moreover, and since the decomposition mechanism continues, the value of the internal pressure will, exceed that of the capillary pressure and the interphase will receed towards the exterior being finally expelled from the particle. Since the pressure of the accompanying gaseous products is large, the observable characteristic marking the completion of the entire ignition process will be a sudden increase in the chamber pressure.

This ignition mechanism has been recently treated by Sangiovanni and Kesten[1], although the physics they use to describe the process seems questionable in several aspects. They assume, for instance, that the transport of the different gaseous products towards the interior of the catalyst particle obeys to a diffusion mechanism where the diffusion coefficients are spatially uniform. The results they obtain show, however, that the mass fractions of the different products of the decomposition of hydrazine can be considered as spatially uniform, but that there exists a severe

pressure gradient within the particle; both results automatically invalidate their assumptions.

In the course of the analysis that follows, it will be shown that, due to the large value of the rate constant for the heterogeneous decomposition of hydrazine, this decomposition takes place in a very narrow zone adjacent to the gas-liquid interphace, so that the mass flux of gaseous hydrazine towards the interior of the particle can be truly adscribed to a diffusion mechanism; however, the mass flux of the decomposition products towards the interior of the particle is mainly due to the convective motion that appears as a result of the existing pressure gradient and not to a diffusion process associated with mass fraction gradients.

Analytical expressions are obtained for the ignition time, i.e., the time period between injection of liquid hydrazine and expulsion of gaseous products from the catalyst particles, which correlate well with available experimental results. This ignition time is obtained as a function of the characteristics of the catalyst particle and of the initial conditions of the chamber for the Shell 405 catalyst.

The theory does also predict the maximum internal pressure, in a given catalyst particle, as a function of both, the initial conditions of the thruster and the particle size of a

given catalyst. This information can lead to criteria for choosing the particle size of the catalyst to be employed in a given mission so as to minimize an early crushing of the catalyst particles that would compromise the entire mission. Furthermore, the theory gives also information on the influence of the different parameters - in particular, the size a_o of the particles, characteristic value of the radius R of the macropores, and the initial temperature of the catalyst bed - on the maximum pressure that can be expected in interior of a catalyst particle during the ignition period.

As a byproduct of the analysis,but by an means less important, the theory does also provide an explanation for the pressure spikes observed in the ignition of hydrazine monopropellant thrusters. Although it was mentioned before that at the end of the induction period, liquid hidrazine is expelled from the catalyst particles, this expulsion takes place only thru the pores in the macropores range. The catalyst is a porous particle with pore sizes ranging from the micropores (10 Å) to the macropores (10^4 Å) being the mean pore size well within the micropore range for which the capillary pressure is extremely large. Therefore at the end of the ignition period liquid hydrazine in the macropores is expelled from the particle although the liquid in the micropores is retained in the particle because the internal pressure is not large enough to overcome the high capillary pressure of the liquid in these micropores. The situation of the catalyst particle at the end of the ignition period can then be physically

visualized as a particle whose most outer part is wetted by liquid hydrazine and is surrounded by an stagnant gas film at high pressure. The liquid retained in the particle keeps vaporizing and decomposing, so that, as long as there is liquid in the particle there will be a feeding source which will keep the chamber pressure at a level well above the nominal pressure.

Naturally the strength of the pressure spikes will depend on the characteristics of the catalyst as well as on the operating conditions of the thruster and catalyst bed packing. For instance, if the mass flow is such that the time needed to fill the interstitial volume of the chamber is smaller then the ignition time, the pressure spikes will appear at full strength, since the gaseous products expelled from the particles can not expand at the beginning of the process; if, by the other hand, the ignition time is smaller than the filling time of the interstitial volume, then, it will be observed a smooth excursion of the chamber pressure above its nominal value. It is also evident that for a given mass flux, a more compact catalyst bed packing will favour the presence of well defined pressure spikes.

II. *PRESSURE BUILD-UP IN A CATALYST PARTICLE*

In order to calculate the pressure build-up in the interior of a catalyst particle, it will be considered that the gaseous products which, as it will be seen later, appear in a narrow

zone close to the interphase as a result of the heterogeneous decomposition of hydrazine, are convected towards the interior of the particle due to the existing pressure gradient.

It will be assumed that this convective mass transfer is only relevant for the macropores for which the flow can be described during most of the ignition time, by a Poiseuille type of equation. The role of the micropores, in this model, would be to provide an empty volume to be filled with the gaseous products.

Therefore the mean velocity of the products, v_m , along the radius of the catalyst particle is given by

$$v_m = \frac{R^2}{8\mu_g \delta} \frac{\partial p}{\partial r} \qquad (1)$$

where

$R \equiv$ characteristic radius of the macropores

$\mu_g \equiv$ viscosity coefficient of the gaseous products

$\delta \equiv$ tortuosity factor (*)

$p \equiv$ pressure of the gas phase

$r \equiv$ radial location of the fluid element.

The mass flux, per unit surface normal to the radius of the catalyst particle, can then be written as

$$J = \rho_g \gamma_v v_m = \frac{1}{8} \frac{\rho_g \gamma_v R^2}{\mu_g \delta} \frac{\partial p}{\partial r} \qquad (2)$$

where

(*) Defined in (12a). Its value is of order one[2].

$J \equiv$ mass flux of gaseous products per unit surface normal to the radius

$\rho_g \equiv$ mean density of the gaseous phase

$\gamma_v \equiv$ void fraction

γ_v , the void fraction, is introduced here so as to take into account the fact that in the unit volume of the catalyst particle only the fraction γ_v can be filled by the gaseous phase.

Eq.2 can be written in a more convenient form when one uses the equation of state for the gas, namely

$$\rho_g = \frac{pM}{R_u T} \tag{3}$$

where

$M \equiv$ mean molecular mass of the gas

$R_u \equiv$ universal gas constant

$T \equiv$ temperature

so that, by using eq (3), eq (2) can be rewritten as

$$\vec{J} = - \frac{1}{\theta} \frac{\gamma_v M R^2}{\mu_g \delta R_u T} p \nabla p \tag{4}$$

The mass conservation equation states that

$$\frac{\partial(\gamma_v \rho_g)}{\partial t} + \nabla . \vec{J} = 0 \tag{5}$$

and, therefore, the equation giving the pressure evolution in the interior of the catalyst particle will be obtained by introducing

in eq (5) the density and the mass flux vector in terms of the pressure as given by eqs (3) and (4); the pressure equation will then be:

$$\frac{\partial p}{\partial t} - \frac{R^2}{8\mu_g \delta} \nabla . (p \nabla p) = 0 \qquad (6)$$

where it has been assumed that during the ignition period the temperature does not significantly depart from its initial value. This assumption will be justified at the end of the study.

The non-dimensional form of eq.6 can be obtained when one uses the following non-dimensional variables

$$\phi = p/p_c \quad , \quad x = r/a_o \quad , \quad \tau = \frac{R^2 p_c}{8\mu_g \delta a_o^2} t \qquad (6a)$$

where

$p_c \equiv$ capillary pressure corresponding to the macropores

$a_o \equiv$ radius of the catalyst particle.

With these variables eq (6) can be written as:

$$\frac{\partial \phi}{\partial \tau} - \nabla . (\phi \nabla \phi) = 0 \qquad (7)$$

or, using spherical coordinates

$$\frac{\partial \phi}{\partial \tau} - \frac{1}{x^2} \frac{\partial}{\partial x} \left(x^2 \phi \frac{\partial \phi}{\partial x} \right) = 0 \qquad (8)$$

which has to be supplemented with appropriate initial and boundary conditions.

By assuming that, initially, the catalyst particle is in a neutral, non poisoning, atmosphere, which eventually could be a vacuum, and that, at a certain instant of time liquid hydrazine is injected and completely surrounds the catalyst particle, the appropriate initial condition for eq (8) is

$$\text{at } \tau = 0 \quad , \quad \phi = \phi_o \quad (\text{eventually } \phi_o = 0) \tag{9}$$

The boundary condition to be fulfilled at the center of the particle simply states that the slope of the pressure distribution must vanish at $r = 0$, namely,

$$\text{at } x = 0 \quad , \quad \frac{\partial \phi}{\partial x} = 0 \tag{10}$$

The remaining boundary condition must be imposed at the interphase, and it states that, at the moving gas-liquid interphase, the mass flux of products towards the interior of the catalyst particle must be equal to the mass flux of gaseous hydrazine resulting from vaporization at the interphace and transported by diffusion towards the interior.

The mathematical form of this boundary condition is, in physical variables

$$\text{at } r = a_i(t) \quad , \quad \rho_g \left(v_m + \frac{da_i}{dt} \right) = D_A \frac{\partial \rho_A}{\partial r}$$

It has been considered here that, in the region close to the interphase, and due to the first decomposition rate, the spatial variation of pressure is entirely negligeable compared with that of hydrazine concentration.

$r = a_i(t)$ donates the radial location of the interphase at the instant of time t and subscript A refers to hydrazine.

Using the non-dimensional variables defined above, together with C_A which is the hydrazine density made non-dimensional with the density of gaseous hydrazine in equilibrium with the liquid phase, $\rho_A)_{vp}$, it is

$$C_A = \frac{\rho_A}{(\rho_A)_{vp}}$$

and taking into account that the diffusion coefficient D_A is a function of the internal pressure of the form:

$$D_A = \frac{D^*p^*}{p}$$

where D^*p^* behaves here as a constant,(*) the boundary condition above can be written in a non-dimensional form as:

$$\text{at } x = x_i(\tau) \quad , \quad \phi^2\left[\frac{\partial\phi}{\partial x} + \frac{dx_i}{d\tau}\right] = \frac{D^*p^*(\rho_A)_{vp}R_uT8\mu_g\delta}{MR^2p_c^3}\,\frac{\partial C_A}{\partial x} \qquad (11)$$

In order to solve eq (8) with initial and boundary conditions given by eqs.9-11, it is necessary to find the pertinent

(*) This constant is taken from ref.1 and its value is $0.0487\ T^{1.823}$ Nw./seg.

values for the position of the interphace as a function of time, namely, $x_i(\tau)$ and, at the same time, the value of the slope of the hydrazine concentration distribution measured at the interphace. This will done in the following sections.

III. *INTERPHACE PENETRATION ANALYSIS*

The radial position of the interphace within the catalyst particle and along a pore of radius R, can be described by the Poiseuille equation, namely:

$$\frac{8\mu_\ell}{R^2}\, y\, \frac{dy}{dt} = \frac{2\sigma\cos\theta}{R} - p \qquad (12)$$

where

$\mu_\ell \equiv$ viscosity coefficient of liquid hydrazine

$R \equiv$ pore radius

$\sigma \equiv$ surface tension of liquid hydrazine

$\theta \equiv$ contact angle

$y \equiv$ pore length, measure from the surface, wetted by liquid hydrazine.

It is obvious from this notation that the radial position of the interphace can be related to y through the tortuosity factor δ by means of the relation:

$$a_i(t) = a_o - \delta y \qquad (12a)$$

Using the non-dimensional variables previously defined,

eq (12) may be written as:

$$-(1 - x_i)\frac{dx_i}{d\tau} = \delta^3 \frac{\mu_g}{\mu_\ell}(1 - \phi) \qquad (13)$$

and the initial condition that x_i has to satisfy is that

$$\text{at} \quad \tau = 0 \quad , \quad x_i = 1 \qquad (14)$$

Eq.13 with this initial condition determines the radial location of the interphace as a function of time. Since the non-dimensional pressure ϕ enters in the right hand side of this equation, it means that eq (13) is coupled with the equation determining the pressure build-up in the interior of the particle and both of them will constitute a set of coupled differential equations that can not be solved separately.

IV. *DISTRIBUTION OF GASEOUS HYDRAZINE IN THE INTERIOR OF THE CATALYST PARTICLE*

By using spherical coordinates, the equation describing the transient mass transfer of hydrazine in the interior of a catalyst particle is given by the equation

$$\frac{1}{r^2}\frac{\partial}{\partial r}\left(\rho_g D_A r^2 \frac{\partial \rho_A/\rho_g}{\partial r}\right) - \frac{\partial \rho_A}{\partial t} = r'_A \qquad (15)$$

where, as mentioned before, D_A is the diffusion coefficient of

gaseous hydrazine in its own products of decomposition (mainly ammonia), which, when the flow field can be described as a continuum varies as the inverse of the pressure field. r'_A is the heterogeneous decomposition rate of hydrazine which, for the range of temperatures of interest for ignition studies, can be written as, assuming that it is proportional to the density of the gaseous hydrazine ρ_A ; $r'_A = k_s(T)\rho_A$ (for k_s see page 26)

The initial condition for eq.(15) states that at $t = 0$, the concentration of hydrazine in the interior of the particle is everywhere zero, i.e.,

$$\text{at} \quad t = 0 \qquad \rho_A(r) = 0 \tag{16}$$

The boundary condition at the center of the particle is a condition of symmetry, namely

$$\text{at} \quad r = 0 \qquad \frac{\partial \rho_A}{\partial r} = 0 \tag{17}$$

and the boundary condition at the interphace establishes that the concentration of gaseous hydrazine at this location must be the corresponding to the gas-liquid thermodynamic equilibrium, i.e.,

$$\text{at} \quad r = a_i(t) \qquad \rho_A = (\rho_A)_{vp} \quad \text{(see page 26)} \tag{18}$$

where $(\rho_A)_{vp}$ is given, as a function of only the temperature, by the Clausius-Clapeyron equation. From the previous equations:

If $C_A = \rho_A / (\rho_A)_{vp}$.

$$\frac{D^*p^*}{a_o^2 p_c k_s} \frac{1}{x^2} \frac{\partial}{\partial x}\left[\frac{1}{\phi} x^2 \frac{\partial C_A}{\partial x}\right] - \frac{R^2 p_c}{8\mu_g \delta a_o^2 k_s} \frac{\partial C_A}{\partial \tau} = C_A \qquad (19)$$

$$\tau = 0 \qquad C_A = 0 \qquad (20)$$

$$x = 0 \qquad \frac{\partial C_A}{\partial x} = 0 \qquad (21)$$

$$x = x_i(\tau) \qquad C_A = 1 \qquad (22)$$

Now, and since $\frac{D^*p^*}{a_o^2 p_c k_s} >> \frac{R^2 p_c}{8\mu_g \delta a_o^2 k_s}$ (*), it means that of the end of a very small initial period of time, the distribution of hydrazine concentration will reach the steady state, given by the solution of the equation

$$\frac{D^*p^*}{a_o^2 p_c k_s} \frac{1}{x^2} \frac{\partial}{\partial x}\left[\frac{1}{\phi} x^2 \frac{\partial C_A}{\partial x}\right] = C_A \qquad (23)$$

with boundary conditions

$$\text{at} \quad x = 0 \qquad \frac{\partial C_A}{\partial x} = 0 \qquad (24)$$

$$\text{and at} \quad x = x_i(\tau) \qquad C_A = 1 \qquad (25)$$

Again, and since the parameter $\frac{D^*p^*}{a_o^2 p_c k_s}$ (*) is a quantity much

(*) Typical values of the parameters are in page 26, and $\mu_g \sim 10^{-4}$ poise.

smaller than one; the problem is of the boundary layer type and the reaction zone, where the concentration of hydrazine is different from zero, will be very narrow and, moreover, this thin reaction zone will be located adjacent to the interphace.

By introducing the variable η, defined as,

$$\eta = (x_i - x)\sqrt{\frac{a_o^2 k_s P_c}{D^* p^*}} \tag{26}$$

eq (23) with boundary conditions (24) and (25) becomes, in the first approximation, in the case in which $\frac{a_o^2 k_s P_c}{D^* p^*}$ is very large

$$\frac{1}{\phi_i}\ \frac{\partial^2 C_A}{\partial \eta^2} = C_A \tag{27}$$

with boundary conditions,

$$\text{at} \qquad \eta = 0 \qquad C_A = 1 \tag{28}$$

and, when $\eta \to \infty$ $\frac{\partial C_A}{\partial \eta} = 0$ (29)

whose solution is

$$C_A = e^{-\sqrt{\phi_i}\,\eta} \tag{30}$$

where, ϕ_i is the value of the non-dimensional pressure, at the interphase.

Therefore, introducing the value of η given by eq.26, into eq.30 we get

$$C_A = \exp\left[(x-x_i)\sqrt{\phi_i \frac{a_o^2 k_s p_c}{D^* p^*}}\right] \tag{31}$$

so that the derivative, with respect to x of the non-dimensional concentration of hydrazine, takes the following value at the interphase

$$\left(\frac{\partial C_A}{\partial x}\right)_{x=x_i} = \sqrt{\phi_i}\sqrt{\frac{a_o^2 k_s p_c}{D^* p^*}} \tag{32}$$

V. *GOVERNING EQUATIONS*

With the results obtained in section III and IV, the evolution of the internal pressure as a function of time will be given by the solution of the following set of equations

$$\frac{\partial \phi}{\partial \tau} - \frac{1}{x^2}\frac{\partial}{\partial x}\left(x^2 \phi \frac{\partial \phi}{\partial x}\right) = 0 \tag{33}$$

$$-(1-x_i)\frac{dx_i}{d\tau} = \frac{\mu_g}{\mu_l}\delta^3(1-\phi) \tag{34}$$

with initial conditions

$$\text{at } \tau = 0 \quad , \quad \phi = 0 \quad , \quad x_i = 1 \tag{35}$$

and boundary conditions

$$\text{at} \quad x = 0 \quad , \quad \frac{\partial \phi}{\partial x} = 0 \tag{36}$$

and at $x = x_i(\tau)$,

$$\phi^{3/2}\left[\frac{\partial \phi}{\partial x} + \frac{dx_i}{d\tau}\right] = \frac{8R_u T \mu_g \delta a_o}{MR^2 p_c^{5/2}} (\rho_A)_{vp} \sqrt{D^* p^* k_s} \tag{37}$$

As it can be seen from eq. 37, the second boundary condition is imposed on a location that is a function of time. To facilitate the integration of this system, of differential equation, the following change of variables will be done so as to have both boundary conditions imposed at fixed locations:

$$\xi = x/x_i(\tau) \quad , \quad \tau = \tau$$

so that

$$\left.\frac{\partial}{\partial \tau}\right|_x = \left.\frac{\partial}{\partial \tau}\right|_\xi - \frac{\partial}{\partial \xi} \frac{x}{x_i^2} \frac{dx_i}{d\tau} = \frac{\partial}{\partial \tau} - \frac{\xi}{x_i} \frac{dx_i}{d\tau} \frac{\partial}{\partial \xi}$$

$$\left.\frac{\partial}{\partial x}\right|_\tau = \frac{1}{x_i} \frac{\partial}{\partial \xi}$$

and the set of eqs 33-37 can be written, in terms of these new variables as follows:

$$\frac{\partial \phi}{\partial \tau} - \frac{\xi}{x_i} \frac{dx_i}{d\tau} \frac{\partial \phi}{\partial \xi} - \frac{1}{\xi^2} \frac{1}{x_i^2} \frac{\partial}{\partial \xi}\left[\xi^2 \phi \frac{\partial \phi}{\partial \xi}\right] = 0 \tag{38}$$

$$-(1-x_i)\frac{dx_i}{d\tau} = \frac{\mu_g}{\mu_l}\delta^3(1-\phi) \qquad (39)$$

with initial conditions

$$\text{at} \quad \tau = 0 \quad , \quad \phi = 0 \quad , \quad x_i = 1 \qquad (40)$$

and boundary conditions

$$\text{at} \quad \xi = 0 \quad , \quad \frac{\partial\phi}{\partial\xi} = 0 \qquad (41)$$

and at $\xi = 1$

$$\phi^{3/2}\left[\frac{1}{x_i}\frac{\partial\phi}{\partial\xi} + \frac{dx_i}{d\xi}\right] = \frac{8R_u T\mu_g \delta a_o}{MR^2 \rho_c^{5/2}}(\rho_A)_{vp}\sqrt{D^* p^* k_s} \qquad (42)$$

that constitute the mathematical problem corresponding to the physical model for the pressure build-up in a given catalyst particle.

The solution of this mathematical problem will be sought by means of a perturbation analysis.

VI. *SOLUTION OF THE MATHEMATICAL PROBLEM*

In order to solve the mathematical problem described by the set of equations 38 and 39 with initial and boundary conditions given by eqs. 40-42, one realizes that, in a first stage of the pressure evolution, the internal pressure in the catalyst particle will be much smaller than the capillary pressure of the liquid in the macropores, indicating that the non-dimensional pressure ϕ,

will be, in this first stage, much smaller than one.

Besides, and for conditions relevant to first starts of hydrazine monopropellant thrusters, the value of $\frac{\mu_g}{\mu_l}\delta^3$ is of the order of 10^{-2}, which is also the order of magnitude of the right hand side of eq.42. Therefore, by calling

$$\frac{\mu_g}{\mu_l}\delta^3 = \varepsilon^2 \tag{42a}$$

one can set

$$\frac{8R_u T \mu_g \delta a_o}{MR^2 p_c^{5/2}} (\rho_{\bar{A}})_{vp} \sqrt{D^* p^* k_s} = A\varepsilon^2 \tag{42b}$$

where ε is a small parameter of order 10^{-1} and A is a parameter whose value, of order one, depends on the initial temperature and on the characteristics of the catalyst particle.

When one attempts the solution of the problem by perturbation schemes where the small parameter is ε, it is easy to see that, in a first stage the appropriate variables are the following:

$$\phi = \varepsilon^{4/5}\phi_o$$

$$\tau = \varepsilon^{-4/5}\tau_o$$

$$x_i = 1 - \varepsilon^{3/5}\chi_o$$

with ϕ_o, τ_o, χ_o of order one at this stage.

Introducing these variables in eqs. 38 to 42 and taking the limit $\epsilon \to 0$, the equations giving ϕ_o and χ_o become, in the first approximation

$$\frac{\partial \phi_o}{\partial \tau_o} - \frac{1}{\xi^2} \frac{\partial}{\partial \xi} \left[\xi^2 \phi_o \frac{\partial \phi_o}{\partial \xi} \right] = 0 \qquad (43)$$

$$\chi_o \frac{d\chi_o}{d\tau_o} = 1 \qquad (44)$$

with initial and boundary conditions

$$\text{at} \quad \tau_o = 0 \quad , \quad \phi_o = 0 \quad , \quad \chi_o = 0 \qquad (45)$$

$$\text{at} \quad \xi = 0 \quad , \quad \frac{\partial \phi_o}{\partial \xi} = 0 \qquad (46)$$

$$\text{and at} \quad \xi = 1 \qquad \phi_o^{3/2} \frac{\partial \phi_o}{\partial \xi} = A \qquad (47)$$

The exact solution of this simplified problem would still require a numerical solution; however, if one is only interested in the asymptotic behavior of the solution for $\tau_o \to \infty$, this behavior can be found from the following physical considerations. Due to the feeding action indicated by the r.h.s. of eq.47, the non-dimensional pressure will increase so that when τ_o is large, $\frac{\partial \phi_o}{\partial \xi}$, evaluated at $\xi = 1$, will be very small; this together with the fact that the slope of the pressure distribution is zero at

$\xi = 0$, indicate that this pressure distribution will asymptotically reach a uniform state. But if ϕ_o tends to $\phi_o(\tau)$, equation (43) can be integrated with respect to ξ - by multiplying both terms by $\xi^2 d\xi$ and integrating between $\xi = 0$ and $\xi = 1$ - to give

$$\frac{d\phi_o}{d\tau_o} = 3A\phi_o^{-1/2}$$

so that, when $\tau_o \to \infty$

$$\phi_o \to \left(\frac{9A}{2}\,\tau_o\right)^{2/3} \tag{48}$$

$$\chi_o \to \sqrt{2\tau_o} \tag{49}$$

This asymptotic behavior for the first stage has the advantage of being independent of the initial condition which, formally, could depart from the values given by eq.45 if one takes into consideration the very early stage of the pressure evolution in which the flow can not be described as a continuum.

Nevertheless, the description of the pressure build-up given by eqs.(48) and (49) will, of course, fail when both χ_o and ϕ_o have grown so much as to make some of the terms neglected of the same order of magnitude of the terms retained.

The problem turns out to be a singular perturbation problem, since the solution already found is not uniformly valid for all τ_o.

In a second stage, the appropriate variables for the description of the pressure evolution are obtained from the matching

requirements with the previous stage. These variables are:

$$\phi = \phi_{11}(\tau_1) + \varepsilon^2 \phi_{12}(\xi, \tau_1) \tag{50a}$$

$$\tau = \varepsilon^{-2} \tau_1 \tag{50b}$$

$$x_i = x_i \tag{50c}$$

with ϕ_{11} , ϕ_{12} , τ_1 and x_1 all of order one.

When one introduces these variables into eqs. (38) to (42), these equations become, in the limit $\varepsilon \to 0$,

$$\frac{d\phi_{11}}{d\tau_1} - \frac{1}{\xi^2} \frac{1}{x_i^2} \frac{\partial}{\partial \xi} \left[\xi^2 \phi_{11} \frac{\partial \phi_{12}}{\partial \xi} \right] = 0 \tag{50d}$$

$$- (1 - x_i) \frac{dx_i}{d\tau_1} = 1 - \phi_{11} \tag{51}$$

with the initial and boundary conditions,

at $\tau_1 \to 0$, ϕ_{11} and x_i are given by the matching conditions with the previous stage

$$\text{at} \quad \xi = 0 \qquad \frac{\partial \phi_{12}}{\partial \xi} = 0 \tag{52}$$

$$\text{at} \quad \xi = 1 \qquad \phi_{11}^{3/2} \left[\frac{1}{x_i} \frac{\partial \phi_{12}}{\partial \xi} + \frac{dx_i}{d\tau_1} \right] = A \tag{53}$$

By multiplying both members of eq. (50d) by $\xi^2 d\xi$ and inte-

grating from $\xi = 0$ to $\xi = 1$, making use of the boundary condition given by eq.(53), one obtains:

$$\frac{d\phi_{11}}{d\tau_1} = \frac{3}{x_i}\left[\frac{A}{\phi_{11}^{1/2}} - \phi_{11}\frac{dx_i}{d\tau_1}\right]$$

Therefore, the evolution of the internal pressure is given in this second stage by the following equations:

$$\frac{d\phi_{11}}{d\tau_1} = \frac{3}{x_i}\left[\frac{A}{\phi_{11}^{1/2}} - \phi_{11}\frac{dx_i}{d\tau_1}\right] \qquad (54)$$

$$\frac{dx_i}{d\tau_1} = -\frac{1 - \phi_{11}}{1 - x_i} \qquad (55)$$

with initial conditions, obtained from the matching conditions with the previous stage, namely,

$$\text{when} \quad \tau_1 \to 0 \quad , \quad \phi_{11} \to \left(\frac{9A}{2}\tau_1\right)^{2/3} \quad , \quad x_i \to 1 - \sqrt{2\tau_1} \qquad (56)$$

In order to gain some insight on the nature of the solution, one can expect from this set, of two coupled ordinary differential equations, in fig.1a, 1b, 1c, are represented the flow lines in the phase plane.

From this figure one can see that ϕ_{11} increases while the interphace moves towards the interior of the catalyst particle

until ϕ_{11} reaches the value of 1, at the moment in which the interphace also reaches the maximum penetration depth. From this moment on, the interphace receeds towards the exterior while the pressure increases until ϕ_{11} is such that

$$x_i = 1 + \frac{\phi_{11}^{3/2}(1-\phi_{11})}{A}$$

corresponding to the maximum value of the internal pressure. The interphace keeps receeding and the pressure decreasing until the liquid is expelled. At this time the internal pressure is above the capillary pressure. This final pressure is almost equal to the capillary pressure for values of A of order of or smaller than one; there is only a significant difference between the final pressure and capillary pressure for large values of A. See figures 1a, 1b, 1c.

Therefore one can infer from this qualitative picture that the expulsion of liquid hydrazine will take place at this stage, that the internal pressure when this expulsion occurs, corresponds almost always to the capillary pressure of the liquid in the macropores, and that the maximum internal pressure is greater than this capillary pressure.

To obtain a quantitative result,the set of equations (54) to (56) were numerically integrated using a WANG 700 B desk calculator, for different values of the parameter A of relevance for

the present study. The results of these integrations have been plotted in figs. 1, 2, 3 and 4. Analytical solutions of equations (54) to (56) have been obtained by using singular perturbation methods for large and small values of A (See Appendix A). In figures 1a and 1c a comparison is made with the numerical results.

In fig.2 it has been represented the time τ_{1ign}, required to complete the entire process, as a function of the parameter A. The asymptotic value of τ_{1ign} for large values of A (see appendix A) is given by

$$\tau_{1ign} = \frac{0.478}{A} \qquad (57a)$$

that gives relative errors smaller than 4% for values of A larger than 50.

For small values of A (see appendix A) the asymptotic expression

$$\tau_{1ign} = \frac{1}{2} + \frac{1 - \left(\frac{2A}{11}\right)^{2/9}}{A} \qquad (57b)$$

gives relative errors smaller than 4% for values of A smaller than 0.1.

For values of A larger than 0.7 the function

$$\tau_{1ign} = \frac{0.46}{A} \qquad (57c)$$

correlates the value of τ_{1ign} as function of A with relative errors

smaller than 4%. In this case the ignition time, defined as the time period between injection of liquid hydrazine and expulsion of the gaseous products from the catalyst particles will be given, in physical variables, by the expression:

$$t_{ign} = 0.46 \frac{Ma_o p_c^{3/2}}{R_u T (\rho_A)_{vp} \sqrt{D^* p^* k_s}} \qquad (58)$$

where

$$p_c = \frac{2\sigma\cos\theta}{R}$$

M = mean molecular mass $\simeq$ 0.017 Kg/mol

R_u = 8.317 Joules/mol °K

$(\rho_A)_{vp} = 2.4944 \times 10^8 T^{-1} \exp(-5175/T)$ Kg/m^3

$D^* p^* = 4.487 \times 10^{-5} \times T^{1.823}$ Nw/sg

$k_s = 10^{10} \exp(-1389/T)$ 1/sg

σ = 0.07312 Nw/m

Using these values, taken from ref[1], the values of A and τ_1 given in formulas (6a), (42a, b), (50b), and the results given in fig.3, the ignition time t_{ign}, has been plotted as a function of the initial temperature for different values of the characteristic radius of the macropores, for a catalyst particle whose radius is of 0.6 mm (25-30 mesh size is plotted in Fig.3a)*.

Formula (58) gives a good approximation to the results presented in fig.3 except for small values of temperature and macro-

* In plotting Figs. 3,3a the values of A have been taken from the correlations (57a,b,c).

pore radius (region to the left of the dotted line in figure 3)*

Comparison of the residence time of liquid hydrazine in a given catalyst particle, as given by expression (58), with available experimental results for the ignition time in hydrazine monopropellant thrusters using the Shell 405 catalyst shows a fairly good agreement between theory and experiment, indicating that the ignition time can be truly adscribed to the proposed mechanism. Therefore the pressure in a given catalyst chamber will depart from the nominal value as soon as the liquid hydrazine is expelled from the catalyst particles.

Finally, and as it was mentioned before, the internal pressure in the catalyst particles reaches a maximum value before the expulsion of gaseous products occurs. In figure 4, the maximum value of the non-dimensional internal pressure has been plotted versus the parameter A. The limiting value of the maximum non-dimensional internal pressure is 5/3 for large values of A (see Appendix A).

As it was already mentioned before, it is important to know the value of this maximum internal pressure and to compare it with the crushing pressure of the catalyst particle, so as to ensure that, in a given mission, there will not be cracking of the catalyst particles.

It is also of much importance to see the influence of the different parameters (in particular the size a_o of the particles,

*In fig.3a obtained directly from (58) a comparison with results of ref.[1] is given.

characteristic value of the radius R of the macropores and initial temperature of the catalyst bed) on this maximum pressure within the particle. To this end, the following analysis is performed so as to determine the effect of small variations of these parameters in the maximum internal pressure

$$p_{max} = p_c \phi_{max} = \frac{2\sigma\cos\theta}{R} \phi_{max}(A)$$

where $\phi_{max}(A)$ has been plotted in fig.4 with A given by

$$A = \frac{8R_u T \mu_l R^{1/2} a_o}{M(2\sigma\cos\theta)^{5/2}\delta^2} (\rho_A)_{vp} \sqrt{D^* p^* k_s} \qquad (59)$$

Therefore, and since

$$\frac{\partial p_{max}}{\partial R} = - \frac{p_{max}}{R} + \frac{2\sigma\cos\theta}{R} \frac{d\phi_{max}}{dA} \frac{A}{2R}$$

$$\frac{\partial p_{max}}{\partial a_o} = \frac{2\sigma\cos\theta}{R} \frac{d\phi_{max}}{dA} \frac{A}{a_o}$$

$$\frac{\partial p_{max}}{\partial T} = \frac{2\sigma\cos\theta}{R} \frac{d\phi_{max}}{dA} \frac{T_A}{T_o^2} A$$

where T_A is the apparent activation temperature -T_A = 5869.5* for the Shell 405 catalyst -, the relative change of the maximum internal pressure, with changes in R , a_o and T_o , can be written as:

* The value of T_A is obtained (pag.26) by adding the activation temperature of $(\rho_A)_{vp}$ and half of the activation temperature of k_s.

$$\frac{\Delta p_{max}}{p_{max}} = - \left(1 - \frac{1}{2} \frac{A}{\phi_{max}} \frac{d\phi_{max}}{dA}\right) \frac{\Delta R}{R} + \frac{A}{\phi_{max}} \frac{d\phi_{max}}{dA} \frac{\Delta a_o}{a_o} -$$

$$+ \frac{T_A}{AT_o} \frac{A}{\phi_{max}} \frac{d\phi_{max}}{dA} \frac{\Delta T_o}{T_o} \qquad (60)$$

From Fig.4 it can be seen that the quantity

$$\frac{A}{\phi_{max}} \frac{d\phi_{max}}{dA}$$

keeps a value smaller than 0.076, for values of A relevant for first starts of hydrazine thrusters. Therefore the most drastic changes in the maximum internal pressure within a catalyst particle can be obtained by increasing the characteristic size of the macropores. It can also be seen that the term within the parenthesis of the first term of equation (60) is positive, consequently an increase in R leads to a reduction of p_{max}.

Changing the size of the catalyst particle a_o has, comparatively, a much smaller effect on the value of this maximum internal pressure.

The maximum internal pressure can also be changed by heating the catalyst bed prior the ignition. The effect of increasing T_o depends on the value of A. If A is of order one, then T_A/AT_o is of order of 20 for $T_o \sim 270°K$, so that the effect

of changing the initial temperature of the bed is similar to change the radius of the characteristic macropores. If by the other hand A is of order of 10, then increasing the initial temperature does not change the value of the maximum internal pressure in a significant way.

To allow an easy application of the above obtained results we also include a graph of $A\delta^2/R^{1/2}a_o$ as a function of temperature (Fig.5). This has been obtained from equation (60) where the following correlation for the viscosity of liquid hydrazine has been taken

$$\log_{10}\mu_l(\text{poise}) = \frac{536}{T(^\circ K)} - 3{,}844 \text{ (ref.3).}$$

REFERENCES

1. SANGIOVANNI, J.J.
   KESTEN, A.S.
   : "Study of Hydrazine Reactor Vacuum Start Characteristics"
   United Aircraft Research Laboratories, UARL H9107 58, December 1969.

2. JASCH, P.M.
   SMITH, D.B.
   SANGIOVANNI, J.J.
   : "Study of Hydrazine Reactor Vacuum Start Characteristics - Computer Program Manual"
   United Aircraft Research Laboratories UARL H9107 61, December, 1969.

3. AUDRIETH, L.F.
   ACKERSON, B.
   : "The Chemistry of Hydrazine"
   John Wiley & Sons Inc. N.Y. (1951)

A P P E N D I X A

Asymptotic Analysis of the Unsteady Behavior of Catalytic Particles

The equations giving the evolution of the pressure ϕ (nondimensionalized with the capillary pressure) and the liquid hydrazine penetration radius x (nondimensionalized with the particle radius) in terms of the nondimensional time τ are

$$\frac{d\phi}{dx} = -\frac{3}{x}\,\frac{1-x}{1-\phi}\,\frac{A}{\phi^{1/2}} - \frac{3}{x}\,\phi \qquad (1)$$

$$\frac{dx}{d\tau} = -\frac{1-\phi}{1-x} \qquad (2)$$

The first term in the right hand side of Eq.(1) represents the effect on the increment of pressure of the hydrazine vaporization and subsequent reaction. The last term represents the increment in pressure associated with the isothermal compression of the gases that have been generated previously. In equation (2), $(1-\phi)$ is the difference between the capillary pressure and the internal pressure, or driving force for the motion of hydrazine toward the interior of the particles.

These equations are to be integrated with the initial conditions

$$\phi = 0 \quad \text{and} \quad x = 1 \quad \text{at} \quad \tau = 0. \qquad (3)$$

Let us now look for the asymptotic solution of Eqs.(1) to (3) for small values of A.

There is a first stage for values of ϕ of order $A^{2/3}$ and τ and x of order 1, so that we shall introduce the variable ψ such that

$$\phi = \psi A^{2/3} \tag{4}$$

so that Eqs.(1) and (2) reduce in first approximation to

$$\frac{d\psi}{dx} = -\frac{3}{x}\,\frac{1-x}{\psi^{1/2}} - \frac{3}{x}\,\psi \tag{5}$$

$$\frac{dx}{d\tau} = -\frac{1}{1-x} \tag{6}$$

Eq.(5) can be integrated with the initial condition $\psi = 0$ at $x=1$ to give

$$\psi^{3/2} = \frac{2}{11}\,x^{-9/2} + \frac{9}{11}\,x - 1 \tag{7}$$

while Eq.(6) with the initial condition $x(0) = 1$ gives

$$x = 1 - \sqrt{2\tau} \tag{8}$$

Eq.(8) ceases to be valid for τ close to 1/2 when x becomes so small that ψ becomes large and we can no longer neglect the counter pressure ϕ in Eq.(2). Then in a second stage when x is very small and ϕ of order unity the equations to be solved are

according to (1) and (2), for the first approximation

$$\frac{d\phi}{dx} = -\frac{3}{x}\phi \tag{9}$$

and

$$\frac{dx}{d\tau} = \phi - 1 \tag{10}$$

Equation (9) can be integrated to yield

$$\phi = cx^{-3}$$

where the constant of integration c has to be chosen as $c=(2A/11)^{2/3}$ from the matching conditions with the solution (7).

Then

$$\phi = \left(\frac{2A}{11}\right)^{2/3} x^{-3} \tag{11}$$

when this result is used in connection with

$$\frac{d\phi}{d\tau} = \frac{3}{x}\phi(1-\phi) \tag{12}$$

which results from Eqs. (9) and (10), we obtain

$$\left(\frac{11}{2A}\right)^{2/9}\left(\tau - \frac{1}{2}\right) = \frac{1}{3}\int\frac{d\phi}{\phi^{4/3}(1-\phi)} = -\phi^{-1/3} - \frac{1}{6}\ln\frac{\left(1-\phi^{1/3}\right)^2}{1+\phi^{1/3}+\phi^{2/3}} -$$

$$-\frac{\text{arctg}}{\sqrt{3}}\left(\frac{1+2\phi^{1/3}}{\sqrt{3}}\right) + \frac{1}{\sqrt{3}}\text{arctg}\frac{1}{\sqrt{3}} \tag{13}$$

The integration constant in Eq.(13) was chosen from the matching

conditions with the previous stage. Thus the second stage is of duration of order $(2A/11)^{2/9}$ and centered around $\tau = 1/2$.

Again the solutions (11) and (12) cease to be valid when ϕ becomes so close to 1 that θ ,

$$\theta = (\phi-1)/A \quad , \tag{14}$$

is of order unity. In this case x is very close to x_o such that

$$\left(\frac{2A}{11}\right)^{2/3} x_o^{-3} = 1 \tag{15}$$

Then in a third stage Eqs.(1) and (2) reduce to

$$\frac{Ax}{3}\,\frac{d\theta}{dx} = \frac{1-\theta-x_o}{\theta} \tag{16}$$

so that

$$\theta\,(1-x_o)\ln(1-x_o-\theta) = -\frac{3}{A}\ln(x/x_o) \tag{17}$$

where the constant of integration has been chosen from the matching conditions with the solution Eq.(11) of the previous stage.

During most of the second stage when θ is of order unity but not too close to 1 and $x_o \ll 1$, Eq.(17) simplifies to

$$\theta + \ln(1-\theta) = -\frac{3}{A}\,\frac{x-x_o}{x_o} \tag{18}$$

To obtain θ as a function of time, we take Eq.(17) or (18) into the

simplified form

$$x_o \frac{d(x/x_o)}{d(A\tau)} = \theta \qquad (19)$$

of Eq.(2) so that we obtain

$$\left(\tau - \frac{1}{2}\right) = - \frac{x_o}{3} \int \frac{d\theta}{\theta - 1} \qquad (20)$$

and the constant of integration has to be obtained from the previous solution

$$\theta - 1 = - \frac{B}{A} e^{- \frac{3(\tau - 1/2)}{x_o}} \qquad (21)$$

with $B = 3\sqrt{3} \exp\left\{-3 - \frac{3}{\sqrt{3}}\left(\text{arctg } \sqrt{3} - \text{arctg } \frac{1}{\sqrt{3}}\right)\right\}$.

The length of this stage is thus of order x_o or $A^{2/9}$, thus very short.

Finally a last stage exists when x is of order unity and θ still of order one, where equation (1) reduces to

$$\theta = (1 - x) \qquad (22)$$

and Eq.(2) reduces to

$$\frac{dx}{d(A\tau)} = 1 \qquad (23)$$

$$\theta + 1 = A(\tau - 1/2) \qquad (24)$$

so that

$$x - x_o = A(\tau - 1/2) \qquad (25)$$

in first approximation, so that finally the ignition time would be given by

$$\tau_I = \frac{1}{2} + \frac{1 - x_o}{A} \qquad (26)$$

Asymptotic solution for large values of A. In this case the penetration of liquid hydrazine $1 - x$ is small of order $1/A^{1/2}$ and occurs during the characteristic time $1/A$ so that we shall use the variables

$$\xi = A^{1/2} (1-x) \quad \text{and} \quad A\tau$$

Then Eq.(1) becomes in first approximation

$$\frac{d\phi}{d\xi} = \frac{3\xi}{(1-\phi)\phi^{1/2}} \qquad (27)$$

so that the effect of the isothermal compression is negligible.

When we integrate (27) with the boundary condition $\phi = 0$ at $\xi = 0$ we obtain

$$\frac{2}{3}\phi^{3/2} - \frac{2}{5}\phi^{5/2} = \frac{3}{2}\xi^2 \qquad (28)$$

On the other hand from Eq.(27) and (2) we obtain

$$\frac{d\phi}{d\tau} = \frac{3}{\phi^{1/2}} A \qquad (29)$$

so that

$$\frac{2}{3}\phi^{3/2} = 3A\tau .$$

or

$$\phi = \left(\frac{9A}{2}\,\tau\right)^{2/3} \qquad (30)$$

The maximum value of ϕ occurs for $\xi = 0$, so that $\phi_{max} = 5/3$,, and the ignition time

$$\tau_I = \left(\frac{5}{3}\right)^{3/2} \frac{2}{9}\,\frac{1}{A} = 0.478/A \qquad (31)$$

A second approximation for $\phi(t)$ is given by

$$\tau A = \frac{2}{9}\,\phi^{3/2} - \frac{1}{\sqrt{A}}\,\frac{2}{3}\,\phi^{3/4}\sqrt{1 - \frac{3}{5}\,\phi}\left[1 + \frac{(1-\phi)\phi^{3/2}}{\frac{4}{9}\,\phi^{3/2}\left(1 - \frac{2}{5}\,\phi\right)}\right]$$

a second approximation for $\phi(\xi)$ is given by

$$\left(\frac{2}{3}\right)^2 \phi^{3/2}\left[1 - \frac{3}{5}\,\phi\right] = \xi^2 + \frac{1}{\sqrt{A}}\int_0^{\phi} \frac{\phi^{1/4}\,d\phi}{\sqrt{1 - \frac{3}{5}\,\phi}}$$

The values of ϕ at $\xi = 0$ which is given in first approximation by $\phi = 5/3$

in second approximation is

$$\phi_o = \frac{5}{3}\left[1 - \frac{\alpha}{\sqrt{A}}\right]$$

and

$$\alpha\left(\frac{5}{3}\right)^{3/2}\left(\frac{2}{3}\right)^2 = \int_0^{5/3} \frac{\phi^{1/4}\,d\phi}{\sqrt{1 - \frac{3}{5}\,\phi}} = \left(\frac{5}{3}\right)^{5/4}\int_0^1 \frac{u^{1/4}\,du}{\sqrt{1 - u}} = \left(\frac{5}{3}\right)^{5/4} \frac{\Gamma\left(\frac{5}{4}\right)\Gamma\left(\frac{1}{2}\right)}{\Gamma\left(\frac{7}{4}\right)}$$

$$\alpha = \left(\frac{5}{3}\right)^{-1/4}\left(\frac{3}{2}\right)^2 \frac{0{,}906 \cdot 1{,}772}{0{,}919} = 3.46$$

As it happens sometimes with asymptotic expansions, the second approximation does not make the asymptotic solution closer to the exact solution, unless very large values of the large parameter are taken. This is due to the fact that the asymptotic expansions are not convergent. Consequently we have taken for the asymptotic solution corresponding to large A the results given in (28), (30) and (31).

- - - - - - - - -

LIST OF FIGURE CAPTIONS

Fig.1.- Non-dimensional pressure as function of non-dimensional interphace location for different values of parameter A.

Fig.2.- Ignition time as function of parameter A.

Fig.3.- Ignition time as function of initial temperature for different pore sizes.

Fig.4.- Maximum non-dimensional pressure servus parameter A.

- - - - - - - - - -

FIG. Nº 1a

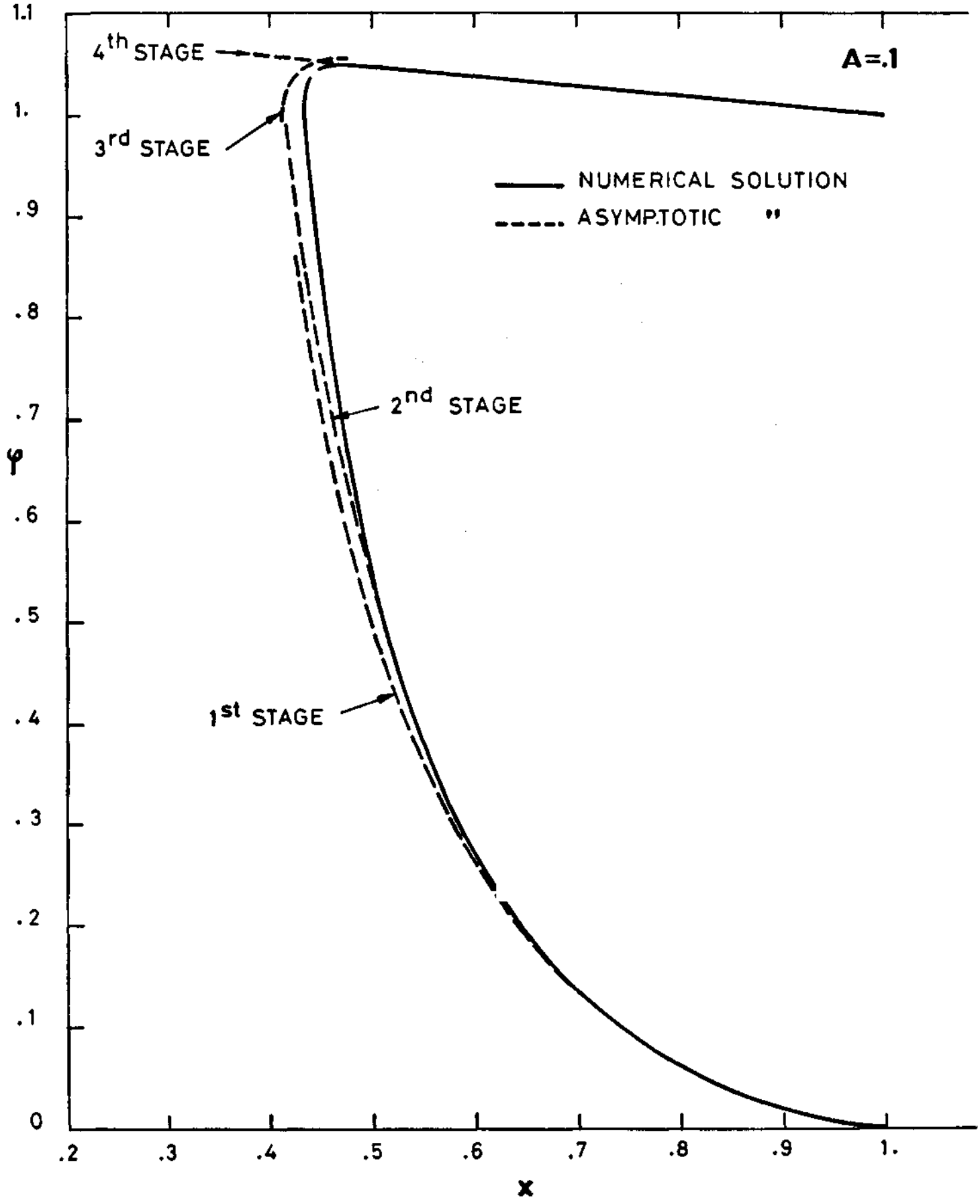
4th STAGE
A=.1
3rd STAGE
NUMERICAL SOLUTION
ASYMPTOTIC "
2nd STAGE
1st STAGE
φ
x
1.1
1.
.9
.8
.7
.6
.5
.4
.3
.2
.1
0
.2
.3
.4
.5
.6
.7
.8
.9
1.

FIG. Nº 1

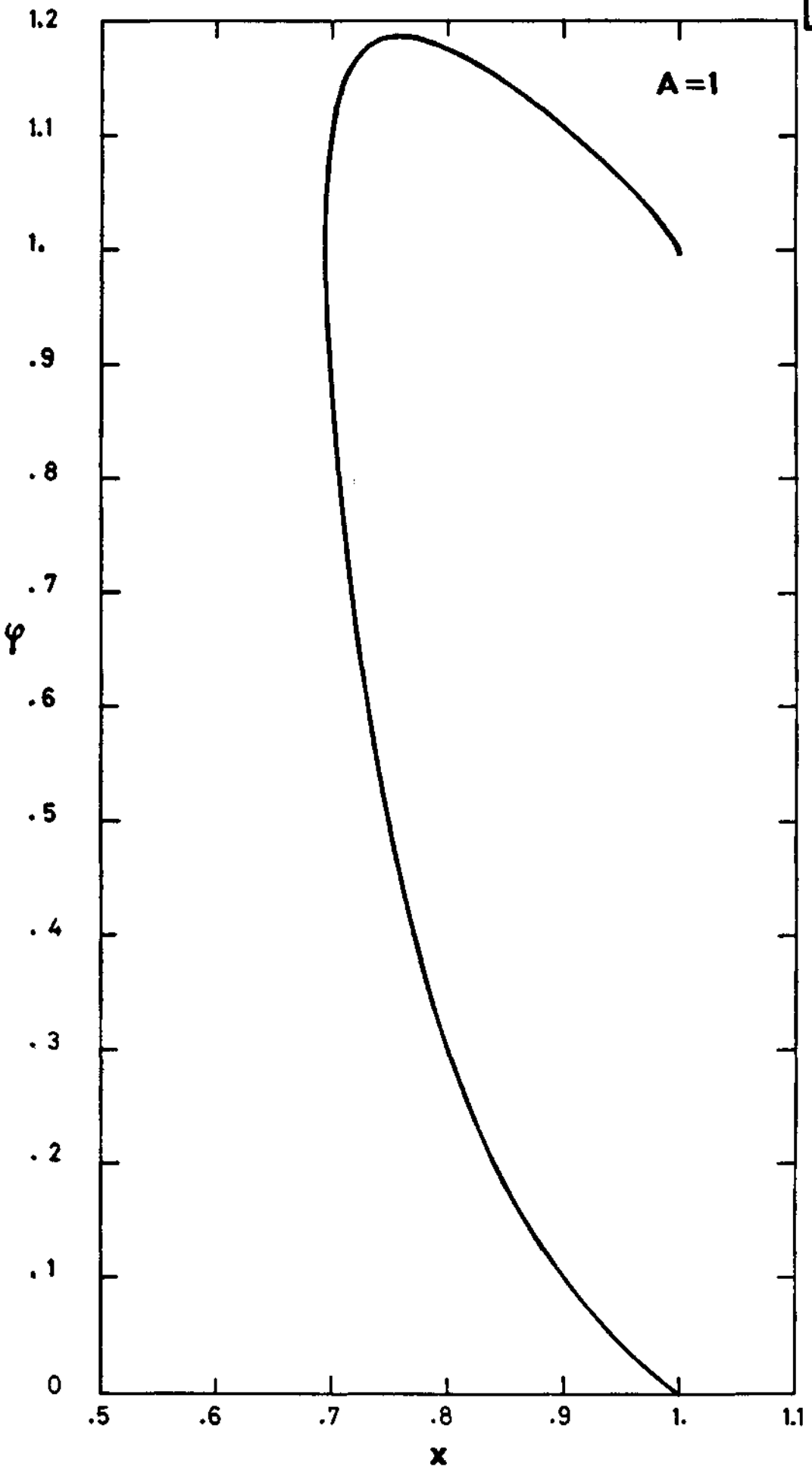

FIG. Nº 1c

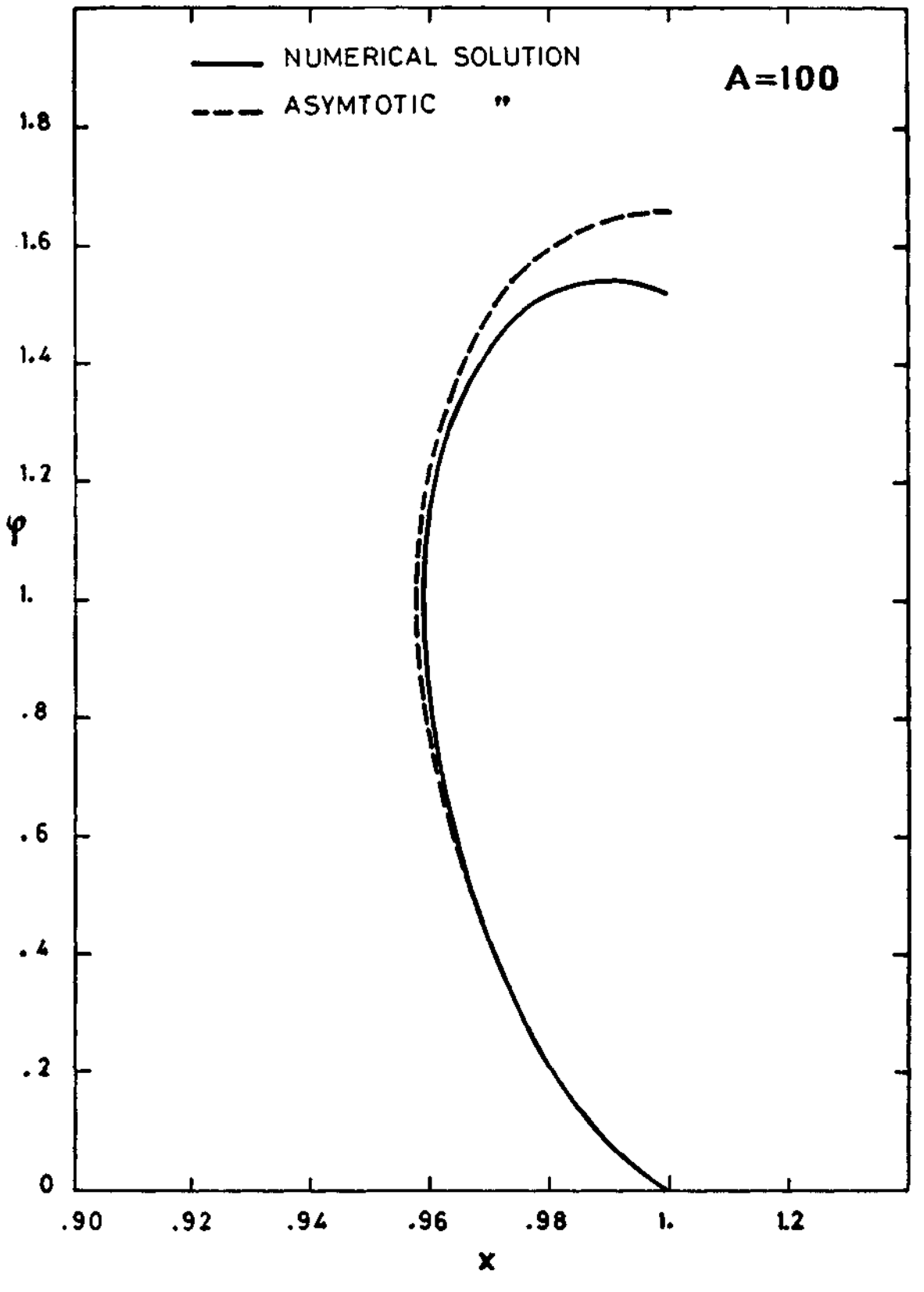
NUMERICAL SOLUTION
ASYMTOTIC "
A=100
1.8
1.6
1.4
1.2
φ
1.
.8
.6
.4
.2
0
.90
.92
.94
.96
.98
1.
1.2
x

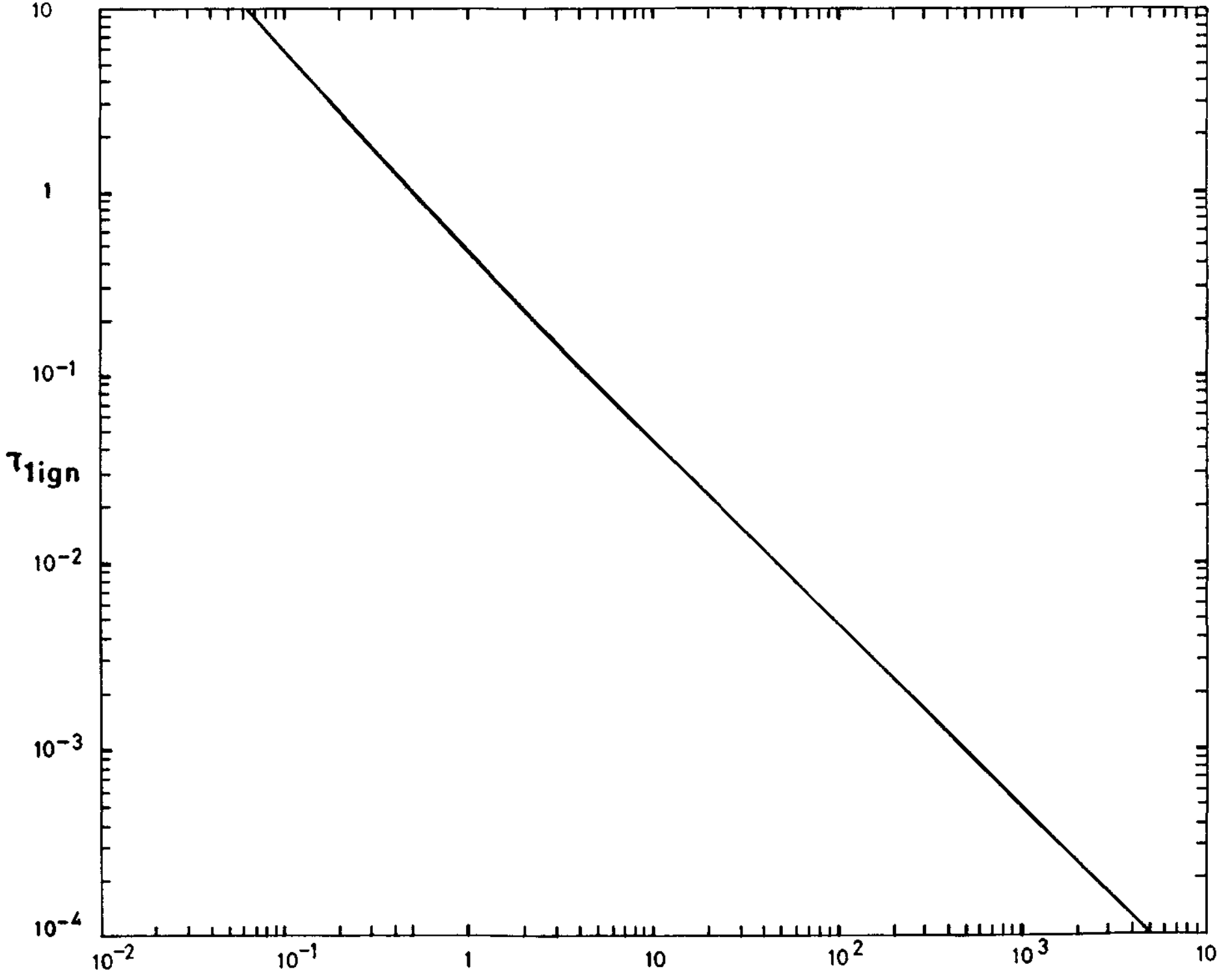

FIG. N° 2

FIG. Nº 3

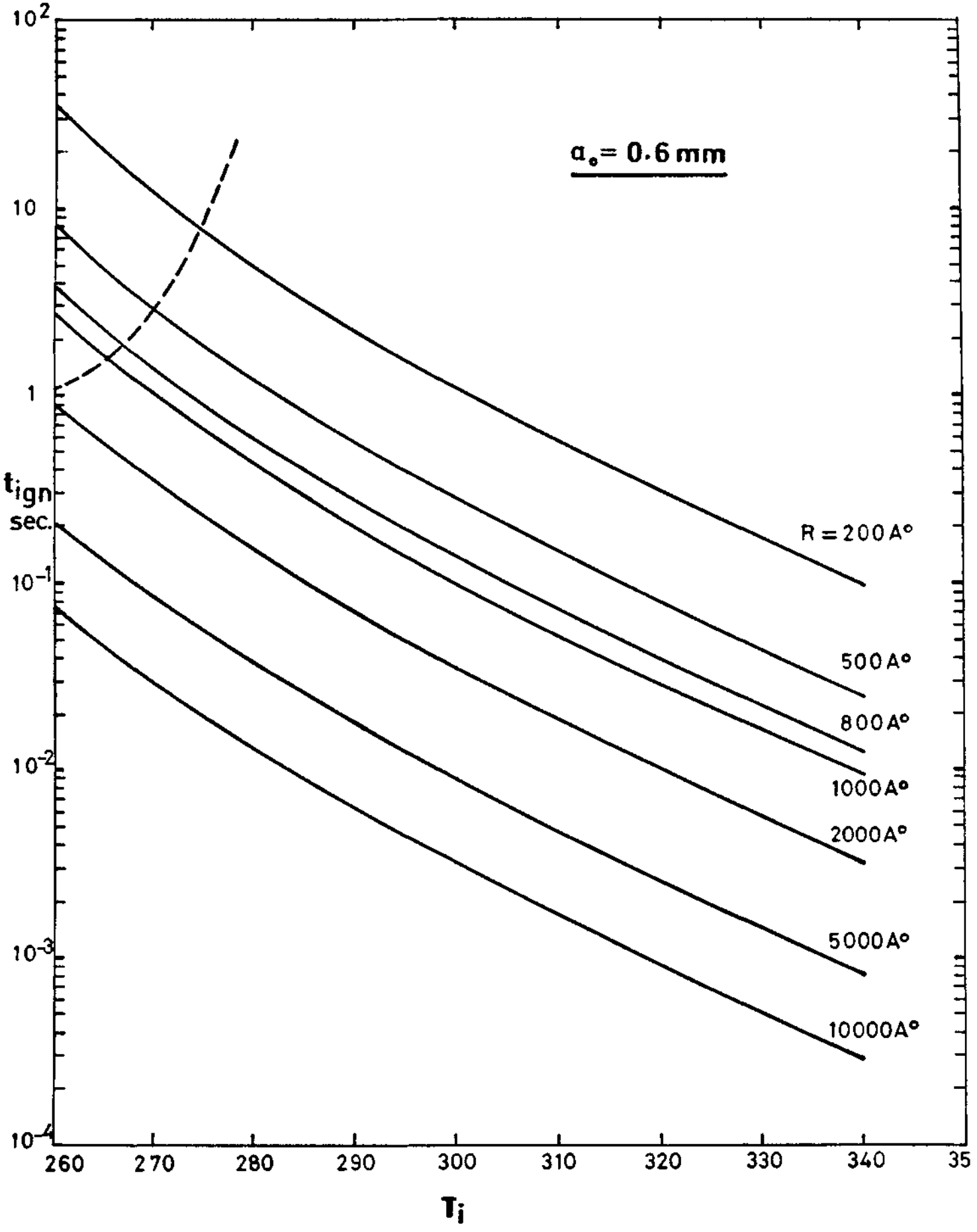
a_o= 0.6 mm
R = 200 A°
500 A°
800 A°
1000 A°
2000 A°
5000 A°
10000 A°
t_{ign} sec.
T_i
10^2
10
1
10^{-1}
10^{-2}
10^{-3}
10^{-4}
260
270
280
290
300
310
320
330
340
35

FIG. Nº 3a

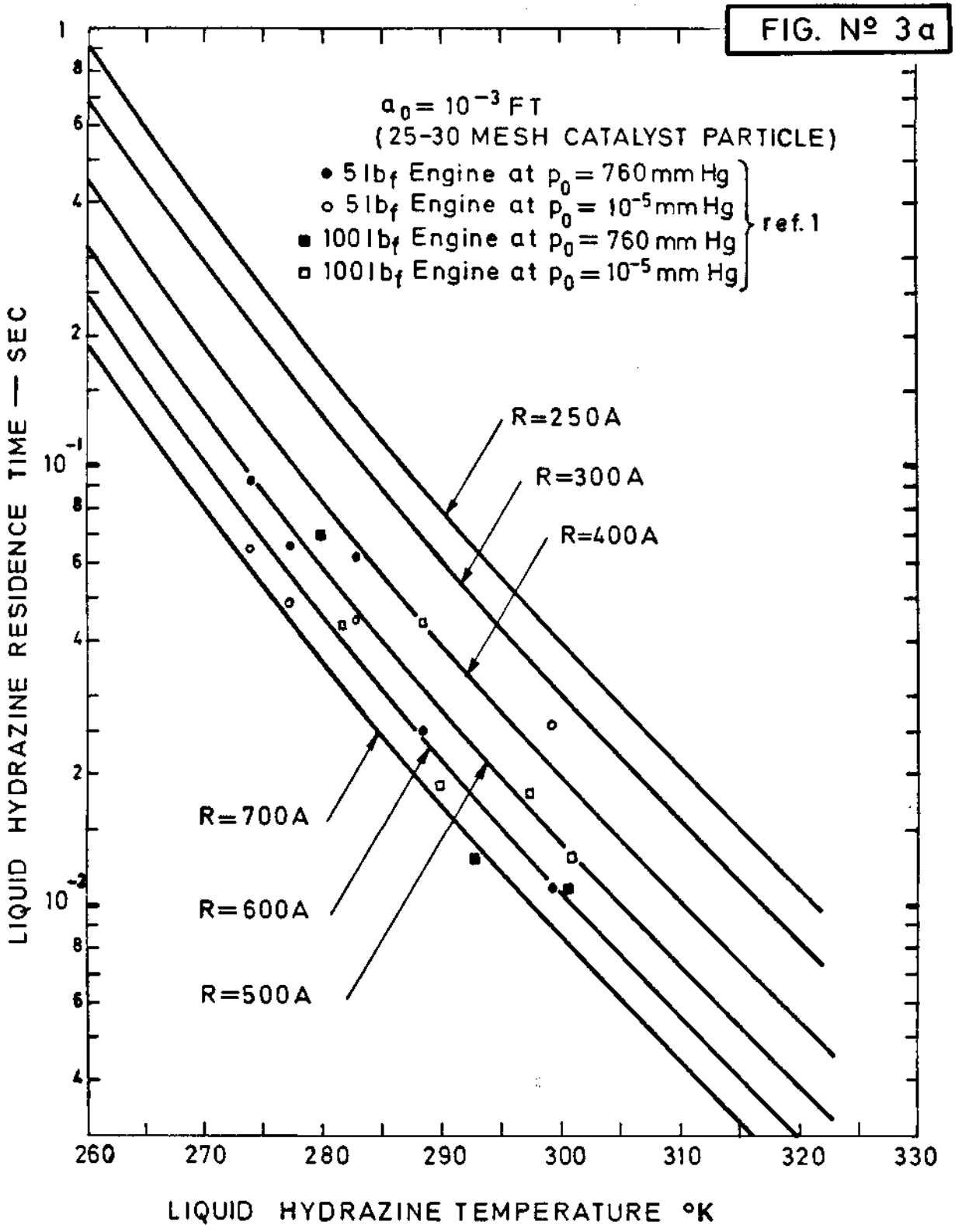
$a_0 = 10^{-3}$ FT
(25-30 MESH CATALYST PARTICLE)
• 5 lb$_f$ Engine at $p_0 = 760$ mm Hg
○ 5 lb$_f$ Engine at $p_0 = 10^{-5}$ mm Hg
■ 100 lb$_f$ Engine at $p_0 = 760$ mm Hg
□ 100 lb$_f$ Engine at $p_0 = 10^{-5}$ mm Hg
ref. 1
R=250A
R=300A
R=400A
R=700A
R=600A
R=500A
LIQUID HYDRAZINE RESIDENCE TIME — SEC
LIQUID HYDRAZINE TEMPERATURE °K
1
10^{-1}
10^{-2}
260
270
280
290
300
310
320
330

FIG. Nº 4

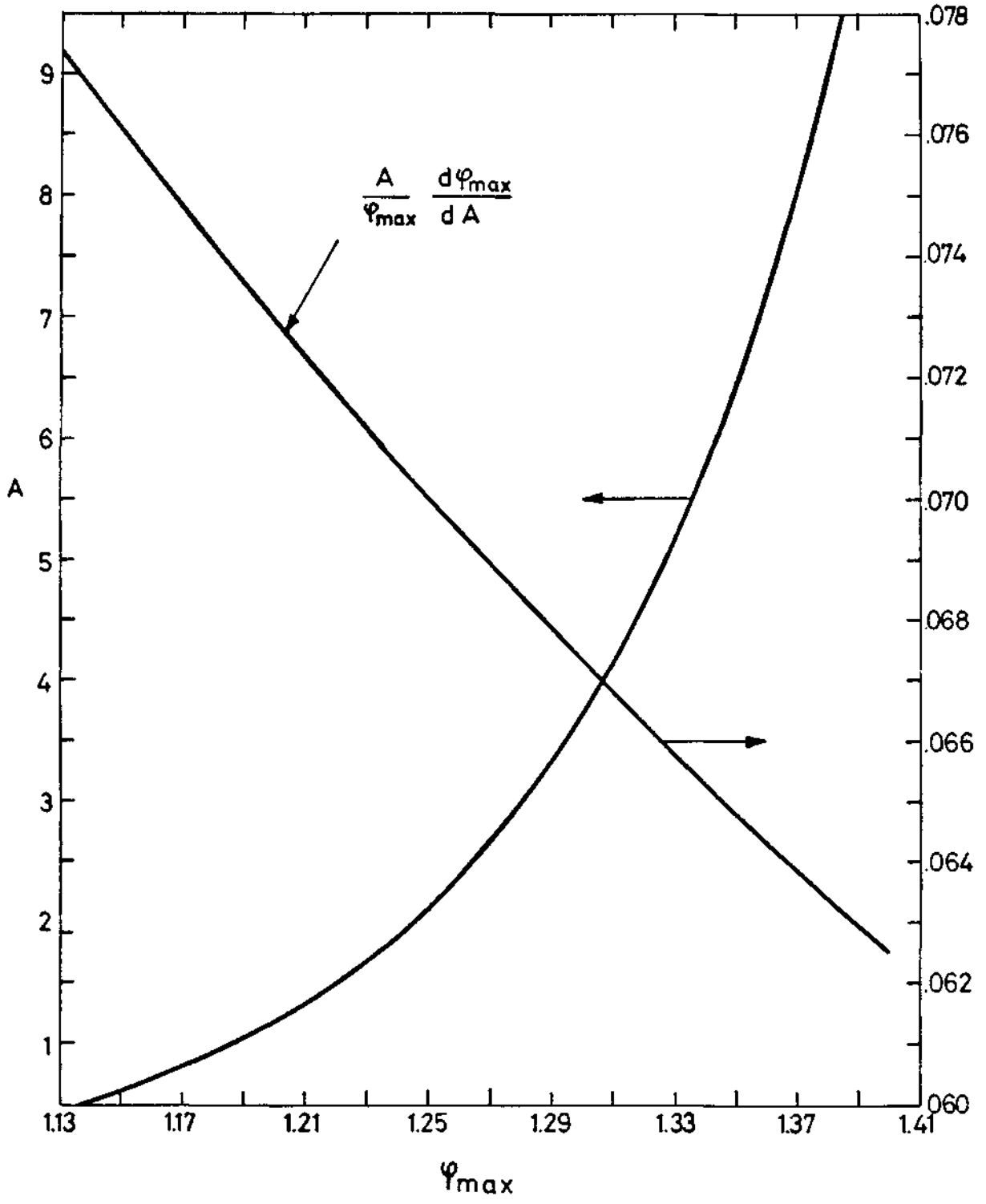
A
$\frac{A}{\varphi_{max}} \frac{d\varphi_{max}}{dA}$
9
8
7
6
5
4
3
2
1
.078
.076
.074
.072
.070
.068
.066
.064
.062
.060
1.13
1.17
1.21
1.25
1.29
1.33
1.37
1.41
φ_{max}

FIG. Nº 5

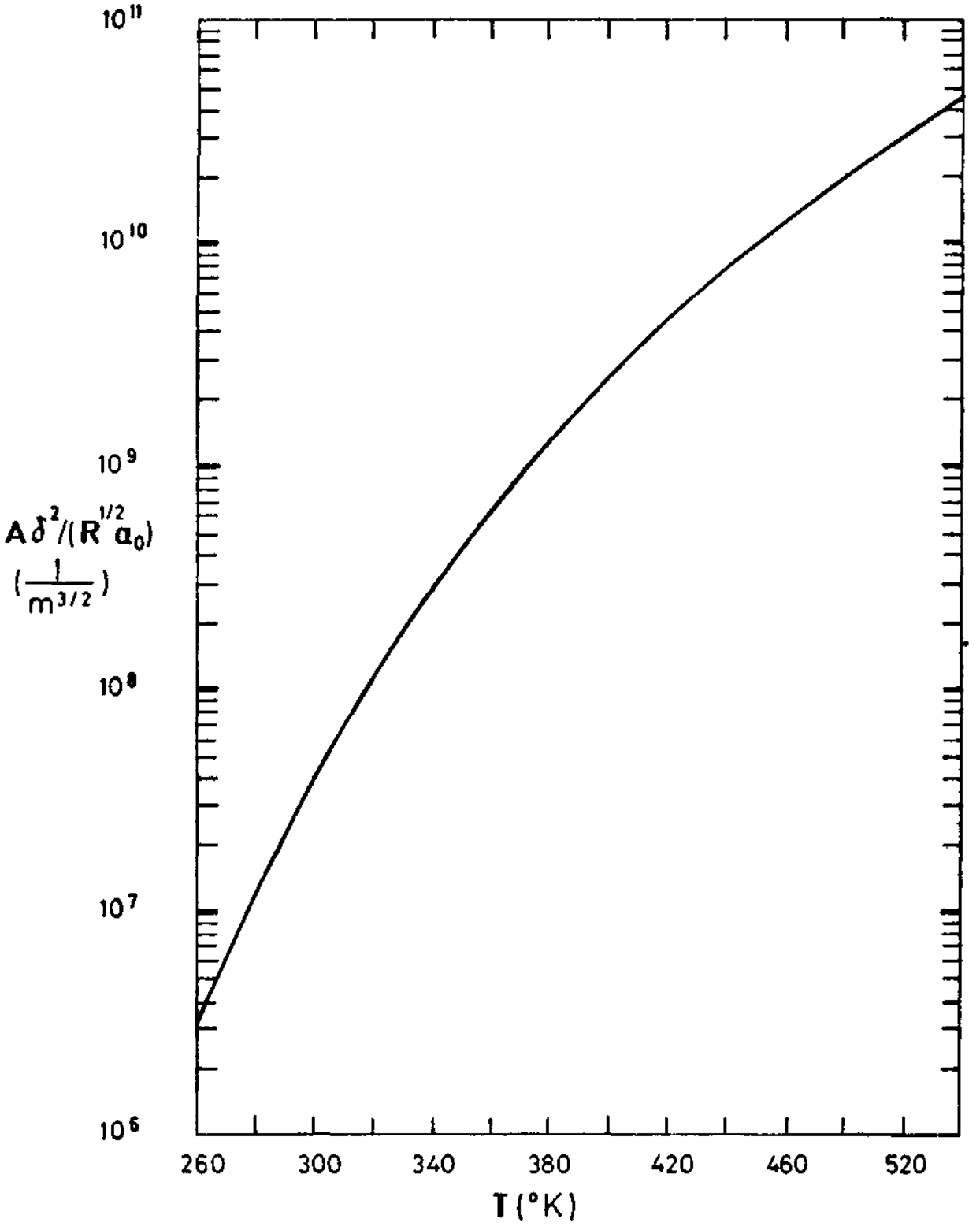
10^{11}
10^{10}
10^{9}
10^{8}
10^{7}
10^{6}
$A\delta^2/(R^{1/2}a_0)$
$(\frac{1}{m^{3/2}})$
260
300
340
380
420
460
520
T (°K)

P A R T II

THE HOMOGENEOUS GAS PHASE DECOMPOSITION OF HYDRAZINE BY SINGULAR PERTURBATION METHODS

Author J.L. Urrutia

LIST OF SYMBOLS

c_1 = non-dimensional molar concentration of species i

k_1 = rate constant of reaction i

K_1 = non-dimensional rate constant

t_1 = non-dimensional time

ϵ = small parameter in asymptotic expansions (set equal to 10^{-2})

ξ_i = normalized molar concentration at each stage, in the evolution

τ = normalized time at each stage.

Subscripts

o = initial condition

- - - - - -

THE HOMOGENEOUS GAS PHASE DECOMPOSITION OF HYDRAZINE BY SINGULAR PERTURBATION METHODS

I. INTRODUCTION

The thermal decomposition of hydrazine has been studied extensively in the past[1-10] and its decomposition mechanism is well understood especially after the work of Eberstein and Glassman[10].

This decomposition mechanism includes one initiation reaction, three propagation reactions, two chain branching reactions and four termination reactions, so that an exact treatment of the evolution of the reaction, even in the simplest circumstances, would require a numerical type of solution.

However, an analytical solution of the evolution of the reaction would give a considerably deeper understanding of the process and its resuls would be of practical significance. For instance, in hydrazine reactors with catalytical combustion chambers, there is a first region in which the heterogeneous decomposition of hydrazine is the only mechanism capable of starting the reaction because the temperature there is practically that of the injected fluid and the thermal decomposition is, at these low temperatures, frozen.

The chamber temperature increases along the axis of the chamber, so that at a certain section both mechanisms of heat release, heterogeneous reaction and gas phase thermal decomposition of hydrazine, can be competitive, and must be included in the study of the evolution of species in a given reactor. This study

would be analytically intractable unless that the complicated kinetic mechanism of the decomposition reaction could be reduced to an overall reaction with an appropriate reaction rate.

The aim of this paper is to see under what circumstances the complicated mechanism of the decomposition of hydrazine can be overlooked and the reaction mechanism described, to a certain approximation, by a single overall reaction with an appropriate reaction rate.

The point of departure is that, when plotting the rate constants of the different elementary reactions playing a role in the decomposition mechanism, as a function of temperature (Fig.1), these rate constants differ one from each other by several orders of magnitude so that it seems appropriate to seek the solution of this problem by perturbation methods in which the small parameters are ratios between rate constants.

It turns out that the mathematical problem is a singular perturbation problem. Several stages are found in the course of the reaction and, at each stage, the detailed kinetic mechanism of the reaction varies, so that different expansions are used for each of the stages and they are matched according to the rules of the method of matched asymptotic expansions.

This paper concerns with the case in which hydrazine is initially highly diluted in He and the initial temperature of the gas mixture is 1000°K. Under these conditions the reaction can be seen to be composed of four stages. However, inspection of the appropriate time scales for each of the stages indicates that this decomposition reaction spends most of the time in the last of these stages.

The appropriate stoichiometry of the reaction, under the said initial conditions, is shown to be:

$$N_2H_4 \rightarrow \frac{2}{3} NH_3 + \frac{2}{3} N_2 + H_2$$

Although the analysis seems to be somehow restricted to the particular initial conditions chosen, it shows, however the feasibility of exten
tions.

II. KINETIC SCHEME

The gas phase decomposition of Hydrazine has been shown by Eberstein and Glassman[10] to involve the following substances and reactions in the temperature range from 750°K to 1000°K.

Initiation Reaction

1) $N_2H_4 + X \rightarrow 2NH_2 + X$ $\quad k_1 = 10^{19} \exp\left[-60000/RT\right]$ cc/mole-sec

Propagation Reactions

2) $N_2H_4 + NH_2 \rightarrow NH_3 + N_2H_3$ $\quad k_2 = 10^{12} \exp\left[-7000/RT\right]$ cc/mole-sec

3) $N_2H_3 + X \rightarrow N_2 + H_2 + H + X$ $\quad k_3 = 10^{13} \exp\left[-20000/RT\right]$ cc/mole-sec

4) $N_2H_4 + H \rightarrow NH_3 + NH_2$ $\quad k_4 = 10^{13} \exp\left[-7000/RT\right]$ cc/mole-sec

Chain Branching Reactions

5) $N_2H_3 + X \rightarrow NH + NH_2 + X$ $\quad k_5 = 10^{12.9} \exp\left[-18000/RT\right]$ cc/mole-sec

6) $N_2H_4 + NH \rightarrow NH_2 + N_2H_3$ $\quad k_6 = 10^{14} \exp\left[-10000/RT\right]$ cc/mole-sec

Termination Reactions

7) $NH_2+N_2H_3 \longrightarrow NH_3+N_2+H_2$	$k_7 = 10^{12.5}$	cc/mole-sec
8) $2N_2H_3 \longrightarrow 2NH_3 + N_2$	$k_8 = 10^{12}$	cc/mole-sec
9) $N_2H_3+H \rightarrow N_2 + 2H_2$	$k_9 = 10^{15}$	cc/mole-sec
10) $2NH_2 \longrightarrow N_2H_4$	$k_{10} = 10^{12.5}$	cc/mole-sec

The analysis that follows concerns with the case in which hydrazine is extremely diluted in He , so that its initial molar concentration is of the order of 10^{-2} times that of Helium.

Let c_i be the molar concentration of substance i normalized with the molar concentration of diluent in the mixture, i.e.,

$c_1 = \{N_2H_4\}/\{X\}$; $c_2 = \{NH_2\}/\{X\}$; $c_3 = \{NH_3\}/\{X\}$

$c_4 = \{N_2H_3\}/\{X\}$; $c_5 = \{H\} / \{X\}$; $c_6 = \{NH\} /\{X\}$

$c_7 = \{N_2\} / \{X\}$; $c_8 = \{H_2\}/ \{X\}$

Now, when the initial temperature of the mixture is of the order of 1000°K, it is apparent from inspection of figure 1 that the rate constants differ one from each other by several orders of magnitude. Dividing each of these rate constants by k_9 , we get for temperatures close to 1000°K,

$k_1/k_9 = K_1\varepsilon^{4.5}$ $k_4/k_9 = K_4\varepsilon^{2}$ $k_7/k_9 = K_7\varepsilon^{1.5}$

$k_2/k_9 = K_2\varepsilon^{2.5}$ $k_5/k_9 = K_5\varepsilon^{3}$ $k_8/k_9 = \varepsilon^{1.5}$

$k_3/k_9 = K_3\varepsilon^{3}$ $k_6/k_9 = K_6\varepsilon^{1.5}$ $k_{10}/k_9 = K_7\varepsilon^{1.5}$

where the K_i are of order one and can be calculated once the exact initial temperature is fixed, and ε is an small number equal to 10^{-2}.

Therefore, the nondimensional rate equations, given by the following set of differential equations:

$$\frac{dc_1}{dt_1} = -K_1\varepsilon^{4.5}c_1 - K_2\varepsilon^{2.5}c_1c_2 - K_2\varepsilon^{2}c_1c_5 - K_6\varepsilon^{1.5}c_1c_6 + K_7\varepsilon^{1.5}c_2^2$$

$$\frac{dc_2}{dt_1} = 2K_1\varepsilon^{4.5}c_1 - K_2\varepsilon^{2.5}c_1c_2 + K_2\varepsilon^{2}c_1c_5 + K_5\varepsilon^{3}c_4 + K_6\varepsilon^{1.5}c_1c_6 - K_7\varepsilon^{1.5}c_2c_4 - 2K_7\varepsilon^{1.5}c_2^2$$

$$\frac{dc_3}{dt_1} = K_2\varepsilon^{2.5}c_1c_2 + K_2\varepsilon^{2}c_1c_5 + K_7\varepsilon^{1.5}c_2c_4 + 2\varepsilon^{1.5}c_4^2$$

$$\frac{dc_4}{dt_1} = K_2\varepsilon^{2.5}c_1c_2 - K_3\varepsilon^{3}c_4 - K_5\varepsilon^{3}c_4 + K_6\varepsilon^{1.5}c_1c_6 - K_7\varepsilon^{1.5}c_2c_4 - 2\varepsilon^{1.5}c_4^2 - c_4c_5$$

$$\frac{dc_5}{dt_1} = K_3\varepsilon^{3}c_4 - K_2\varepsilon^{2}c_1c_5 - c_4c_5$$

$$\frac{dc_6}{dt_1} = K_5\varepsilon^{3}c_4 - K_6\varepsilon^{1.5}c_1c_6$$

$$\frac{dc_7}{dt_1} = K_3\varepsilon^{3}c_4 + K_7\varepsilon^{1.5}c_2c_4 + \varepsilon^{1.5}c_4^2 + c_4c_5$$

$$\frac{dc_8}{dt_1} = K_3\varepsilon^{3}c_4 + K_7\varepsilon^{1.5}c_2c_4 + 2c_4c_5$$

where t_1 is a non-dimensional time variable related with the physical time by means of the following expresion:

$$t_1 = k_9\{X\}t$$

III. FIRST STAGE OF THE REACTION

In the absence of intermediates in the initial mixture, the only mechanism capable of starting the reaction of decomposition of hydrazine is the initiation reaction 1); once some NH_2 has been produced by this reaction, reactions 2), 3) and 5) enter into play and generate more intermediates and products.

Being the initiation reaction the crucial step in this stage, it is obvious that the rate of appearance of NH_2 must be goberned precisely by this initiation reaction. This consideration directly leads to the conclusion that this rate must be,in this first stage, of the order of $\varepsilon^{5.5}$, and that the appropriate variables to study the evolution of the different species, at this stage, will be the following

$$c_1 = \varepsilon\xi_1 \qquad c_4 = \varepsilon^4\xi_4 \qquad c_7 = \varepsilon^{4.5}\xi_7$$

$$c_2 = \varepsilon^3\xi_2 \qquad c_5 = \varepsilon^{4.5}\xi_5 \qquad c_8 = \varepsilon^{4.5}\xi_8$$

$$c_3 = \varepsilon^4\xi_3 \qquad c_6 = \varepsilon^{4.5}\xi_6 \qquad \tau = \varepsilon^{2.5}t_1$$

where ξ_i and τ are, all of them, of order one.

In the limit $\varepsilon \to 0$, the rate equations take the following form:

$$\frac{d\xi_1}{d\tau} = 0 \qquad \frac{d\xi_4}{d\tau} = K_2\xi_1\xi_2 \qquad \frac{d\xi_7}{d\tau} = K_3\xi_4$$

$$\frac{d\xi_2}{d\tau} = 2K_1\xi_1 \qquad \frac{d\xi_5}{d\tau} = K_3\xi_4 \qquad \frac{d\xi_8}{d\tau} = K_3\xi_4$$

$$\frac{d\xi_3}{d\tau} = K_2\xi_1\xi_2 \qquad \frac{d\xi_6}{d\tau} = K_5\xi_4 - K_6\xi_1\xi_6$$

with the initial conditions

$$\xi_i = 0 \ (i - 2, \text{---}8) \qquad \xi_1 = (\xi_1)_o$$

The solutions of this set of differential equations is easily found to be:

$$\xi_1 = (\xi_1)_o \qquad \xi_2 = 2K_1(\xi_1)_o\tau$$

$$\xi_3 = K_1K_2(\xi_1)_o\tau^2 \qquad \xi_4 = K_1K_2(\xi_1)_o^2\tau^2$$

$$\xi_5 = \frac{1}{3}K_1K_2K_3(\xi_1)_o^2\tau^3$$

$$\xi_6 = \frac{K_1K_2K_5}{K_6}\left[-\frac{2}{K_6^2(\xi_1)_o}e^{-K_6(\xi_1)_o\tau} + \frac{2}{K_6^2(\xi_1)_o} - \frac{2}{K_6}\tau + (\xi_1)_o\tau^2\right]$$

$$\xi_7 = \frac{1}{3}K_1K_2K_3(\xi_1)_o^2\tau^3 \qquad \xi_8 = \frac{1}{3}K_1K_2K_3(\xi_1)_o^2\tau^3$$

The simplified kinetic scheme appropriate at this stage is the

following:

1) $N_2H_4 + X \longrightarrow 2NH_2 + X$

2) $N_2H_4 + NH_2 \longrightarrow NH_3 + N_2H_3$

3) $N_2H_3 + X \longrightarrow N_2 + H_2 + H + X$

5) $N_2H_3 + X \longrightarrow NH + NH_2 + X$

6) $N_2H_4 + NH \longrightarrow NH_2 + N_2H_3$

This stage ceases to be valid when both c_4 and c_5 become large enough as to make significant the contribution of reaction 3) and 9).

IV. SECOND STAGE OF THE REACTION

The appropriate variables in this stage are the following:

$c_1 = \varepsilon\xi_1$ $\quad$ $c_4 = \varepsilon^3\xi_4$ $\quad$ $c_7 = \varepsilon^3\xi_7$

$c_2 = \varepsilon^{2.5}\xi_2$ $\quad$ $c_5 = \varepsilon^3\xi_5$ $\quad$ $c_8 = \varepsilon^3\xi_8$

$c_3 = \varepsilon^3\xi_3$ $\quad$ $c_6 = \varepsilon^{3.5}\xi_6$ $\quad$ $\tau = \varepsilon^3 t_1$

where ξ_i and τ are of order one in this stage.

The corresponding rate equations, in the limit $\varepsilon \to 0$ become:

$$\frac{d\xi_1}{d\tau} = 0 \qquad \frac{d\xi_4}{d\tau} = K_2\xi_1\xi_2 - K_3\xi_4 - \xi_4\xi_5 \qquad \frac{d\xi_7}{d\tau} = K_3\xi_4 + \xi_4\xi_5$$

$$\frac{d\xi_2}{d\tau} = 2K_1\xi_1 \qquad \frac{d\xi_5}{d\tau} = K_3\xi_4 - K_2\xi_1\xi_5 - \xi_4\xi_5 \qquad \frac{d\xi_8}{d\tau} = K_3\xi_4 + 2\xi_4\xi_5$$

$$\frac{d\xi_3}{d\tau} = K_2\xi_1\xi_2 + K_2\xi_1\xi_5 \qquad 0 = K_5\xi_4 - K_6\xi_1\xi_6$$

The initial conditions are substituded by the matching conditions with the previous stage.

The fact that the rate equation for NH reduces to

$$0 = K_5\xi_4 - K_6\xi_1\xi_6$$

indicates that this intermediate reaches the steady state already in this second stage of the reaction.

The solution of this set of equations with initial conditions given by the matching conditions with the precedent stage, can be reduced to the integration of the set of equations:

$$\frac{d\xi_4}{d\tau} = 2K_1K_2(\xi_1)_o\tau - K_3\xi_4 - \xi_4\xi_5$$

$$\frac{d\xi_5}{d\tau} = K_3\xi_4 - K_2(\xi_1)_o\xi_5 - \xi_4\xi_5$$

with the initial condition that, at $\tau = 0$ $\xi_4 = \xi_5 = 0$.

Although a detailed knowledge of the evolution of species in this stage, would require numerical integration of these equations, however the asymptotic solution for $\tau \to \infty$ gives enough

information so as to establish the matching conditions with the following stage.

It can be seen that when $\tau \to \infty$ the species behave in the following manner:

$$\xi_1 = (\xi_1)_o \qquad \xi_4 \longrightarrow \frac{K_1K_2}{K_3}(\xi_1)_o\tau \qquad \xi_7 \longrightarrow K_1K_2(\xi_1)_o^2\tau^2$$

$$\xi_2 \longrightarrow 2K_1(\xi_1)_o\tau \qquad \xi_5 \longrightarrow K_3 \qquad \xi_8 \longrightarrow \frac{3}{2}K_1K_2(\xi_1)_o^2\tau^2$$

$$\xi_3 \longrightarrow K_1K_2(\xi_1)_o^2\tau^2 \qquad \xi_6 \longrightarrow \frac{K_1K_2K_5}{K_6}(\xi_1)_o\tau$$

This asymptotic solution is not uniformly valid; it ceases to be valid when the species have grown enough as to invalidate the simplified kinetic scheme for this stage.

The kinetic scheme appropriate, at this stage,is

$$N_2H_4 + X \longrightarrow 2NH_2 + X$$

$$N_2H_4 + NH_2 \longrightarrow NH_3 + N_2H_3$$

$$N_2H_4 + H \longrightarrow NH_3 + NH_2$$

$$N_2H_3 + X \longrightarrow NH + NH_2 + X$$

$$N_2H_3 + X \longrightarrow N_2 + H_2 + H + X$$

$$N_2H_4 + NH \longrightarrow NH_2 + N_2H_3$$

$$N_2H_3 + H \longrightarrow N_2 + 2H_2$$

together with the steady state for NH.

V. THIRD STAGE OF THE REACTION

When the intermediate NH_2 has grown enough as to make the contribution of reaction 10) important, the second stage ceases to be valid and the evolution of the species are described by a different mechanism. The appropriate variables for this stage are, in this stage, the following:

$$c_1 = \varepsilon\xi_1 \qquad c_4 = \varepsilon^{2.5}\xi_4 \qquad c_7 = \varepsilon^2\xi_7$$

$$c_2 = \varepsilon^2\xi_2 \qquad c_5 = \varepsilon^3\xi_5 \qquad c_8 = \varepsilon^2\xi_8$$

$$c_3 = \varepsilon^2\xi_3 \qquad c_6 = \varepsilon^3\xi_6 \qquad \tau = \varepsilon^{3.5}t_1$$

The corresponding rate equations, in the limit $\varepsilon \to 0$, take in this stage, the following form:

$$\frac{d\xi_1}{d\tau} = 0$$

$$\frac{d\xi_2}{d\tau} = 2K_1\xi_1 - K_2\xi_1\xi_2 + K_5\xi_4 + K_6\xi_1\xi_6 - 2K_7\xi_2^2$$

$$\frac{d\xi_3}{d\tau} = K_2\xi_1\xi_2$$

$$0 = K_2\xi_1\xi_2 - K_3\xi_4 - K_5\xi_4 + K_6\xi_1\xi_6 - \xi_4\xi_5$$

$$0 = K_3\xi_4 - \xi_4\xi_5$$

$$0 = K_5\xi_4 - K_6\xi_1\xi_6$$

$$\frac{d\xi_7}{d\tau} = K_3\xi_4 + \xi_4\xi_5 \qquad \frac{d\xi_8}{d\tau} = K_3\xi_4 + 2\xi_4\xi_5$$

indicating that the kinetic scheme is, at this stage:

$$N_2H_4 + X \rightarrow 2NH_2 + X$$

$$N_2H_4 + NH_2 \rightarrow NH_3 + N_2H_3$$

$$N_2H_3 + X \rightarrow N_2 + H_2 + H + X$$

$$N_2H_3 + H \rightarrow N_2 + 2H_2$$

$$N_2H_3 + X \rightarrow NH + NH_2 + X$$

$$N_2H_4 + NH \rightarrow NH_2 + N_2H_2$$

$$2NH_2 \rightarrow N_2H_4$$

with the steady state condition for the intermediates N_2H_3 , H and NH . Replacing the initial conditions by the matching conditions with the precedent stage, the solution of this set of equations is:

$$\xi_1 = (\xi_1)_o \qquad \xi_2 = A+(A-B)/\{(B/A)\exp(\alpha\tau)-1\}$$

$$\xi_3 = K_2(\xi_1)_o\xi_2\tau + \frac{K_2(\xi_1)_o}{\alpha}(A-B)\,\mathrm{Ln}\,\frac{B - A\,\exp(-\alpha\tau)}{B - A}$$

$$\xi_4 = K_2(\xi_1)_o\xi_2/2K_3$$

$$\xi_5 = K_3$$

$$\xi_6 = K_2K_5\xi_2/2K_6$$

$$\xi_7 = \xi_3$$

$$\xi_8 = 3\xi_3/2$$

where:

$$A = \frac{(K_5-K_3)(\xi_1)_o + \sqrt{(K_5-K_3)^2K_2^2(\xi_1)_o^2 + 8K_1K_7K_3^2(\xi_1)_o}}{4K_3K_7}$$

$$B = \frac{(K_5-K_3)(\xi_1)_o - \sqrt{(K_5-K_3)^2K_2^2(\xi_1)_o^2 + 8K_1K_7K_3^2(\xi_1)_o}}{4K_3K_7}$$

$$\alpha = \frac{1}{K_3}\sqrt{(K_5-K_3)^2K_2^2(\xi_1)_o^2 + 8K_1K_7K_3^2(\xi_1)_o}$$

The asymptotic behavior of the solution, when $\tau \to \infty$ is the following:

$\xi_1 = (\xi_1)_o$ $\qquad$ $\xi_4 \to K_2A(\xi_1)_o/2K_3$ $\qquad$ $\xi_7 \to AK_2(\xi_1)_o\tau$

$\xi_2 \to A$ $\qquad$ $\xi_5 = K_3$ $\qquad$ $\xi_8 \to 3AK_2(\xi_1)_o/2$

$\xi_3 \to K_2(\xi_1)_oA\tau$ $\qquad$ $\xi_6 \to AK_2K_5/2K_6$

and it can be seen that this stage ends up when the concentration of the products reach values of the same order of magnitude as the initial concentration of gaseous hydrazine.

VI. FOURTH STAGE OF THE REACTION

The appropriate variables to study the evolution of the

reaction at this stage are:

$$c_1 = \varepsilon\xi_1 \qquad c_4 = \varepsilon^{2.5}\xi_4 \qquad c_7 = \varepsilon\xi_7$$

$$c_2 = \varepsilon^2\xi_2 \qquad c_5 = \varepsilon^3\xi_5 \qquad c_8 = \varepsilon\xi_8$$

$$c_3 = \varepsilon\xi_3 \qquad c_6 = \varepsilon^3\xi_6 \qquad \tau = \varepsilon^{4.5}t_1$$

and the rate equations, in the limit $\varepsilon \to 0$ become:

$$\frac{d\xi_1}{d\tau} = -K_1\xi_1 - K_2\xi_1\xi_2 - K_6\xi_1\xi_6 + K_7\xi_2^2$$

$$0 = 2K_1\xi_1 - K_2\xi_1\xi_2 + K_5\xi_4 + K_6\xi_1\xi_6 - 2K_7\xi_2^2$$

$$\frac{d\xi_3}{d\tau} = K_2\xi_1\xi_2$$

$$0 = K_2\xi_1\xi_2 - K_3\xi_4 - K_5\xi_4 + K_6\xi_1\xi_6 - \xi_4\xi_5$$

$$0 = K_3\xi_4 - \xi_4\xi_5$$

$$0 = K_5\xi_4 - K_6\xi_1\xi_6$$

$$\frac{d\xi_7}{d\tau} = K_3\xi_4 + \xi_4\xi_5$$

$$\frac{d\xi_8}{d\tau} = K_3\xi_4 + 2\xi_4\xi_5$$

indicating that the simplified kinetic scheme, at this stage,

hence for most of the reaction time,is the following:

$$N_2H_4 + X \longrightarrow 2NH_2 + X$$

$$N_2H_4 + NH_2 \longrightarrow NH_3 + N_2H_3$$

$$N_2H_3 + X \longrightarrow N_2 + H_2 + H + X$$

$$N_2H_3 + X \longrightarrow NH + NH_2 + X$$

$$N_2H_4 + NH \longrightarrow NH_2 + N_2H_3$$

$$2NH_2 \longrightarrow N_2H_4$$

$$N_2H_3 + H \longrightarrow N_2 + 2H_2$$

with the steady state condition for all the intermediates.

The overall stoichiometry of the reaction that results is

$$N_2H_4 \longrightarrow \frac{2}{3} NH_3 + \frac{2}{3} N_2 + H_2$$

The solution of the evolution of species, in this stage, can be more easily obtained by writing this set of equations in the following form:

$$\frac{d\xi_1}{d\tau} = -\frac{3}{2} K_2 \xi_1 \xi_2$$

$$0 = 2K_1\xi_1 - K_2\xi_1\xi_2 + 2K_5\xi_4 - 2K_7\xi_2^2$$

$$0 = K_2\xi_1\xi_2 - K_3\xi_4 - \xi_4\xi_5$$

$$\xi_5 = K_3$$

$$\xi_4 = \frac{K_2}{2K_3} \xi_1\xi_2$$

$$\frac{d\xi_3}{d\tau} = K_2\xi_1\xi_2$$

$$\frac{d\xi_7}{d\tau} = K_2\xi_1\xi_2$$

$$\frac{d\xi_8}{d\tau} = \frac{3}{2} K_2\xi_1\xi_2$$

whose solution, when one imposes the matching conditions with the third stage can be reduced to the solution of:

$$\frac{d\xi_1}{d\tau} = -\frac{3}{2} K_2\xi_1\xi_2 \qquad (4\text{-}1)$$

with

$$\frac{\xi_1}{2K_7\xi_2} = \frac{(\xi_1)_o}{2K_7A} \exp\left[\frac{K_1K_3}{K_2(K_5-K_3)} (3K_2\tau - 4/A)\right] \qquad (4\text{-}2)$$

where A is the same constant of the previous stage.

and

$$\xi_1 = \frac{2K_7\xi_2^2}{2K_1 - K_2\xi_2 + (K_2K_5/K_3)\xi_2} \qquad (4\text{-}3)$$

It is convenient to integrate this equation, to introduce the following parameters and variables:

$$E = \frac{K_2}{2K_1}\sqrt{\frac{K_1}{K_7}}\ \frac{K_5 - K_3}{K_3}$$

$$\xi_2 = \sqrt{\frac{K_1}{K_7}}\ \frac{1}{Ey}$$

$$\xi_1 = \frac{1}{E^2} \quad \frac{1}{y(y+1)} \;,\; \tau_1 = \frac{3}{2} K_2 \sqrt{\frac{K_1}{K_7}}\, \tau$$

so that the problem in these variables reduces to the solution of the equation:

$$\left(2 - \frac{1}{1+y}\right) dy = \frac{1}{E}\, d\tau_1$$

with the initital condition

$$\tau_1 = 0 \quad , \quad y_i = -\frac{1}{2} + \sqrt{\frac{1}{4} + \frac{1}{E^2 \xi_{10}}}$$

The solution is:

$$2(y-y_i) - \mathrm{Ln}\, \frac{1+y}{1+y_i} = \frac{\tau_1}{E}$$

with

$$\xi_1 = \frac{1}{E^2} \quad \frac{1}{y(1+y)}$$

and

$$\xi_2 = \sqrt{\frac{K_1}{K_7}} \quad \frac{1}{Ey}$$

It is important to realize that the temperature of the mixture enters in this solution through the parameters E, $\frac{K_1}{K_7}$ and y_i.

Fig.2 presents a plot of the evolution of hydrazine, ammonia, nitrogen and hydrogen as a function of time.

CONCLUSION

As shown in the course of the analysis, the homogeneous gas phase decomposition of hydrazine can be analyzed using perturbation techniques. The reaction can be visualized as composed of four stages with different kinetic mechanisms. However, inspection of the appropriate time scale for each of these stages indicates that the decomposition reaction spends most of the reaction time in the last of these stages, so that the complicated mechanisms of the reaction can be reduced, in a first approximation, to the overall reaction

$$N_2H_4 \longrightarrow \frac{2}{3} NH_3 + \frac{2}{3} N_2 + H_2$$

for the particular conditions of temperature and degree of dilution of the mixture here studied.

The calculated reaction rate is not a simple function of temperature and concentration, and can not be considered, except in a rough qualitative approximation to present a linear dependence with hydrazine concentration. Comparison with the experimental results of Eberstein and Glassman indicate a fairly good agreement for the absolute value of the rate constant. However, the theory predicts that the reaction is not first order so that, when one consider the reaction as a first order reaction, the rate constant will depend on the pressure; this could be an explanation of the scattering of the experimental results that can be observed in Fig.3 of ref.[10].

The disagreement between the predicted stoichiometry and the one observed experimentally by Eberstein and Glassman can be thought to derive from the fact that most of their experimental results were for temperatures of the mixtures around

950°K while, in this paper, the temperature of the mixture was centered in 1000°K.

REFERENCES

1. MURRAY, R.C. and HALL, A.R. : Trans.Faraday Soc 47, 743 (1951)

2. ADAMS, G.K. and STOCKS, G.W. : Fourth Symposium (International) on Combustion, p.239, Williams and Wilkins, 1953.

3. GRAY, P., LEE, J.C., LEACH, H.A., and TAYLOR, D.C. : Sixth Symposium (International) on Combustion, p.255, Reinhold, 1956.

4. GILBERT, M. and ALTMAN, D. : "Mechanism and Flame Speed for Hydrazine Decomposition" Progress Report 20-278, Jet Propulsion Lab., Pasadena, California, 1955.

5. DE JAEGERE, S. and VAN TIGGETEN, A. : Rev.Inst.Franc Petrolé. Ann. Combust. Liquides 12, (1958)

6. HALL, A.R. and WOLFHAND, H.G. : Trans. Foraday Soc. 52, 1520 (1956)

7. SZWARC, M. : Proc. Roy. Soc. (London) A 198, 267 1949.

8. RAMSAY, D.A. : J.Phys. Chem. 57, 415 (1953)

9. GILBERT, M. : "The Hydrazine Flame" Jet Propulsion

Lab. Report 20-318, Pasadena, California March 1957.

10. EBERSTEIN, I.J. and GLASSMAN, I. : Tenth Symposium (International) on Combustion p.365, The Combustion Institute 1965.

- - - - - - - - -

LIST OF FIGURE CAPTIONS

Fig.1.- Rate constants as function of temperature.

Fig.2.- Evolution of hydrazine, ammonia, nitrogen and hydrogen as function of time.

FIG. Nº 1

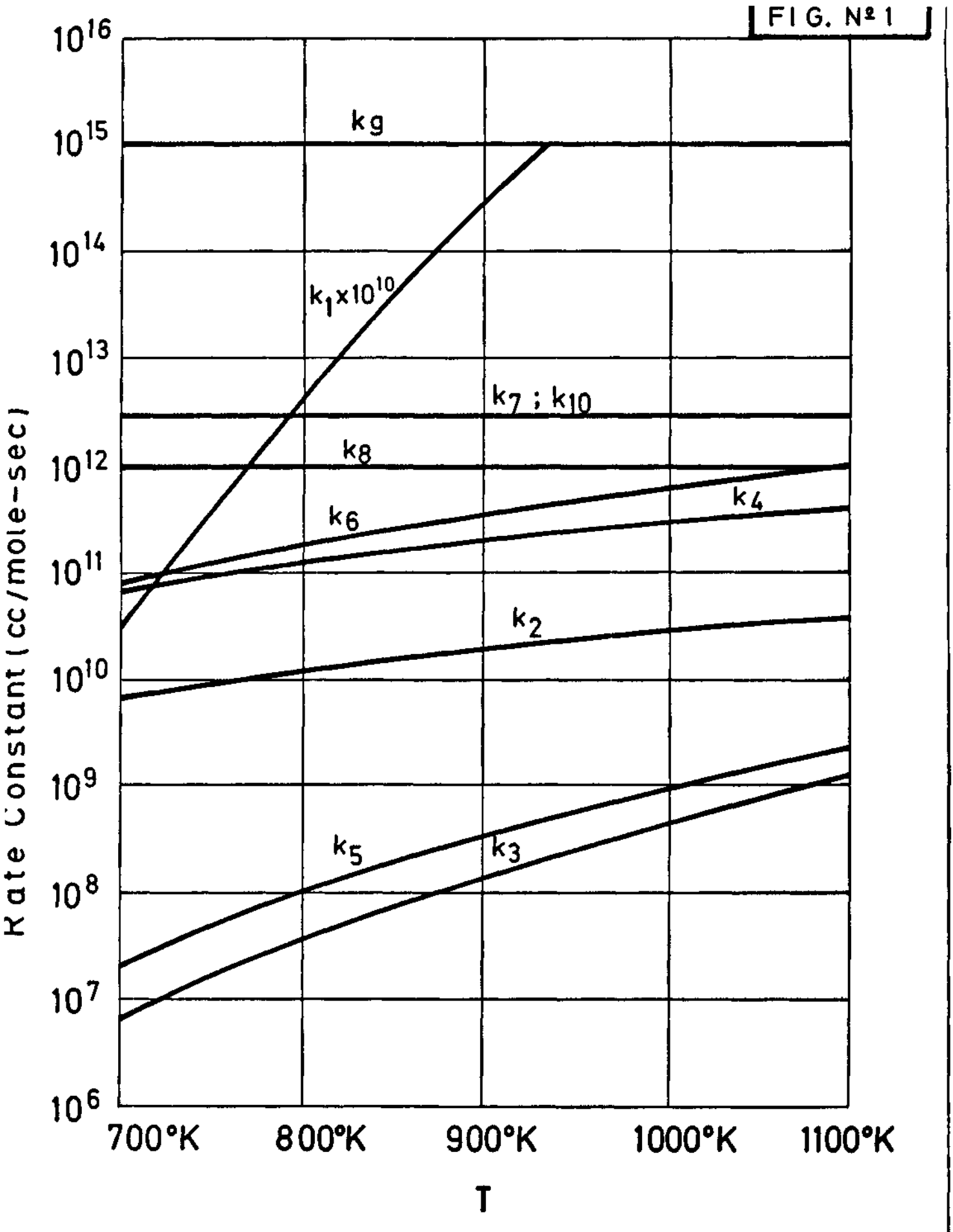
Rate Constant (cc/mole-sec)
10^{16}
10^{15}
10^{14}
10^{13}
10^{12}
10^{11}
10^{10}
10^{9}
10^{8}
10^{7}
10^{6}
k_g
$k_1 \times 10^{10}$
$k_7 ; k_{10}$
k_8
k_6
k_4
k_2
k_5
k_3
700°K
800°K
900°K
1000°K
1100°K
T

FIG. Nº 2

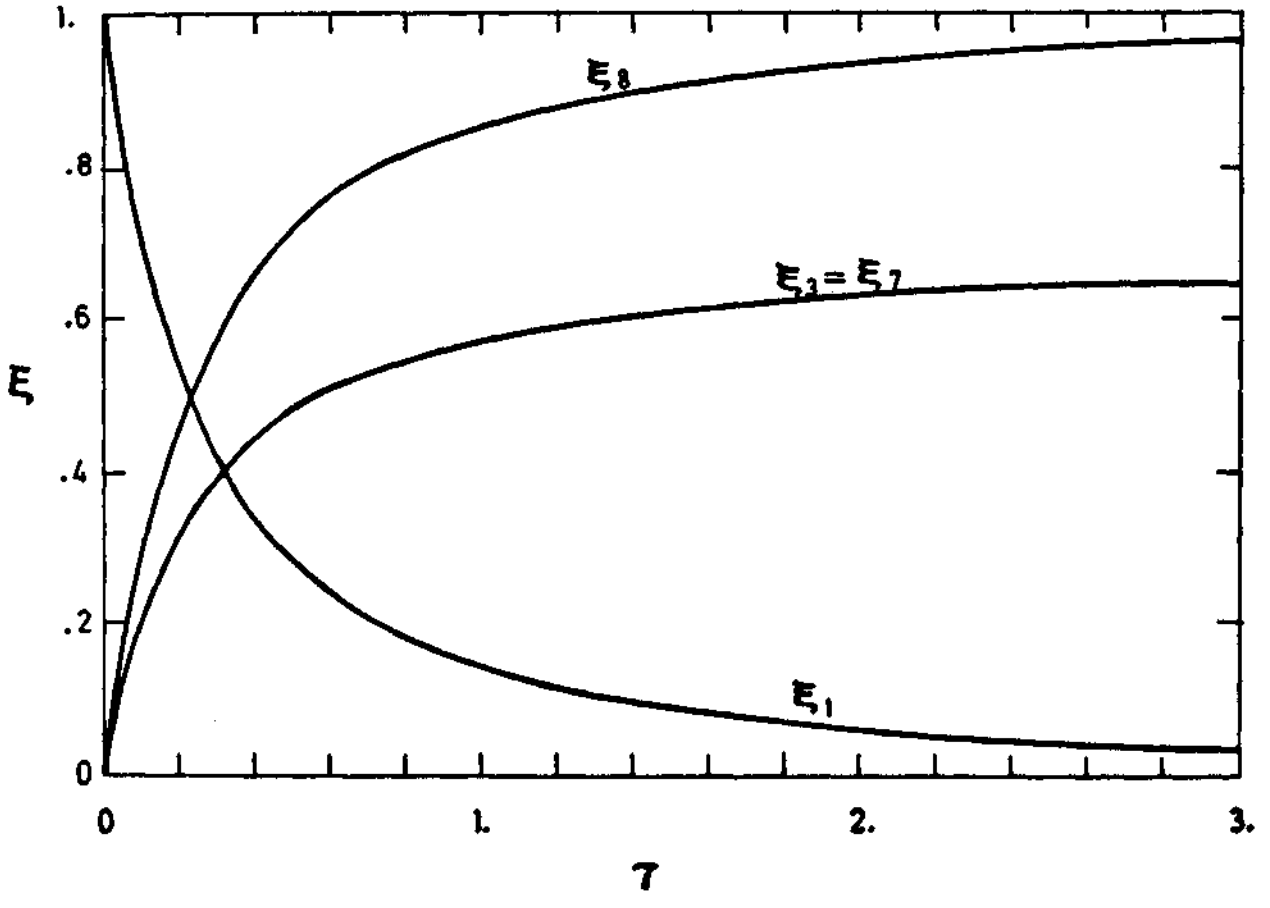

PART III

STEADY HEAT AND MASS TRANSFER IN POROUS CATALYST PARTICLES

Authors J.L. Urrutia
A. Liñán

LIST OF SYMBOLS

a = particle radius

b = frequency factor

c = molar concentration

D = effective diffusion coefficient

H = molar heat of reaction

K = effective heat conduction coefficient

$\dot{N}$ = rate of mole consumption per particle

P = nondimensional gradient defined in (B3)

p = pressure

r = radial distance

T = temperature

u = variable defined in (A2)

x = nondimensional parameter defined in (9)

y = " " " (9)

α = parameter defined in (36)

β = " " " (7)

Γ = Euler Gamma function

γ = nondimensional activation energy

Δ = reduced Damköhler number

δ = parameter defined in (34)

η = effectiveness factor

θ = parameter defined in (36)

ν = modified Nusselt number

σ = modified Sherwood number

ϕ_s = Thiele modulus

ψ = variable defined in (54)

ω = function defined in (34)

Subscripts

a = activation

s = surface

- - - - - - - -

STEADY HEAT AND MASS TRANSFER IN POROUS CATALYST PARTICLES

- - - - - - - -

I. *INTRODUCTION AND FORMULATION*

In catalytic packed bed reactors the reaction chamber is filled with porous particles, which present a large internal surface with active sites where chemical reactions between reactive species take place after being absorbed at the surface.

Because of the consumption of reacting species within the catalytic particles, differences in concentration of these species appear within the particle to provide the driving force for the species to diffuse from the outer surface toward the interior. Similarly, the mean concentration of the reactive species in the interstitial fluid surrounding the particle differs from the concentration at the particle surface,so that transfer of reactants between the interstitial fluid and the catalytic particles occurs.

Thus, the reacting mixture, flowing along the chamber through the interstices, looses reactive species, which by diffusion enter the catalytic particles, and incorporates the reaction products coming out of the particles. If the reaction is exothermic, the heat evolved in the reaction will, under steady state conditions, leave the interior of the particle by heat conduction

to increase the thermal energy of the interstitial fluid. The temperature and composition of the interstitial fluid will change as it flows along the chamber, as a result of the sinks of reactants and sources of heat and products provided by the catalytic particles. See Petersen (1965), Aris (1965) and Aris (1969).

In this paper we shall show how asymptotic methods can be used to calculate the distributions of temperature and concentration within a spherical catalytic particle under steady state conditions. We shall analyze the case when a chemical decomposition reaction of a species takes place within the particle. This reaction is considered to be one-step irreversible, with a mole consumption rate per unit volume, given by the following Arrhenius expression

$$\dot{n} = bc^n \exp(-T_a/T) \qquad (1)$$

in terms of the local molar concentration c of the reactant species and the local temperature T. In (1), b is a pre-exponential factor, proportional to the internal surface area,per unit volume, of the catalytic particle, n is the reaction order and T_a is the activation temperature of the reaction. The energy absortion rate, per unit volume, due to the chemical reaction is $H\dot{n}$ where H is the molar heat of reaction, negative for exothermic reactions.

We shall assume that the temperature and composition of

the interstitial fluid surrounding the particle is uniform; so that we can use the assumption of spherical symmetry, and describe the concentration and temperature distributions within the particle in terms of the functions c(r) and T(r) of the radial distance r from the center of the particle.

These functions satisfy the equations of species and energy conservation, which can be solved for given surface values, c_s and T_s, of c and T to yield, in particular, the reactant and energy input to the particle from the interstitial fluid.

The conservation equations for mass and energy, under quasi-steady conditions reduce, see Peterson (1965) and Aris (1965)

$$D\left(\frac{d^2c}{dr^2} + \frac{2}{r}\frac{dc}{dr}\right) = \dot{n} \qquad (2)$$

$$K\left(\frac{d^2T}{dr^2} + \frac{2}{r}\frac{dT}{dr}\right) = H\dot{n} \qquad (3)$$

showing how the chemical production term is balanced by diffusion and heat conduction. D and K are the effective diffusion and heat conduction coefficients, which we assume to be constant.

These equations are to be solved with the boundary conditions

$$r = a \; : \; c = c_s \; , \; T = T_s \qquad (4)$$

$$r = 0 \; : \; dc/dr = dT/dr = 0 \qquad (5)$$

where a is the particle radius.

The effects on the decomposition rate of the shape of the particles and of non-uniformities of the external distributions of concentration and temperature can be found in the literature. See for example Bischoff (1968), Volkman and Kehat (1969), Rester and Aris (1969) and Hlaváček and Kubíček (1970).

From Eqs.(1)-(4), we obtain the relation

$$(T - T_s)/T_s = \beta(1-c/c_s) \ , \tag{6}$$

named after Pratter, between the temperature and concentration. The parameter β is the maximum possible increment in temperature, relative to the surface temperature, obtained when $c = 0$,

$$\beta = -c_s HD/KT_s \tag{7}$$

The reaction rate expression (1) and the linear relation (6) can be used together with Eq.(2) to provide a differential equation, which we shall write below in non-dimensional form as

$$\frac{d^2y}{dx^2} + \frac{2}{x}\frac{dy}{dx} = \phi_s^2 y^n \exp\frac{\gamma\beta(1-y)}{1+\beta(1-y)} \tag{8}$$

in terms of the nondimensional variables

$$y = c/c_s \quad , \quad x = r/a \tag{9}$$

and the parameters β and

$$\gamma = T_a/T_s \quad ,, \quad \phi_s^2 = (a^2/D)be^{-T_a/T_s}c_s^{n-1} \tag{10}$$

The parameter γ is the nondimensional activation energy of the reaction, and ϕ_s^2 , the squared Thiele modulus,is the ratio of the characteristic diffusion and reaction times. The ratio ϕ_s is named after Thiele (1939) in the Chemical Engineering literature, while in the Combustion literature ϕ_s^2 is named after Damköhler (1936).

Eq (8) is to be solved with the boundary conditions

$$dy/dx = 0 \quad \text{at} \quad x = 0 \tag{11}$$

and

$$y = 1 \quad \text{at} \quad x = 1 \tag{12}$$

As part of the solution we shall obtain the value of dy/dx at x = 1, which when multiplied by $4\pi aDc_s$ gives the rate of mole consumption per particle $\dot{N}$. We shall write $\dot{N}$ as

$$\dot{N} = 4\pi aDc_s\left(\frac{dy}{dx}\right)_1 = \eta bc_s^n e^{-T_a/T_s}\, 4\pi a^3/3 \tag{13}$$

the product of the effectiveness factor η , introduced by Thiele (1939), times the rate of mole consumption per particle that we would have in the absence of internal diffusional resistance; that is, when $c = c_s$ everywhere in the interior of the particle. The relation (13) can be written as

$$\eta = 3\phi_s^{-2}(dy/dx)_{x=1} \tag{14}$$

The parameter

$$\Phi = \eta\phi_s^2 = 3(dy/dx)_{x=1} \qquad (15)$$

the "observable" reaction rate per unit volume, made nondimensional by dividing by $c_s D/a^2$, is a direct measure of the decomposition rate per particle

$$\dot{N} = \Phi 4\pi a D c_s/3 \qquad (16)$$

It was introduced by Weisz to generate a criterium, $\Phi < 1$, in terms of observable quantities to insure that there is no falsification of kinetic effects due to internal diffusion resistance. See Weisz and Hicks (1962).

The problem of solving Eq.(8), with the boundary conditions (11) and (12) has received considerable attention in the literature. For the work in the Chemical Engineering literature, see for example the reviews by Satterfield and Sherwood (1963), Petersen (1965), Aris (1969) and Satterfield (1970). For the work related with the Combustion or Thermal Explosion literature see Gray and Lee (1967) and Frank-Kamenetskii (1969).

Weisz and Hicks (1962) published the results of numerical integrations of Eq.(1) in the form of curves giving the effectiveness factor η in terms of the Thiele modulus ϕ_s , for first order reactions and some representative values of the parameters β and γ . The numerical integrations by Weisz and Hicks have shown the existence of multiple solutions within a range of Thiele numbers; the solution is unique for small and large values of the Thiele

number..

The problem of existence and uniqueness of the solution has received considerable attention. See, for example, Gavalas (1968), Hlaváček et al. (1968), Luss (1969), and Copelowitz and Aris (1970).

We shall devote this analysis to the solution of Eq.(8) for large values of γ . We shall try to obtain, if possible, closed form expressions for the effectiveness factor η , or the parameter Φ , in terms of γ , β , ϕ_s and n. Very often γ is large enough, from 10 to 50, so that an asymptotic analysis for large γ is well justified. See Satterfield (1970) for the range of values of these parameters of interest in chemical reactors and how they depend on the phisicochemical characteristics of the catalytic particles.

We shall begin with the analysis in Section II of the cases for which $\gamma\beta$ is of order unity to recover, in particular, the results of Tinkler and Metzner (1961). Then we shall proceed to the analysis for large $\gamma|\beta|$, first for endothermic reactions in Section III, and then for exothermic reactions in the ignition regime, Section IV, and in the thin reaction zone regime, Section V.

We shall consider in Appendix C how the external resistance effects could be taken into account.

II. *ENDOTHERMIC AND EXOTHERMIC REACTIONS WITH SMALL OR MODERATE HEAT EFFECTS*

We shall in this section look for the solution of Eq (8) for values of the heat release parameter β very small compared with unity, so that the particle is nearly isothermal. We shall include in the analysis the cases with an activation energy γ large enough that $\gamma\beta = \beta_1$ is of order unity, and, thus, the non-isothermal effects are important.

We shall write the solution of Eq.(8) in the form of a power series expansion in powers of β for fixed values of x, ϕ_s^2, β_1 and n

$$y = y_o + \beta y_1 + \text{---} \tag{17}$$

When this expansion is substituted in Eqs.(8-10), the following equation is obtained for y_o ,

$$\frac{d^2y_o}{dx^2} + \frac{2}{x}\frac{dy_o}{dx} = \phi_s^2 e^{\beta_1 y_o} y_o^n e^{-\beta_1 y_o} \tag{18}$$

with the boundary conditions *

$$dy_o/dx = 0 \quad \text{at} \quad x = 0 \tag{19}$$

$$y_o = 1 \quad \text{at} \quad x = 1 \tag{20}$$

The effectiveness factor η , and Φ , are given, with errors of order β , in terms of $y_o(x)$ by

$$\Phi = \eta\phi_s^2 = 3(dy_o/dx)_{x=1} \tag{21}$$

Thus Φ is, for a given reaction order n, a function of ϕ_s^2 and β_1.

* For values of $n < 1$, and sufficiently large ϕ_s the reactant does not penetrate beyond a certain radius x_s ; $y = 0$ for $x < x_s$.

Eq (18) was obtained, and solved using an analog computer, by Tinkler and Metzner (1961) for the case n = 1. Fig.1 and Fig.2 show the utilization factor η and Φ as a function of ϕ_s for several values of $\beta_1 = \gamma\beta$. Multiplicity of solutions occur for values of $\gamma\beta > 4.5$. Very often the particles present a large internal resistance to the diffusional transport of mass, but very small resistance to heat conduction, so that γβ is very small. Thus we shall give below the form of the utilization or effectiveness factor η for small values of γβ .

Eq (8) in the particular case n = 1, β = 0, or Eq (18) for $\beta_1 = 0$, has the solution

$$y = (x\,\mathrm{sh}\phi_s)^{-1}\,\mathrm{sh}(\phi_s x) \tag{22}$$

satisfying the boundary conditions (11) and (12).

The corresponding expression for the utilization factor η is

$$\eta = 3\phi_s^{-2}(\phi_s\,\mathrm{cth}\phi_s - 1) \tag{23a}$$

or

$$\Phi = 3(\phi_s\,\mathrm{cth}\phi_s - 1) \tag{23b}$$

a well known result in the Chemical Engineering literature.

We shall show in Appendix A, that for small values of γβ, and n = 1

$$\Phi/3 = \eta\phi_s^2/3 = p_o(\phi_s^2) + \gamma\beta p_1(\phi_s^2) + \ldots \tag{24}$$

where

$$p_o(u) = \sqrt{u}\,\mathrm{cth}\sqrt{u} - 1$$

$$p_1(u) = -(p_o + p_o^2 - u)/2 - \frac{1}{2\sqrt{u}}\left(\frac{\sqrt{u}}{\mathrm{sh}\sqrt{u}}\right)^3 \int_o^u \sqrt{x}\left(\frac{\mathrm{sh}\sqrt{x}}{\sqrt{x}}\right)^3 dx$$

The functions p_o and g of ϕ_s are plotted in Fig.3.

In Appendix B the first two terms of an asymptotic expansion of η for large values of ϕ_s are obtained, from (Eq 18) for $n = 1$, as

$$\eta = \frac{3\sqrt{2}}{\gamma\beta\phi_s}\,(e^{\gamma\beta} - 1 - \gamma\beta)^{1/2}\left[1 - \frac{\sqrt{2}\,\exp(\gamma\beta/2)\,I}{\phi_s\{\exp(\gamma\beta) - 1 - \gamma\beta\}}\right] \qquad (25)$$

where $I = \int_o^{\gamma\beta} \{1 - (1+u)\exp(-u)\}^{1/2} du$

In this case the decomposition reaction occurs in a thin surface layer. Fig.4 shows $\eta\phi_s$ as a function of $\gamma\beta$, as given by the first term of the expansion (25). The one term and two term expansions of η for large values of ϕ_s are also shown in Fig. 1 and 2.

For the cases $\beta = 0$ and $n \neq 1$ see for example Volkman and Kehat (1969) or the review by Satterfield (1970). We obtain in Appendix A expansions, for arbitrary n and small and large values of ϕ_s, of the nondimensional "observable" reaction rate Φ.

Thus, for large values of ϕ_s, the reaction, occurs in a

thin surface layer, with

$$\Phi = 3\phi_s\sqrt{2/(n+1)} - 3\{1 + (n-1)/4\}^{-1} + \text{---} \qquad (26)$$

For small values of ϕ_s , no falsification of the kinetics occurs in first approximation, because the reactant concentration is approximately equal to c_s , and

$$\Phi = \phi_s^2\{1 - \phi_s^2 n/15 + \phi_s^4 n(3n-1)/315 + \text{---}\} \qquad (27)$$

For zero order reactions, Eq (18) reduces to

$$\frac{d^2y_o}{dx^2} + \frac{2}{x}\frac{dy_o}{dx} = \phi_s^2 e^{\beta_1(1-y_o)} \qquad (28)$$

to be solved with the boundary conditions (19) and (20).*

It can be written in the form

$$\frac{d^2\theta}{dx^2} + \frac{2}{x}\frac{d\theta}{dx} = -\delta e^{\theta} \qquad (29)$$

and the boundary conditions

$$d\theta/dx = 0 \quad \text{at} \quad x = 0 \qquad (30)$$

$$\theta = 0 \quad \text{at} \quad x = 1 \qquad (31)$$

in terms of the non-dimensional temperature increment

$$\theta = \beta_1(1-y_o) = (T-T_s)T_a/T_s^2 \qquad (32)$$

* Negative values of y_o can appear in the solution, unless the chemical production term is written equal to zero for $y_o \leq 0$. This limits the range of validity in ϕ_s , of the solution.

and the reduced Damköhler number

$$\delta = \phi_s^2 \gamma\beta \tag{33}$$

The problem of Eqs (29)-(31) is encountered also in connection with Astrophysical problems, see Chandrasekhar (1939), the thermal failure of dielectrics, see Von Karman (1924), and in thermal explosion problems, see Frank-Kamenetskii (1969). We shall also encounter Eq (29) in the following two sections, when analyzing the catalytic particle behaviour for large values of γ , and $-\beta$ of order unity or β of order unity in the near ignition regime. A numerical solution of Eq (29) was first given by Emden (1907).

For a literature review concerning this equation and approximate treatments, see Hlaváček and Marek (1968).

From the solution of Eq (29) we can obtain, in particular the non-dimensional particle reaction rate Φ as a function of δ given by

$$\gamma\beta\Phi = \eta\delta = \omega = -3(d\theta/dx)_{x=1} \tag{34}$$

where ω is a function of the parameter δ .

Enig (1966) was able to generate from Eqs (29)-(31) the following differential equation

$$d\omega/d\delta = (9\delta - 3\omega)/\delta(6-\omega) \tag{35}$$

which, when solved with the initial condition $\omega = 0$ for $\delta = 0$,

yields the non-dimensional particle reaction rate ω as a function of δ . For exothermic reactions $\delta > 0$ and $\omega > 0$; for endothermic reactions both ω and δ are negative.

We can obtain Eq (35) directly from Eq (29), if we notice that Eq (29) is invariant under the transformation group

$$\theta \to \theta + \alpha \quad , \quad x \to e^{-\alpha/2} x \tag{36}$$

Eq (29) will now be written in terms of the variables

$$p = -3x \frac{d\theta}{dx} \quad \text{and} \quad u = \delta x^2 e^{\theta} \quad , \tag{37}$$

chosen so that they are invariant under the same transformation group (36) and, in addition, $p = \omega$ and $u = \delta$ at $x = 1$.

From the definition of u and p we first obtain

$$du/dx = (2-p/3)u/x$$

and then we easily obtain from Eq (29) the equation

$$dp/du = (9u-3p)/u(6-p) \tag{38}$$

which, when integrated with the initial condition $p = 0$ at $u = 0$, obtained from Eq (30), it yield, $p = p(u)$. When the integration is carried out to $x = 1$, when $u = \delta$, we obtain $p = \omega$. Thus, as we wanted tc show, $p = p(u)$ is identical to $\omega = \omega(\delta)$.

Fig.5, gives both η and ω as functions of δ for exothermic reactions. Fig 6 gives η and $-\omega$ as a function of $-\delta$ for endo-

thermic reaction. Figs.5 and 6 show also $\theta(0)$ in terms of δ.

No solution of Eq (35), or Eq (29), exists for $\delta > \delta_I = 3.322$. At $\delta = \delta_I$, $\omega = \omega_I = 6$. The solution of Eq (35) spirals around the critical point $\omega = 6$, $\delta = 2$. For δ close to 2, Eq (29) has a large number of solutions growing to infinity when $\delta \to 2$. Only the lower branch of the curve $\omega(\delta)$ may be expected to be stable.

For small values of ω

$$\delta = \omega - \omega^2/15 - \omega^3/1575 + \text{---} \qquad (39)$$

For endothermic reactions, a solution of Eq (35) exists for all values of δ , and it is unique. An approximate representation of the relation between δ and ω is given for negative δ by

$$\delta = \omega(1-\omega/10+\omega^2/540)(1-\omega/30)^{-1} \qquad (40)$$

III. *ENDOTHERMIC REACTIONS WITH LARGE HEAT EFFECTS*

We shall look in this section for the solution of Eq (8) for large values of γ and β negative of order unity, so that $-\gamma\beta >> 1$.

In these cases the concentration differences are small, $(1-y) << 1$, within the particles; otherwise, the negative Arrhenius exponent in Eq (8) would become very large and, consequently, the chemical reaction would be freezed. The non-dimensional tem-

perature rise θ , defined in Eq (32) of the previous section, stays of order unity.

We shall write the solution of Eq (8) in the form of a power expansion

$$y = 1 - \theta/\gamma\beta - \theta_1/(\gamma\beta)^2 + \text{---} \qquad (41)$$

When it is substituted in Eqs (8), (11) and (12) we obtain Eqs. (29)-(31) for θ , independently of the reaction order. Eq (29) is obtained directly from Eq (8) if the Arrhenius exponent is linearized, following Frank-Kamenetskii, because $\gamma >> 1$, and if the reactant consumption is neglected, because $-\gamma\beta >> 1$. Thus the following approximation

$$\phi_s^2 y^n \exp \frac{\gamma\beta(1-y)}{1+\gamma\beta(1-y)/\gamma} \approx \phi_s^2 \exp\{\gamma\beta(1-y)\} \qquad (42)$$

is made in the chemical consumption term of Eq (8).

The results obtained in the previous section, when analizing endothermic zero order reactions for large activation energies, are thus directly applicable to the present case. In particular, the non-dimensional particle decomposition rate, $\Phi = \omega/\gamma\beta$, and the utilization factor, $\eta = \omega/\delta$, are given in terms of the reduced Damköhler number, $\delta = \phi_s^2\gamma\beta$, by means of the solution $\omega(\delta)$ of Eq (35) for negative δ . The functions $\phi/\gamma\beta$ and η of δ have been plotted in Fig.6. As indicated in the previous section, an accurate representation of $\delta(\omega)$, with the correct asymptotic behaviour

for small ($-\delta$) and for large ($-\delta$), is given by Eq (40).

The effect of the reactant consumption, can be easily taken into account in first approximation by introducing in the right hand side of Eq (42) and of Eq (29) the factor $\exp(-n\theta/\gamma\beta)$, which is an approximate representation of $y^n \simeq (1 - \theta/\gamma\beta)^n$ for small values of $n\theta/\gamma\beta$. This is equivalent to a modification of the activation energy from $\gamma\beta$ to $\gamma\beta(1-n/\gamma\beta)$.

Thus, when the effects of reactant consumption are retained in first approximation, the particle reaction rate and the utilization factor are given by the relations

$$\left(1- n/\gamma\beta\right)\gamma\beta\Phi \simeq \eta\delta_e = \omega(\delta_e) \qquad (43)$$

where $\delta_e = \phi_s^2\gamma\beta(1-n/\gamma\beta)$.

IV. *EXOTHERMIC REACTIONS. IGNITION REGIME*

For exothermic reactions with large temperature effects $\gamma\beta >> 1$, very small changes in the reactant concentration cause large changes in the reaction rate. In this section will shall look for the asymptotic solution of Eq (8) for large values of $\gamma\beta$, for values of the Thiele modulus such that $(1-y)$ is of order $1/\gamma\beta$.

We find under these conditions two types of solutions for each Thiele modulus below a critical "ignition" value. In one

of the solutions the particle decomposition rate, or ω , is small because the temperature rise has been small in the interior of the particle. In the other solutions ω is larger because the temperature rise in the interior of the particle has been significant.

We shall use in analyzing this "ignition" regime of decomposition the expansion (41) for y, which when substituted in Eqs (8), (11) and (12) yields, as in the previous section, Eqs (29)-(31) for θ , independently of the reaction order.

The particle consumption rate Φ and the utilization factor η are given by Eq (34), where ω is obtained as a function of δ by solving Eq (35) for positive δ . The functions $\eta(\delta)$ and $\omega(\delta)$ are represented in Fig.5. They are seen to be multivalued for $\delta < \delta_c = 3.322$.

The effects of reactant consumption can be taken into account in first approximation, as in the previous section. The particle decomposition rate Φ and utilization factor η are then given by Eq (43) with relative errors of order $1/\gamma$.

Notice that solutions corresponding to the ignition regime exist only for

$$\phi_s^2 \gamma\beta(1-n/\gamma\beta) < 3.322 \qquad (44)$$

If higher order corrections to the solution were desired, the asymptotic problem should be posed as to find the solution of

Eq (8) and the Thiele modulus resulting in a given value of ω of order unity. The expansion (41) should be complemented with an expansion

$$\delta = \delta_o + \delta_1/\gamma\beta + \text{---} \tag{45}$$

for the Thiele modulus. In this way the difficulties associated with the fact that the interval of multiplicity of solutions of Eq (8) would change with the order of approximation is eliminated.

See Copelowitz and Aris (1970) for a numerical analysis of Eq (8) under ignition conditions and a discussion of the multiplicity of solutions.

V. *EXOTHERMIC REACTIONS. THIN REACTION ZONE REGIME*

For large values of the nondimensional activation energy, $\gamma\beta \gg 1$, there exists a regime of decomposition for which, as sketched in Fig 7, a thin reaction zone separates an interior region of equilibrium, for $x < x_r$, with

$$y = 0 \quad \text{and} \quad \theta/\gamma = (T-T_s)/T_s = \beta \tag{46}$$

from an outer region where the chemical reaction is frozen. In the outer region, $x > x_r$, where the reaction term in the right hand side of Eq (8) is negligible, the distribution of concentration is determined by the diffusion equation

$$\frac{d^2y}{dx^2} + \frac{2}{x}\frac{dy}{dx} = 0 \tag{47}$$

A first integral yields

$$x^2 dy/dx = \Phi/3 \qquad (48)$$

in terms of the particle decomposition rate Φ , defined in Eq (15). When Eq (48) is integrated with the boundary condition (12), we obtain, for $x > x_r$,

$$y = 1 + (1-1/x)\Phi/3 \qquad (49)$$

The temperature distribution is obtained from the Pratter relation (6), $\theta = \gamma\beta(1-y)$.

The distributions of temperature and concentration are sketched in Fig.7.

The continuity of y and θ at the reaction zone, $x = x_r$, provides the relation

$$x_r = \Phi/(\Phi+3) \qquad (50)$$

between x_r and the observed particle decomposition rate Φ .

To obtain a relation between Φ and the Thiele modulus, we need to analyze the structure of the thin reaction zone, following the procedure used by Liñan (1974) in his analysis of the structure of diffusion flames.

The reaction zone is thin because, due to the large temperature sensitivity of the reaction rate, the chemical reaction is freezed as soon as the temperature drops below its maximum value, $T_m = T_s(1+\beta)$, by an amount large compared with T_m^2/T_a . This can

be clearly shown by writing the Arrhenius factor $\exp(-T_a/T)$ in the form

$$e^{-T_a/T} = e^{-T_a/T_m}\, e^{(T_a/T_m)(T-T_m)/T}$$

The Arrhenius factor, for large values of T_a/T_m, becomes exponentially small compared with its maximum value, obtained in the interior edge of the reaction zone, unless the negative exponent $(T_a/T_m)(T-T_m)/T$ stays of order unity. Through the reaction zone the nondimensional temperature drop

$$(T_m-T)T_a/T_m^2 = \psi = y\gamma\beta/(1+\beta)^2 \qquad (51)$$

is of order unity. The thickness of the reaction zone δ_r is small, of order T_m/T_a, so that the gradient of temperature in the reaction zone, of order $T_m^2/T_a\delta_r$, is of the order of the temperature gradient in the outer frozen region, $(T_m-T_s)/(1-x_r)$.

Thus, for values of x_r and β of order unity, the orders of magnitude y_r of y in the reaction region and the thickness δ_r are of order $(1+\beta)^2/\gamma\beta$. The orders of magnitude of the three terms of Eq (8) are given by

$$d^2y/dx^2 \sim y_r/\delta_r^2 \sim \gamma\beta/(1+\beta)^2$$

$$(2/x)dy/dx \sim y_r/\delta_r \sim 1$$

and

$$\phi_s^2 y^n \exp\frac{\gamma\beta(1-y)}{1+\beta(1-y)} \sim \phi_s^2\gamma^{-n}\exp\frac{\gamma\beta}{1+\beta}$$

In the thin reaction zone, the term $(2/x)dy/dx$ representing

the effects of the spherical geometry can be neglected, with relative errors of order $1/\gamma\beta$, compared with the one-dimensional diffusion term d^2y/dx^2, which is thus balanced by the reaction term. Thus in the thin reaction zone regime, the reduced Damköhler number Δ ,

$$\Delta = \phi_s^2\{(1+\beta)^2/\gamma\beta\}^{n+1}\exp\{\gamma\beta/(1+\beta)\} \qquad (52)$$

is of order unity. We shall obtain below, from the detailed analysis of the reaction zone structure, the asymptotic form of the relation $\Delta = \Delta(\phi)$ for large values of $\beta\gamma$.

In the thin reaction zone, as the order of magnitude analysis given above indicated, the diffusion operator in the left hand side of Eq (8) can in first approximation be replaced by the one-dimensional term d^2y/dx^2. The Arrhenius exponent in Eq (8) can be linearized around its value at $y = 0$. Thus, for large values of $\gamma\beta$ the conservation Eq (8), reduces in the reaction zone to

$$\frac{d^2y}{dx^2} = \phi_s^2 y^n \exp\frac{\gamma\beta}{1+\beta}\exp\frac{-\gamma\beta y}{(1+\beta)^2} \qquad (53)$$

or, if written in terms of the variables

$$\psi = \gamma\beta y/(1+\beta)^2 \quad \text{and} \quad \xi = (x-x_r)\gamma\beta/(1+\beta)^2 , \qquad (54)$$

$$\frac{d^2\psi}{d\xi^2} = \Delta\psi^n\exp(-\psi) \qquad (55)$$

Eq (55) can be integrated once to yield

$$\frac{1}{2}\left(\frac{d\psi}{d\xi}\right)^2 = \Delta\int_0^{\psi} z^n e^{-z} dz \qquad (56)$$

if we require the solution to coincide for large negative values of β with the solution, Eq (46), for the interior equilibrium region. That is,

$$\psi \to 0 \qquad \text{for} \qquad \xi \to -\infty \qquad (57)$$

which implies $d\psi/d\xi = 0$ for $\psi = 0$.

By requiring that the solution of Eq (56) should also coincide for $\xi \to \infty$ with the form for $(x-x_r) \to 0$ of the solution (49), we obtain

$$(d\psi/d\xi)_{\xi\to\infty} = \Phi/3x_r^2 = (\Phi+3)^2/3\Phi \qquad (58)$$

which together with Eq (56) leads to the relation

$$(\Phi+3)^2/3\Phi = (2\Delta\Gamma_{n+1})^{1/2} \qquad (59)$$

where Γ_{n+1} is the Euler Gamma function

$$\Gamma_{n+1} = \int_0^{\infty} z^n e^{-z} dz$$

The right hand side of Eq (59) is proportional to the Thiele modulus

$$\sqrt{2\Delta\Gamma_{n+1}} = 2\alpha\phi_s \qquad (60)$$

where

$$\alpha = \sqrt{\Gamma_{n+1}/2}\,\{(1+\beta)^2/\gamma\beta\}^{(n+1)/2}\exp\{\gamma\beta/2(1+\beta)\} \qquad (61)$$

So that Eq (59) is an explicit function of the Thiele modulus in terms of the non-dimensional particle reaction rate. Eq (59) can also be written as

$$\Phi = \eta\phi_s^2 = 3(\alpha\phi_s-1)\{1 \pm \sqrt{1-(\alpha\phi_s-1)^{-2}}\} \qquad (62)$$

giving Φ explicitely in terms of $\alpha\phi_s$

The two-valued functions Φ and η/α^2 of $\alpha\phi_s$ have been plotted in Fig.8. The thin reaction zone solution exists only for values of ϕ_s above a minimum "extinction" value ϕ_{SE} given by the relation

$$\phi_{SE} = 2/\alpha = \sqrt{8/\Gamma_{n+1}}\{\gamma\beta/(1+\beta)^2\}^{(n+1)/2}\exp\{-\gamma\beta/2(1+\beta)\} \qquad (63)$$

The lower branch of the curves giving Φ and η/α^2 as functions of $\alpha\phi_s$, represented with dashed lines in Fig.8, are very likely unstable. When $\alpha\phi_s \sim \gamma\beta$, the values of x_r and δ_r are of the same order for the lower branch, so that the one-dimensional treatment, Eq (53), of the reaction zone is no longer valid.

For large values of $\alpha\phi_s$, the reaction zone corresponding to the upper stable branches of Fig.8, approaches the particle surface, $x_r \to 1$; most of the particle is in equilibrium, and both the reaction zone and the outer frozen diffusion region are thin

and with a planar structure. Φ and η take the limiting form

$$\Phi \doteq 6\alpha\phi_s \quad \text{and} \quad \eta \doteq 6\alpha/\phi_s \tag{64}$$

in agreement with the asymptotic description given by Petersen (1965).

Notice that the parameter $\alpha\phi_s$ can also be written as

$$\alpha\phi_s \doteq (\phi_m\sqrt{\Gamma_{n+1}/2})\{(1+\beta)^2/\gamma\beta\}^{(n+1)/2} \tag{65}$$

where

$$\gamma\beta/(1+\beta)^2 = (T_m-T_s)T_a/T_m^2 \tag{66}$$

and

$$\phi_m = \phi_s\exp\{\gamma\beta/2(1+\beta)\} \tag{67}$$

is the Thiele modulus based on the maximum temperature T_m.

If higher order approximations were desired, we would pose our problem as to find, for large values of $\gamma\beta$, the Thiele modulus ϕ_s and the solution of Eq (8), resulting in a given value of Φ, of order unity. We would write the solution in the form of three "matched asymptotic expansions", see Cole (1968). That is: An interior expansion

$$y = 0 + (\gamma\beta)^{-2}y_1(x) + \text{---}$$

for the near-equilibrium region, an outer expansion, given by Eq (49) to all algebraic orders in $(\gamma\beta)^{-1}$, for the outer frozen

region, and an expansion

$$y = \psi(1+\beta)^2/\gamma\beta + \psi_1/(\gamma\beta)^2 + \text{---}$$

for the transition, reaction zone, region, with ψ , ψ_1 , --- functions of the variable ξ .

In addition, the reduced Damköhler number Δ , defined by Eq (52), would also be expanded in powers of $(\gamma\beta)^{-1}$

$$\Delta = \Delta_o + (\gamma\beta)^{-1}\Delta_1 + \text{---}$$

so that, only in first approximation, $\Delta = \Delta_o$ would be given by Eq (59).

The analysis of the thin reaction zone regime, given here for spherical particles, can be easily extended to cover particles with the form of infinite slabs or infinite cylinders.

The half-thickness of the slab and the radius of the cylinder should be used as the characteristic length in the definition of the Thiele modulus and to dimensionalize the distance to the center plane or axis of the particle. The non-dimensional particle reaction rate, $\Phi = \eta\phi_s^2$, is equal to 1 and 2 times the gradient dy/dx at the particle surface x = 1 for the one dimensional and cylindrical cases, respectively; while the corresponding thin reaction zone location is given by $x_r = 1 - 1/\Phi$ and $x_r = \exp(-2/\Phi)$, respectively.

The reaction zone structure is described by Eq (55), and

the relation between the reduced Thiele modulus $2\alpha\phi_s$ and Φ is

$$2\alpha\phi_s = \Phi \tag{68}$$

for infinite slabs, and

$$2\alpha\phi_s = (\Phi/2)\exp(2/\Phi) \tag{69}$$

for cylindrical particles. This relation (69) is also shown in Fig.8. In this case, there exists a minimum,extinction, value ϕ_{SE} of ϕ_s for the thin reaction zone regime to exist,

$$\phi_{SE} = e/2\alpha \tag{70}$$

Of the two branches of the $\phi(\alpha\phi_s)$ curve, for $\phi_s > \phi_{SE}$, the lower branch corresponds, very possibly to an unstable mode of decomposition.

The thin reaction zone analysis ceases to be valid when x_r becomes small, of the order, $1/\gamma\beta$, of the thickness of the reaction zone.

If the Thiele modulus were defined in terms of the ratio of the particle volume to the external particle surface we would obtain a number ϕ_s' equal to 1, 1/2, 1/3 times the Thiele modulus ϕ_s based on the half-thickness or radius of the particle. In Fig.9 we have plotted η/α^2 in terms of $\alpha\phi_s'$ for infinite slabs, infinite cylinder and spheres. The asymptotic form of the effectiveness factor for large values of the Thiele modulus coincide for the three types of particles if the Thiele modulus is based on the ratio of particle volume to particle surface.

VI. CONCLUSIONS.

We have carried out in the previous sections asymptotic analyses of Eq.(8), for small values of β and $\gamma\beta$ of order unity or small in Section II, for large values of $(-\gamma\beta)$ in Section III, and for large values of $\gamma\beta$ in Sections IV and V. In Appendix A we consider the cases where $\gamma\beta$ is small compared with unity, and in Appendix B we extend to the second approximation the asymptotic analysis of Petersen for large ϕ_s .

These analyses were carried out with the purpose of generating closed form expressions for the effectiveness factor η and the apparent particle consumption rate Φ in terms of the overall order of the reaction n, the Thiele modulus ϕ_s , the heat release parameter β and the activation energy γ ; all these variables based on the concentration c_s and temperature T_s of the fluid at the particle surface. These closed form expressions can be used in studying the evolution of reactants through catalytic packed bed reactors. In Appendix C we show how these expressions can be used to determine the reaction rate per particle in terms of the mean properties of the interstitial fluid and the Nusselt and Sherwood numbers.

The analysis of Section II for small values of β corresponds to nearly isothermal particles; if the reaction rate is very sensitively dependent on temperature, $\gamma\beta \sim 1$, these effects cause significant departures of the values of the effectiveness factor η

and Φ from their isothermal values (for $\gamma\beta=0$). For small values of β, both Φ and η are found to be, in first approximation, function only of $\gamma\beta$ and ϕ_s for each reaction order n.

For first order reactions and $\gamma\beta$ of order unity, we carried out the numerical integration of the simplified Eq (18), obtained from Eq (8) by linearization of the Arrhenius exponent, to reproduce the results, presented in Figs. 1 and 2, of Tinkler and Metzner (1961). Multiple solution were found for $\gamma\beta > 4.5$. For zero order reactions we carried out an analysis, similar to that of Hlavacek and Marek (1968) to obtain, by numerical integration of Eq.(35), a relation between $\omega = \Phi\gamma\beta$ and $\delta = \phi_s^2\gamma\beta$. The results are plotted in Fig.5 and 6 for exothermic and endothermic reactions, respectively The expansion (39) for small δ has also been plotted in Fig.5. Eq.(40) gives $\delta(\omega)$ for endothermic reactions with errors lower than one per cent.

In Appendix A we present a perturbation analysis of Eq. (8) for small values of $\gamma\beta$, to account for the incipient non-isothermal particle effects. This analysis leads to the closed form expressions, Eqs.(24) and (A22), for n=1 and n=0, respectively.

The analysis of Section III was devoted to endothermic reactions with large values of the parameter $(-\gamma\beta)$ and $-\beta$ of order unity. No concentration differences are found within the particle, in first approximation, under these conditions; so that we obtain

for arbitrary reaction orders the relation $\delta(\omega)$ obtained in the previous section for zero order reactions. Eq.(40) is an approximate representation of this relation.

Sections IV and V were devoted to the analysis of exothermic reactions, for large values of $\gamma\beta$ and β of order unity. Under these conditions there are two possible decomposition regimes. In one regime, the ignition regime analyzed in Section IV, the particle is nearly isothermal and no significant differences in concentration are found within the particle; so that,again we are led in first approximation to the relation $\omega(\delta)$ represented in Fig.5, which we obtained in Section III for zero order reactions. When the incepient effects of the differences in concentration within the particles are taken into account the relation between Φ and ϕ_s and $\gamma\beta$ takes the form of Eq.(43) for both endothermic and exothermic reactions. The ignition regime is only found for values of ϕ_s satisfying the relation (44).

For large activation energies, $\gamma\beta \gg 1$, there is a second decomposition regime, analyzed in Section V, for which, as sketched in Fig.7, the decomposition reaction occurs in a thin reaction layer. The reaction layer separates an interior equilibrium region, where $y = 0$ and $\theta = \beta$, from an outer region, where the chemical reaction is frozen, because of the temperature drop from its maximum value. The asymptotic analysis carried out for

arbitrary reaction orders and also for infinite slabs and infinite cylinders, led to closed form expressions for Φ and η in terms of ϕ_s and $\gamma\beta$ and β. These expressions are represented in Figs. 8 and 9. The thin reaction zone regime was found to exist only for values of ϕ_s above an "extinction" value ϕ_{SE}, for which closed form expressions are given in Section V.

Fig.10 shows the effectiveness factor as function of ϕ_s for several values of $\gamma\beta$ and β, as resulting from the asymptotic analyses. No significant differences are found with the numerical results of Weisz and Hicks (1962).

A P P E N D I X A

We shall in this Appendix look for the solution of Eq (8), with the boundary conditions given by Eqs (11) and (12), for small values of both β and $\gamma\beta$, in order to calculate the incipient effects of the non-uniformities in the particle temperature on the effectiveness factor.

In the particular case $\gamma\beta = 0$, Eq (8) reduces to the Emden-Fowler equation

$$\frac{d^2y}{dx^2} + \frac{2}{x}\frac{dy}{dx} = \phi_s^2 y^n \qquad (A1)$$

which has received considerable attention in the literature. See the recent review by Wong (1975).

We want to find the solution of Eq (A1) and, in particular, calculate the observed reaction rate

$$\Phi = 3(dy/dx)_{x=1}$$

We shall introduce the variables

$$p = (x/y)dy/dx \quad \text{and} \quad u = \phi_s^2 x^2 y^{n-1} \qquad (A2)$$

which are invariant, like Eq (A1), under the continuous transformation group

$$y \to \alpha y \quad , \quad x \to \alpha^{(1-n)/2} x \qquad (A3)$$

From the definitions (A2), we obtain

$$\frac{udy}{ydu} = \frac{p}{2+(n-1)p} \qquad (A4)$$

When Eq (A1) is written in terms of the variables p and u, we obtain the equation

$$\frac{dp}{du} = \frac{u-p^2-p}{u\{2+(n-1)p\}} \qquad (A5)$$

which, when integrated with the initial condition $p = 0$, at $u = 0$, yields *

$$p = p_o(u, n) \qquad (A6)$$

When $x = 1$: $y = 1$, $u = \phi_s^2$ and $p = \Phi/3$; so that

$$\Phi = 3p_o(\phi_s^2 , n) \qquad (A7)$$

For $n = 0$, the solution of Eq (A5) is, if $u < 6$

$$p_o(u, 0) = u/3 \qquad (A8)$$

For $n = 1$, the solution is

$$p_o(u , 1) = \sqrt{u}\ \mathrm{ctanh}\sqrt{u} - 1 \qquad (A9)$$

which together with Eq (A7) provide the relation between Φ and ϕ_s^2.

For arbitrary n , and small values of u , the solution of Eq (A5) is

$$p_o = (u/3)\{1 - nu/15 + n(3n-1)u^2/315 + ---\} \qquad (A10)$$

For large values of u

$$p_o = \{2u/(n+1)\}^{1/2} - \{1+(n-1)/4\}^{-1} + --- \qquad (A11)$$

* If $n < 1$, this initial condition can only be used if the resulting $p_o(\phi_s^2,n) < 2/(1-n)$; for larger ϕ_s the reactant does not reach the center of the particle.

The purpose of this Appendix is to obtain the solution of Eq (8) for small values of β and $\gamma\beta$, when the solution will be a small perturbation of the solution (A6) for the case $\gamma\beta = 0$. For this reason, we shall write Eq (8) in terms of the variables p and u defined by Eqs (A2). Thus we obtain the equation

$$\{2 + (n-1)p\}\frac{dp}{du} = \exp \frac{\gamma\beta(1- y)}{1+\beta(1-y)} - (p+p^2)/u \qquad (A12)$$

together with Eq (A4) and the boundary conditions

$$p = 0 \quad \text{at} \quad u = 0 \qquad (A13)$$

and

$$y = 1 \quad \text{at} \quad u = \phi_s^2 \qquad (A14)$$

to calculate p(u),and in particular $\Phi = 3p(\phi_s^2)$.

We shall write the solution,for small values of β and $\gamma\beta$, of Eqs (A4) and (A12) in the form of expansions

$$p = p_o + \gamma\beta p_1 + \text{---} \qquad (A15)$$

$$y = y_o + \gamma\beta y_1 + \text{---} \qquad (A16)$$

which when substituted in Eqs (A4) and (A12) yield Eq (A5) for p_o , and

$$\ln y_o = -\int_u^{\phi_s^2} \{2+(n-1)p_o\}^{-1} p_o du/u \qquad (A17)$$

for $y_o(u)$.

In the particular cases, $n = 0$, if $\phi_s^2 < 6$,

$$y_o(u) = (\phi_s^2-6)/(u-6) \qquad (A18)$$

and for $n = 1$

$$y_o(u) = \frac{\sinh\sqrt{u}}{\sqrt{u}} \frac{\phi_s}{\sinh\phi_s} \tag{A19}$$

For $p_1(u)$ we obtain the equation

$$\{2 + (n-1)p_o\}\frac{dp_1}{du} + (n-1)p_1\frac{dp_o}{du} + p_1 \frac{(1+2p_o)}{u} = 1 - y_o \tag{A20}$$

which when integrated, with the initial condition $p_1(0) = 0$, until $u = \phi_s^2$ will yield the first two terms of the expansion for Φ

$$\Phi = 3p_o(\phi_s^2, n) + 3\gamma\beta p_1(\phi_s^2, n) + \text{---} \tag{A21}$$

For $n = 0$, we obtain, from Eq (A20), for $\phi_s^2 < 6$

$$\Phi = \phi_s^2 + \gamma\beta\phi_s^4/15 + \text{---} \tag{A22}$$

in agreement with Eq (39). For $n = 1$, we obtain, after elaborate calculations,

$$p_1 = (-p_o - p_o^2 + \phi_s^2)/2 - \frac{1}{2\phi_s}\left(\frac{\phi_s}{\sh\phi_s}\right) \int_o^{\phi_s^2} \sqrt{x} \left(\frac{\sh\sqrt{x}}{\sqrt{x}}\right)^3 dx \tag{A23}$$

The functions $p_o(\phi_s)$ and $p_1(\phi_s)$ have been plotted in Fig.3.

A P P E N D I X B

In this appendix we shall obtain the first two terms of an asymptotic solution of Eq (8) for large values of ϕ_s . The first term is given by Petersen (1965).

When the formal limit $\phi_s \to \infty$ is taken in Eq (8), with y and their derivatives with respect to x assumed to be of order unity, we obtain the limiting equilibrium equation

$$y = 0 \tag{B1}$$

This does not hold close to the particle surface in a thin reaction layer where y changes from 0 to 1. The thickness of this layer is, of order ϕ_s^{-1}, such that the first diffusion term of Eq (8) is of the same order, ϕ_s^2, as the reaction term.

To describe the reaction zone structure we shall write Eq (8) in terms of the variable

$$\xi = (1-x)\phi_s \tag{B2}$$

and the nondimensional gradient

$$P = -dy/d\xi \tag{B3}$$

so that Eq (8) becomes

$$P \frac{dP}{dy} - \frac{2/\phi_s}{1-\xi/\phi_s} P = R(y) \tag{B4}$$

where

$$R(y) = y^n \exp \frac{\gamma\beta(1-y)}{1+\beta(1-y)} \qquad (B5)$$

Eqs (B3) and (B4) are to be integrated with the boundary conditions

$$P = 0 \quad \text{at} \quad \xi = \phi_s \qquad (B6)$$

$$\xi = 0 \quad \text{at} \quad y = 1 \qquad (B7)$$

The nondimensional particle reaction rate Φ is given in terms of the value P(1) of P for y = 1 by

$$\Phi = 3\,\phi_s P(1) \qquad (B8)$$

The solution of Eqs (B3) and (B4) will be written in the form of the expansions

$$P = P_o(y) + \phi_s^{-1} P\,(y) + \text{---} \qquad (B9)$$

$$\xi = \xi_o(y) + \phi_s^{-1}\xi_1(y) + \text{---} \qquad (B10)$$

We then obtain the equations

$$P_o dP_o/dy = R(y) \qquad (B11)$$

$$d(P_o P_1)dy = 2P_o \qquad (B12)$$

and

$$d\xi_o/dy = -P_o^{-1} \quad , \quad d\xi_1/dy = P_1 P_o^{-2} \qquad (B13)$$

These equations will be integrated with the boundary conditions

$$\xi_o = \xi_1 = 0 \quad \text{at} \quad y = 1 \qquad (B14)$$

resulting from Eq (B7), and the conditions,

$$\xi_o \to \infty \quad , \quad P_o = P_1 = 0 \quad \text{at} \quad y = 0 \ , \tag{B15}$$

obtained by matching with the interior equilibrium solution y = 0.

Thus we obtain

$$P_o = \left\{2\int_o^y R(y)dy\right\}^{1/2} \tag{B16}$$

and

$$P_o P_1 = 2\int_o^y P_o dy \tag{B17}$$

The nondimensional particle consumption rate Φ and the effectiveness factor η are given by the expansions

$$\Phi = \phi_s^2 \eta = 3\phi_s P_o(1) + 3P_1(1) + \text{---} \tag{B18}$$

where

$$P_o(1) = \left\{2\int_o^1 R(y)dy\right\}^{1/2} \tag{B19}$$

and

$$P_1(1) = \left\{P_o(1)\right\}^{-1} 2\int_o^1 P_o(y)dy \tag{B20}$$

In the particular case $\gamma\beta = 0$,

$$P_o(1) = \sqrt{2/(n+1)} \quad ,, \quad P_1(1) = 4/(n+3) \tag{B21}$$

For values of $\beta << 1$ and $\gamma\beta$ of order unity

$$P_o(y) = \left[\pm 2|\gamma\beta|^{-n-1}\exp(\gamma\beta)\int_o^{\gamma\beta y} |\psi|^n e^{-\psi} d\psi\right]^{1/2} \tag{B22}$$

with the - sign chosen for negative β . The integral can be written in terms of incomplete Gamma functions. Eqs (B17) and (B22) can be used to obtain Eq (25) for η when $n = 1$. For $n = 0$, we obtain

$$P_o(1) = \{(2/\gamma\beta)(\exp\gamma\beta - 1)\}^{1/2} \qquad (B23)$$

and

$$P_1(1) = \frac{4}{\gamma\beta}\left[-1 + \frac{\tanh^{-1}X}{X}\right] \qquad (B24a)$$

with $X = \{1 - \exp(-\gamma\beta)\}^{1/2}$, for $\gamma\beta > 0$ and

$$P_1(1) = \frac{-4}{\gamma\beta}\left[1 - \frac{\tan^{-1}Y}{Y}\right] \qquad (B25b)$$

with $Y = \{\exp(-\gamma\beta) - 1\}^{1/2}$ for $\gamma\beta < 0$.

The asymptotic form of $P_o(1)$ and $P_1(1)$ for large values of $\gamma\beta$ and β of order unity can be obtained from Eqs (B19) and (B20) without much difficulty. The resulting expressions can be obtained directly from Eq (35) of Section II for negative β as

$$\gamma\beta\Phi = -3\sqrt{-2\gamma\beta}\,\phi_s + 12 + \text{---} \qquad (B26)$$

and, from Eq (62) of Section V, for positive β as

$$\Phi = 6\alpha\phi_s - 6 + \text{---} \qquad (B27)$$

$$D(dc/dr)_{r=a} = K_c(c_i - c_s) \qquad (C1)$$

$$K(dT/dr)_{r=a} = h\ (T_i - T_s) \qquad (C2)$$

where K_c and h are overall heat and mass transfer coefficients.

The gradient of temperature is given in terms of the concentration gradient by the equation

$$(dT/dr)_{r=a} = -\beta(T_s/c_s)(dc/dr)_{r=a} \qquad (C3)$$

as a result of the Pratter relation(6).

The concentration gradient was written, Eq (15), in terms of the non-dimensional observable reaction rate Φ , as

$$(dc/dr)_{r=a} = (c_s/a)\Phi/3 \qquad (C4)$$

From Eqs (C1)-(C4), we can obtain the relations

$$(\sigma\beta/\nu)(c_i/c_s - 1) = (1-T_i/T_s) \qquad (C5)$$

and

$$3\sigma(c_i/c_s - 1) = \Phi \qquad (C6)$$

where σ and ν are the modified Sherwood and Nusselt numbers

$$\sigma = K_c a/D \quad \text{and} \quad \nu = ha/K \qquad (C7)$$

In our previous study we obtained, for the possible decomposition regimes, expressions for Φ in terms of the Thiele modulus ϕ_s , the nondimensional activation energy γ ,and the heat release parameter β , all based on the temperature T_s and concentration c_s

at the particle surface. The resulting relation

$$\Phi = \Phi(\phi_s, \gamma, \beta) \tag{C8}$$

or equivalently

$$\phi_s = \phi_s(\Phi, \gamma, \beta) \tag{C9}$$

together with Eq (C5) and (C6) can be used to calculate T_s and c_s in terms of c_i and T_i.

We shall write below these relations in terms of the Thiele modulus ϕ_i, the nondimensional activation energy γ_i, and the heat release parameter β_i based on T_i and c_i. According to the definitions given by Eqs (7) and (10), we can write

$$\gamma = \gamma_i(T_i/T_s) \quad ,, \quad \beta = \beta_i(T_i/T_s)(c_s/c_i) \tag{C10a}$$

$$\phi_s = \phi_i(c_s/c_i)^{(n-1)/2} e^{-\gamma_i(T_i/T_s-1)/2} \tag{C10b}$$

When Eq.(C5) is written in terms of the variable β_i, we obtain

$$(T_s/T_i - 1) = (\sigma\beta_i/\nu)(1 - c_s/c_i) \tag{C11}$$

The relations of the form (C9) obtained in our analyses of the different regimes of decomposition, can be combined with Eqs. (C6) and (C10) to yield an explicit relation

$$\phi_i(c_s/c_i)^{(n-1)/2} e^{-\gamma_i(T_i/T_s-1)/2} =$$

$$\phi_s\{3\sigma(c_i/c_s-1) \ , \ \gamma_i(T_i/T_s) \ , \ \beta_i(T_i/T_s)(c_s/c_i)\} \tag{C12}$$

between ϕ_i and c_s , or T_s , for given values of T_i , c_i and the Sherwood and Nusselt numbers σ and ν.

The mass and heat transfer rates $K_c(c_i-c_s)$ and $h(T_i-T_s)$ are also linear functions of c_s, or T_s; so that from Eq (C12) we can easily obtain an explicit relation for ϕ_i in term of the heat or mass transfer rate, for given ν , σ , T_i and c_i. The effectiveness factor η_i,based on the interstitial properties, defined by the equation

$$K_c(c_i - c_s) = (Dc_i/a)\eta_i\phi_i^2/3 \qquad (C13)$$

so that

$$\eta_i = 3\sigma(1 - c_s/c_i)\phi_i^{-2} \qquad (C14)$$

can also written explicitely in terms of the surface concentration.

The explicit relation (C9) leading to the explicit relation (C12) for ϕ_i in terms of c_s or, as a consequence, the mass transfer rate, can be used for parametric studies to find the regions of multiplicity of decomposition modes.

In the limit $\nu \to \infty$ and $\sigma \to \infty$, c_s and T_s coincide with c_i and T_i,and the analysis of the main text is directly applicable,because there is no external heat and mass transfer resistance. The influence of external heat and mass transfer resistance on the decomposition rates by catalytic particles, and the conditions for uniqueness or multiplicity of decomposition modes, has been

considered, among others, by Hlaváček, Marek and Kubíček (1968), Kesten (1969), and Creswell (1970) who integrated the conservation Eqs (2) and (3) with mixed boundary conditions. Hatfield and Aris (1969) treated the problem of infinite slabs, for which the mass conservation equation can be solved in terms of quadratures for all the decomposition regimes. Mc Greavy and Creswell (1969),and later Kehoe and Butt (1970), used an approach similar to the one presented here,in considering the cases when the Thiele modulus ϕ_s is large enough for the reaction to occur in a thin surface layer, so that the asymptotic analysis of Petersen is applicable.

We shall indicate below how Eq (C12) simplifies for the limiting regimes discussed in our analysis.

For values of $\gamma\beta << 1$, corresponding to $\gamma_i\beta_i << 1$, the particle can be considered isothermal in first approximation. We obtained a relation, Eq (A7) of Appendix A, for Φ in terms of ϕ_s , which was written explicitely, Eqs (A8) and (A9) for zero order and first order reactions. For first order reactions, we obtained the relation

$$\Phi = 3(\phi_s \mathrm{cth}\phi_s - 1) \qquad (C15)$$

which should be inverted to generate $\phi_s(\Phi)$.

Notice that for $\gamma_i\beta_i << 1$ the dependence of ϕ in (C12) on the last two parameters disappears. The incipient non-isothermal

effects in the particle reaction rate were taken into account in Appendix A to generate the relation (A21) between Φ , ϕ_s and $\gamma\beta$.

The asymptotic decomposition regime for large ϕ_s was analyzed in Appendix B , where we obtained Eq (B18) for Φ in terms of ϕ_s . From the expansion (B18) we can obtain the expansion

$$\phi_s = \{3P_o(1)\}^{-1}\{\Phi - 3P_1(1) + \text{---}\} \qquad (C16)$$

where P_o and P_1 are functions of $\gamma\beta$ and β , involving integrals of the reaction rate. We gave P_o and P_1 , explicitely, for zero and first order reactions, and values of $\gamma\beta$ of order unity or large.

We analyzed in the main text also the cases where $|\gamma\beta| \gg 1$ leading to a relation between $\delta = \phi_s^2\gamma\beta$ and $\omega = \phi\gamma\beta$, obtained from Eq (35). For endothermic reaction Eq (40) is an approximate explicit representation of $\delta(\omega)$ as seen in Fig.6. For exothermic reactions the solution of Eq (35) is represented in Fig.5. The curve $\omega(\delta)$ is multivalued in the range $1.63 < \delta < 3.32$; no solution exists for $\delta > 3.32$. Only the lower branch of the curve may be expected to correspond to a stable, weak, mode of decomposition. As seen in Fig.5 the three term expansion, Eq (39), for small values of ω gives a fairly accurate representation for the lower branch of $\omega(\delta)$. A, strong, mode of decomposition exists for $\gamma\beta > 1$, for which the relation between ϕ_s and ω is given by Eq (59), or

$$2\alpha\phi_s = (\Phi+3)^2/3\Phi \qquad (C17)$$

where α is given by Eq (61).

R E F E R E N C E S

Aris, R. (1965): "Introduction to the Analysis of Chemical Reactors". Prentice-Hall.

Aris, R. (1969):"Elementary Chemical Reaction Analysis". Prentice-Hall.

Bischoff, K.B. (1968): "Effectiveness factors and temperature distributions for catalyst particles in non-uniform environments". Chem. Engng. Sci. 23, 451-456.

Cole, J.D. (1968): "Perturbation Methods in Applied Mechanics". Blaisdell.

Copelowitz, I. and Aris, R.(1970): "Communications on the theory of diffusion and reaction-V Findings and conjectures concerning the multiplicity of solutions". Chem. Engng. Sci. 25, 906-909.

Cresswell, D.L. (1970): "On the uniqueness of the steady state of a catalytic pellet involving both intraphase and interphase transport". Chem. Engng. Sci. 25, 267-275.

Chandrasekhar, S. (1939): " An Introduction to the Study of Stellar Structure". University of Chicago Press.

Damköhler, G. (1936): "Einflüsse der Strömung, Diffusion und des Wärmeüberganges auf die Leistung von Reaktionsöfen" Z. Elektrochem. Angew. Physik. Chem., 42, 846-862.

Emden, R. (1907). Gaskugeln. Anwendungen der mechanischen Warmentheorie auf Kosmologie und metereologische Probleme. B.G. Teubner Leipzig.

Enig, J.W. (1966): "Critical parameters in the Poisson-Boltzmaun equation of steady-state thermal explosion theory. Comb. and Flame, 10,197-199.

Frank-Kamenetskii, D.A. (1969): "Diffusion and Heat Transfer in Chemical Kinetics". Plenum Press.

Gavalas, G.R. (1968): "Nonlinear Differential Equations of Chemically Reacting Systems". Springer-Verlag.

Gray, P. and Lee, P.R. (1967): "Thermal explosion theory". Oxidation and Combustion Reviews. Vol.2. Edited by C.F.H. Tipper. Elsevier.

Hatfield, B. and Aris, R. (1969): "Communications of the theory of diffusior and reaction-IV Combined effects of internal and external diffusion in the non-isothermal case". Chem. Engng. Sci. 24, 1213-1222.

Hlaváček, V. and Marek, M. (1968): "Modelling of chemical reactors-IX Non-isothermal zero-order reaction within a porous catalyst particle". Chem. Engng. Sci., 23, 865-880.

Hlaváček, V., Marek, M. and Kubíček, M. (1968): "Modelling of chemical reactors-X Multiple solutions of enthalpy and mass balances for a catalytic reaction within a porous catalyst particle". Chem. Engng. Sci. 23, 1083-1097.

Hlaváček, V. and Kubíček, M. (1970): "Modelling of chemical reactors-XX Heat and mass transfer in porous catalyst. The particle in a non-uniform external field. Chem. Engng. Sci. 25, 1527-1536.

Kehoe, J.P.G. and Butt J.B.(1970): "Boundary layer effects in

heterogeneous catalytic reactions. Chem. Engng. Sci. 25, 345-347.

Kesten, A.S. (1969):"An integral method for evaluating the effects of film and pore diffusion of heat and mass on reaction rates in porous catalyst particles. AIChE Journal 15, 128-131.

Liñan, A. (1974): "The asymptotic structure of counter - flow diffusion flames for large activation energies". Acta Astronautica, 1, 1007-1039.

Luss, D. (1969): "On the uniqueness of a large distributed parameter system with chemical reaction and heat and mass diffusion" Chem. Engng. Sci. 24, 879-883.

McGreavy, C. and Creswell, D.L. (1969): "Non-isothermal effectivenes factors". Chem. Engng. Sci. 24, 608-611.

Petersen, E.E. (1965): "Chemical Reaction Analysis". Prentice-Hall.

Rester, S. and Aris, R. (1969): "Communications on the theory of diffusion and reaction-II the effect of shape on the effectiveness factor". Chem. Engng. Sci. 24, 793-795.

Satterfield, C.N. and Sherwood, T.K. (1963): "The Role of Diffusion in Catalysis". Addison-Wesley.

Satterfield, C.N. (1970): "Mass Transfer in Heterogeneous Catalysis" M.I.T. Press, Cambridge Mass.

Thiele, E.W. (1939): "Relation between catalytic activity and size of particle". Ind. Engng. Chem., 31, 916.

Tinkler, J.D. and Metzner, A.B. (1961)."Reaction rates in non-

isothermal catalysts". Ind. Engng. Chem. 53,663.

Volkman, Y. and Kehat, E. (1969): "Computation of effectiveness factors" Chem. Engng. Sci. 24, 1531-1532.

Von Karman, Th. (1924): "Über das thermisch-elektrische Gleichgewicht in festen Isolatoren". Archiv für Elektrotechnik, 13, 174-180.

Weisz, P.B. and Hicks, J.S. (1962): "The behaviour of porous catalyst particles in view of internal mass and heat diffusion effects". Chem. Engng. Sci. 17, 265-275.

Wong, J.S.W. (1975): "On the generalized Emden-Fowler equation" SIAM Review, 17, 339-360.

LIST OF FIGURE CAPTIONS

Fig.1 The effectiveness factor for small values of β , as a function of the Thiele modulus and the parameter $\gamma\beta$. ($n = 1$).

Fig.2 The nondimensional observable particle reaction rate Φ for small values of β , as a function of the Thiele modulus and the parameter $\gamma\beta$. First order reactions.

Fig.3 The first two terms of the expansion, Eq.(24), of $\Phi/3$ and η for small values of $\gamma\beta$, as a function of ϕ_s for $n = 1$.

Fig.4 The asymptotic form of the effectiveness factor for $\phi_s \to \infty$ as a function of $\gamma\beta$ for several values of β , for first order reactions.

Fig.5 The effectiveness factor η, $\theta(0)$ and $\omega = \Phi\gamma\beta$ as functions of $\delta = \phi_s^2\gamma\beta$, for exothermic reactions of zero order or exothermic reactions of arbitrary order with large $\gamma\beta$, in the "ignition" regime. The dashed line corresponds to the expansion (39) for small ω .

Fig.6 The effectiveness factor η, $\theta(0)$ and $-\omega = \Phi\gamma\beta$ as functions of $-\delta = \phi_s^2\gamma\beta$, for endothermic zero order reactions or reactions of arbitrary order with $-\gamma\beta$ large.

Fig.7 Schematic representation of the distributions of concentration and temperature within a catalytic particle for large values of $\gamma\beta$ in the thin reaction zone regime. The dashed lines correspond to the asymptotic distributions in the limit $\gamma\beta \to \infty$, with a fixed Damköhler number Δ .

Fig.8 The functions Φ and η/α^2 of the reduced Thiele modulus $2\alpha\phi_s$, for large values of $\gamma\beta$ in the thin reaction zone

regime; for spheres (solid lines) and infinite cylinders (dashed lines).

Fig. 9 The functions Φ and η/α^2 of the reduced Thiele modulus $2\alpha\phi_s'$, for large values of $\gamma\beta$ in the thin reaction zone regime; for infinite slabs ($\phi_s' = \phi_s$, lines with dots and dashes), infinite cylinders ($\phi_s' = \phi_s/2$, dashed lines) and spheres ($\phi_s' = \phi_s/3$, solid lines).

Fig.10 The effectiveness factor η as a function of ϕ_s for some typical values of $\gamma\beta$ and β as obtained, for first order reactions, from the asymptotic analyses for the various decomposition regimes.

FIG. Nº 1

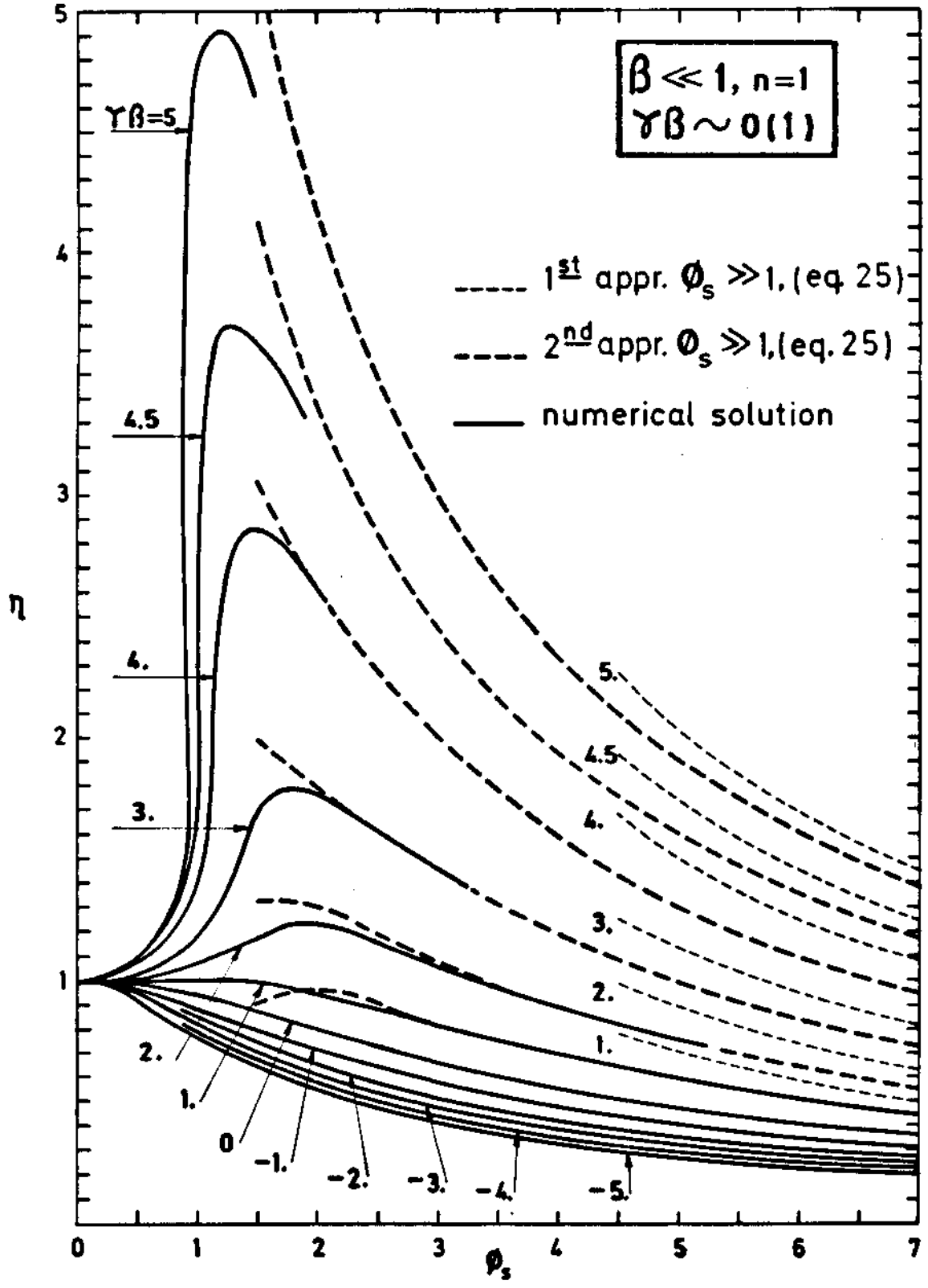
β ≪ 1, n=1
γβ ~ 0(1)
1st appr. Ø_s ≫ 1, (eq. 25)
2nd appr. Ø_s ≫ 1, (eq. 25)
numerical solution
γβ=5
4.5
4.
3.
2.
1.
0
-1.
-2.
-3.
-4.
-5.
η
Ø_s

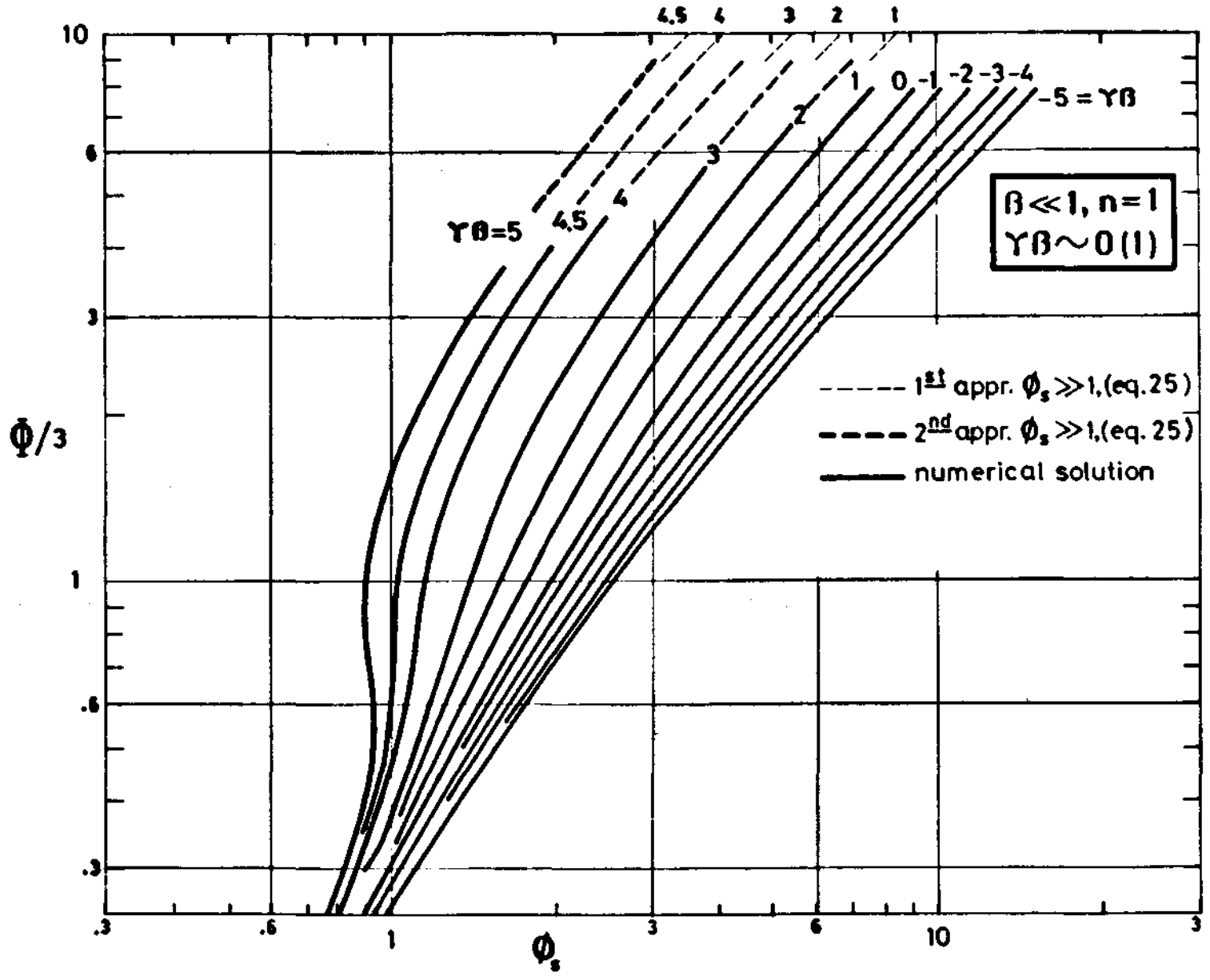
4.5
4
3
2
1
10
6
3
1
.6
.3
Φ/3
1
0
-1
-2
-3
-4
-5 = Υβ
Υβ=5
4.5
4
3
2
β≪1, n=1
Υβ∼0(1)
1st appr. φs≫1,(eq.25)
2nd appr. φs≫1,(eq.25)
numerical solution
.3
.6
1
3
6
10
φs

FIG. Nº 2

FIG. Nº 3

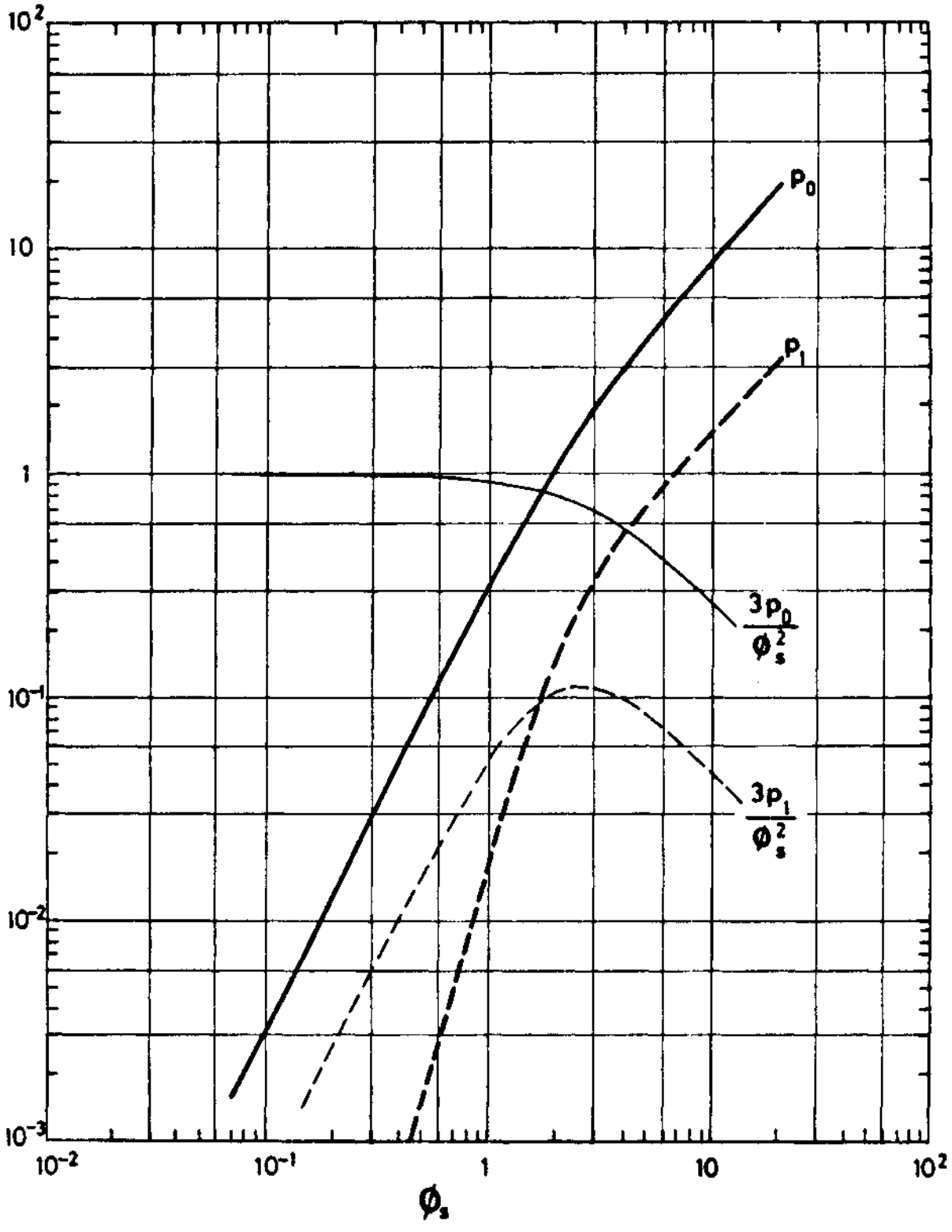
10^2
10
1
10^{-1}
10^{-2}
10^{-3}
10^{-2}
10^{-1}
1
10
10^2
ϕ_s
p_0
p_1
$\frac{3p_0}{\phi_s^2}$
$\frac{3p_1}{\phi_s^2}$

FIG. Nº 4

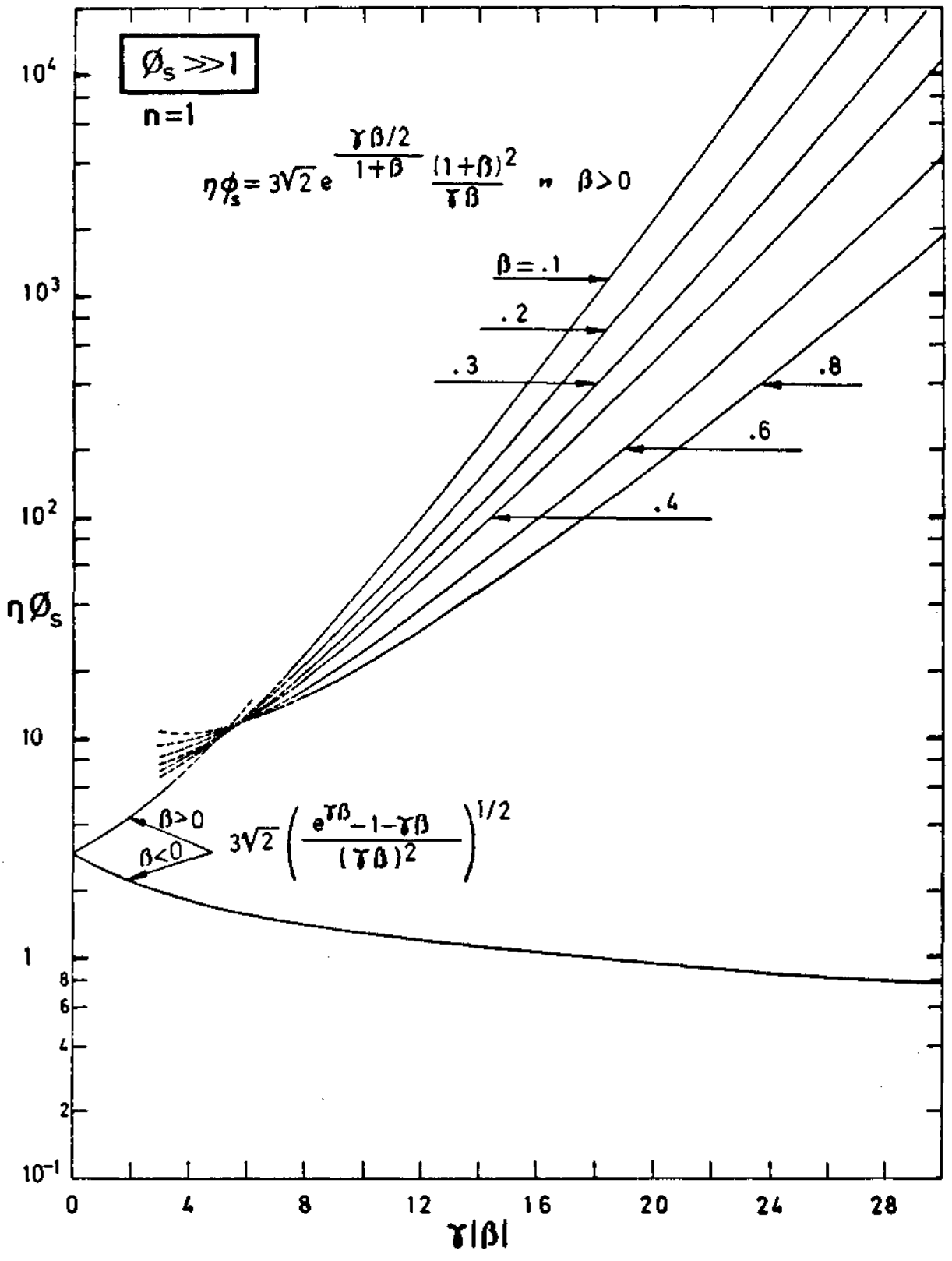
$\phi_s \gg 1$
n=1
$\eta\phi_s = 3\sqrt{2}\, e^{\frac{\gamma\beta/2}{1+\beta}} \frac{(1+\beta)^2}{\gamma\beta}$; $\beta>0$
$\beta = .1$
.2
.3
.4
.6
.8
$\beta>0$
$\beta<0$
$3\sqrt{2}\left(\frac{e^{\gamma\beta}-1-\gamma\beta}{(\gamma\beta)^2}\right)^{1/2}$
$\eta\phi_s$
$\gamma|\beta|$
10^4
10^3
10^2
10
1
10^{-1}
8
6
4
2
0
4
8
12
16
20
24
28

FIG. Nº 5

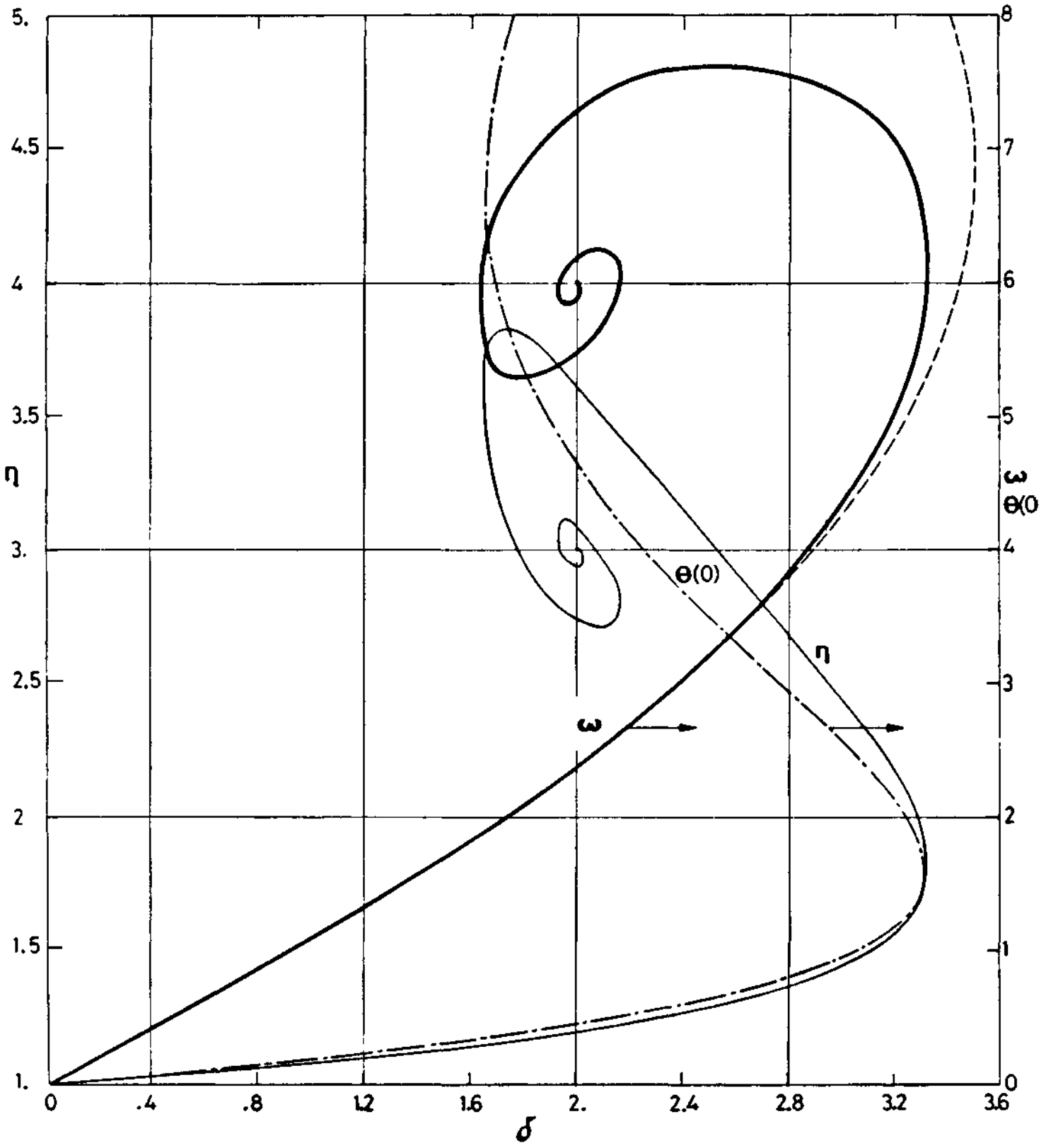

FIG. Nº 6

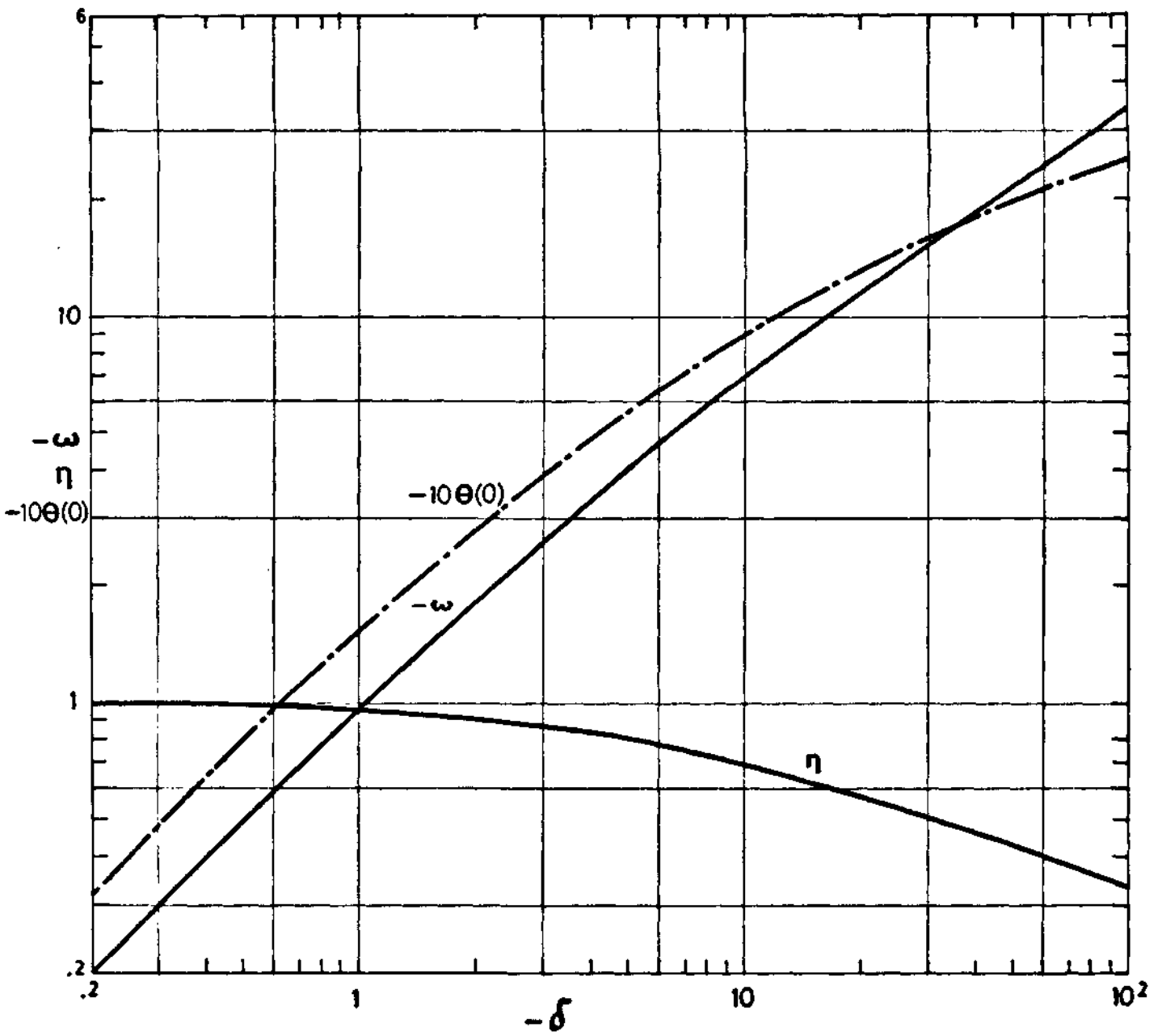

FIG. Nº 7

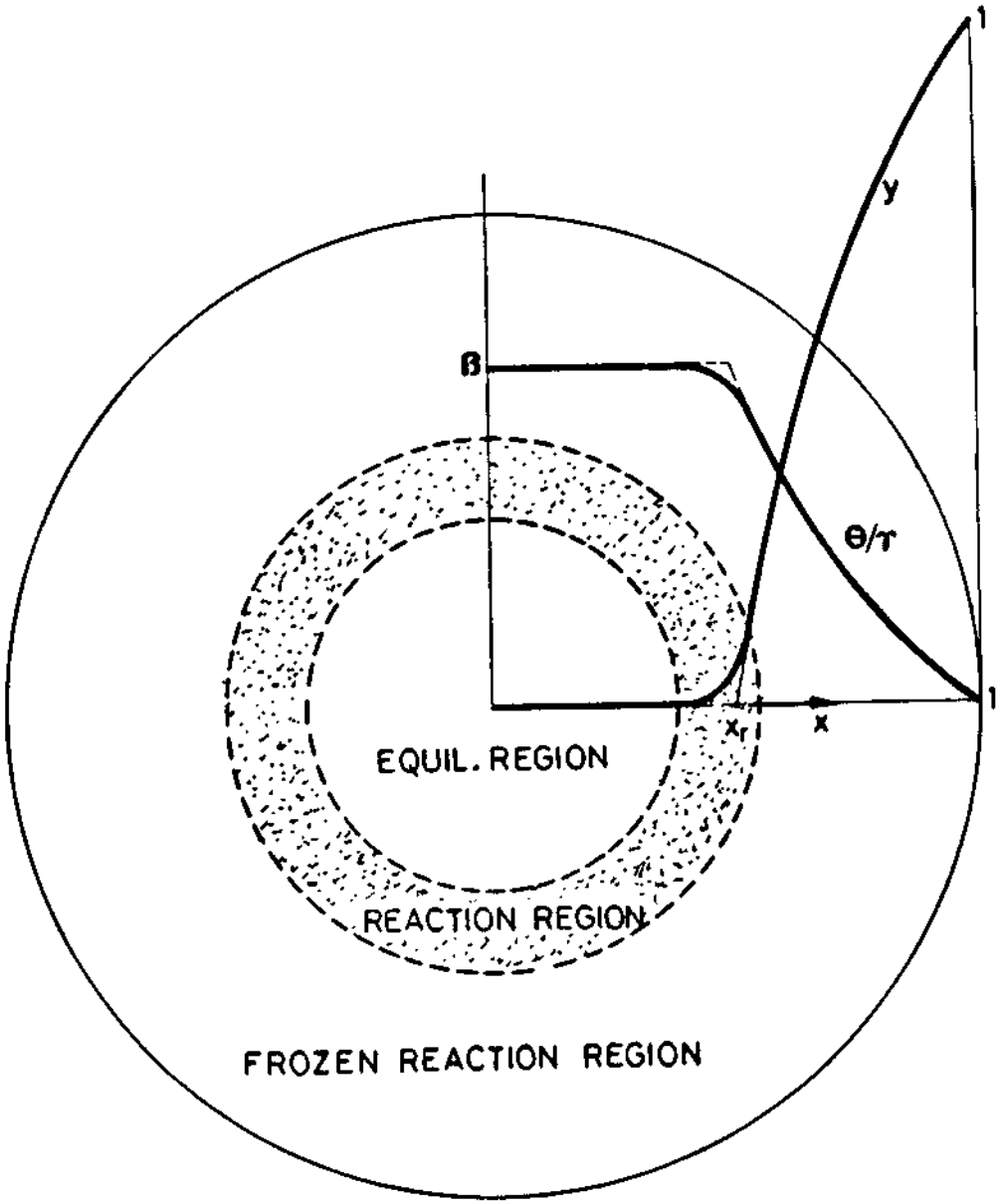
1
y
β
θ/τ
1
r
x_r
x
EQUIL. REGION
REACTION REGION
FROZEN REACTION REGION

FIG. Nº 8

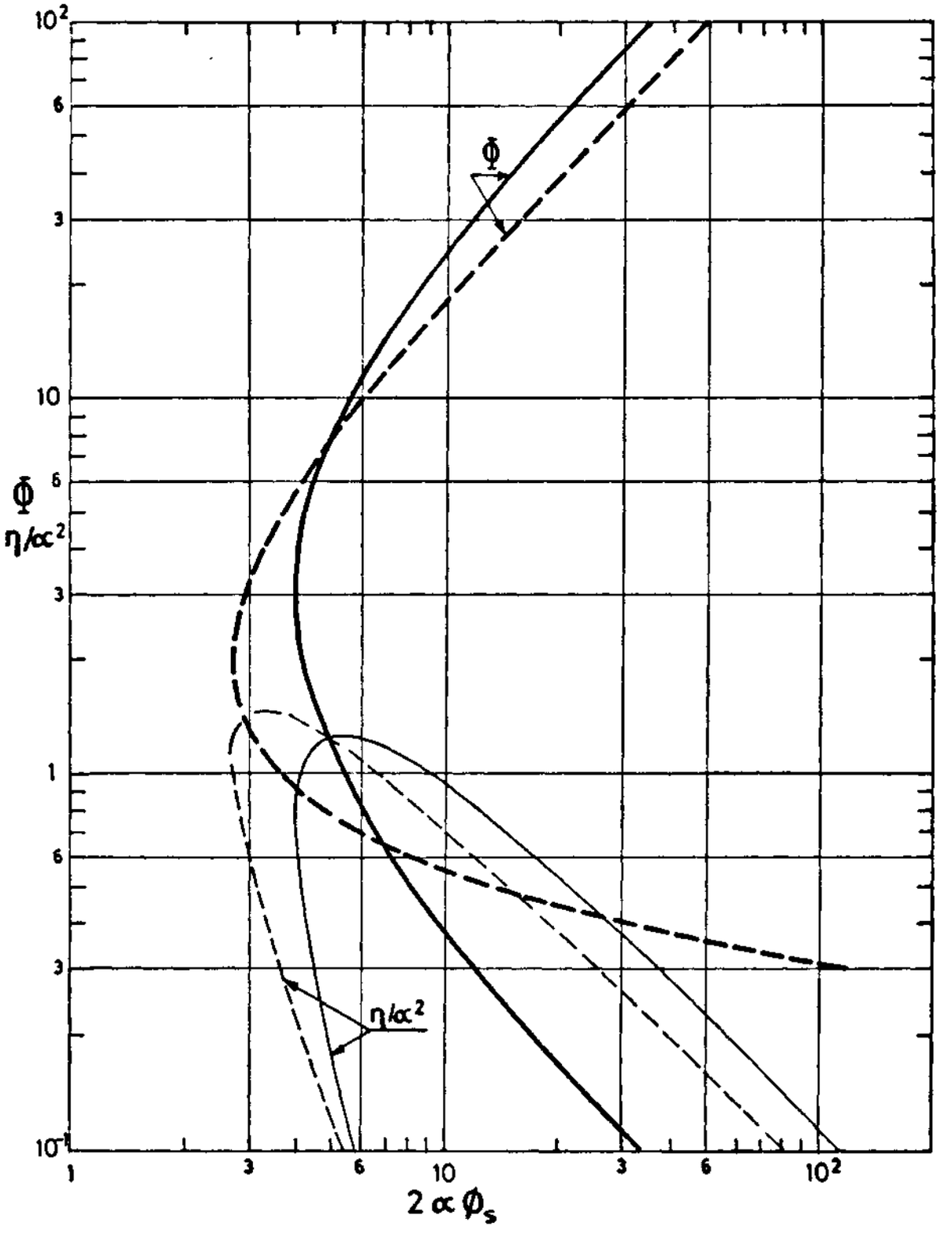
10^2
6
3
10
6
3
1
6
3
10^{-1}
Φ
$\eta/\alpha c^2$
Φ
$\eta/\alpha c^2$
1
3
6
10
3
6
10^2
$2\alpha\phi_s$

FIG. Nº 9

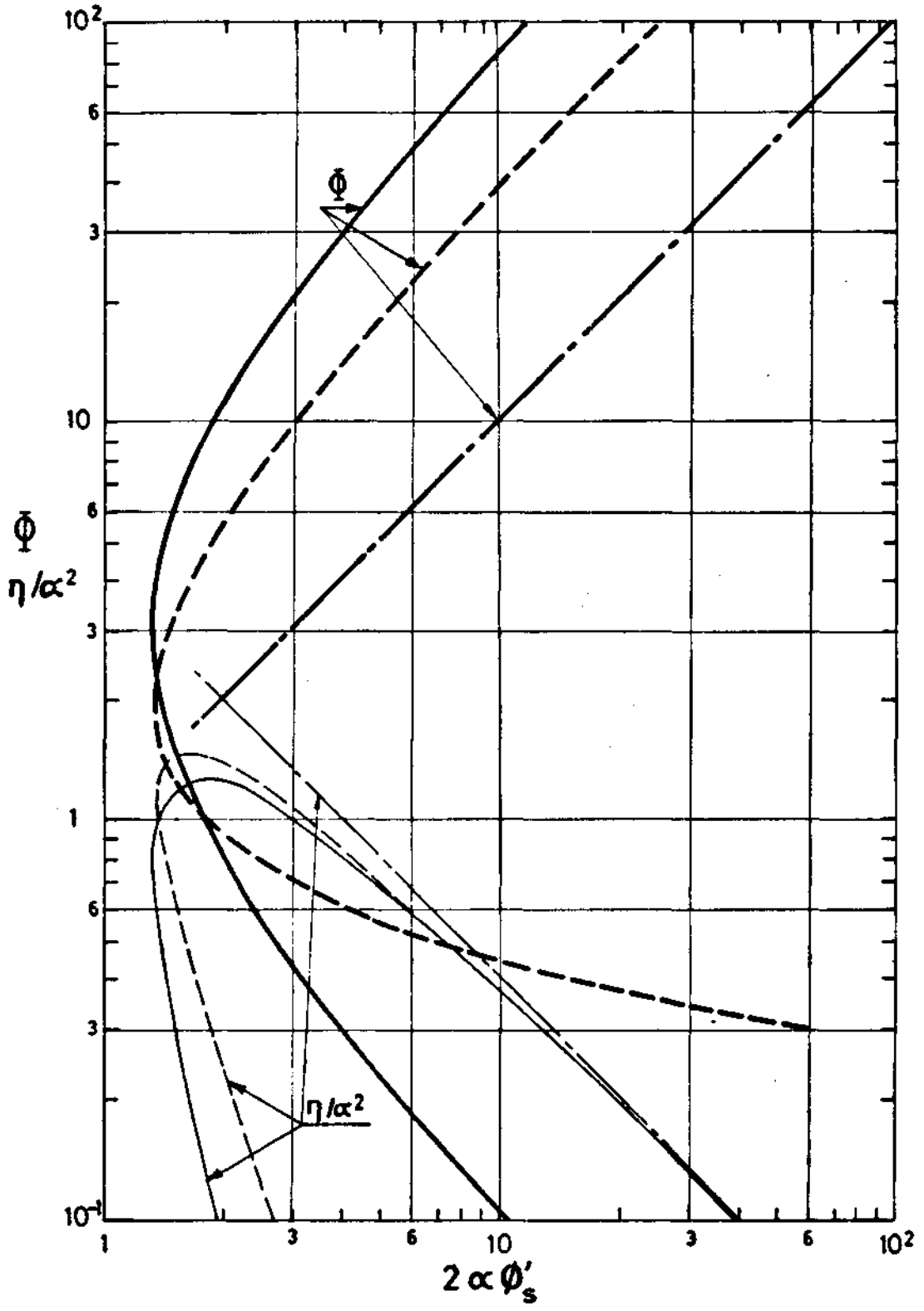

FIG. Nº 10

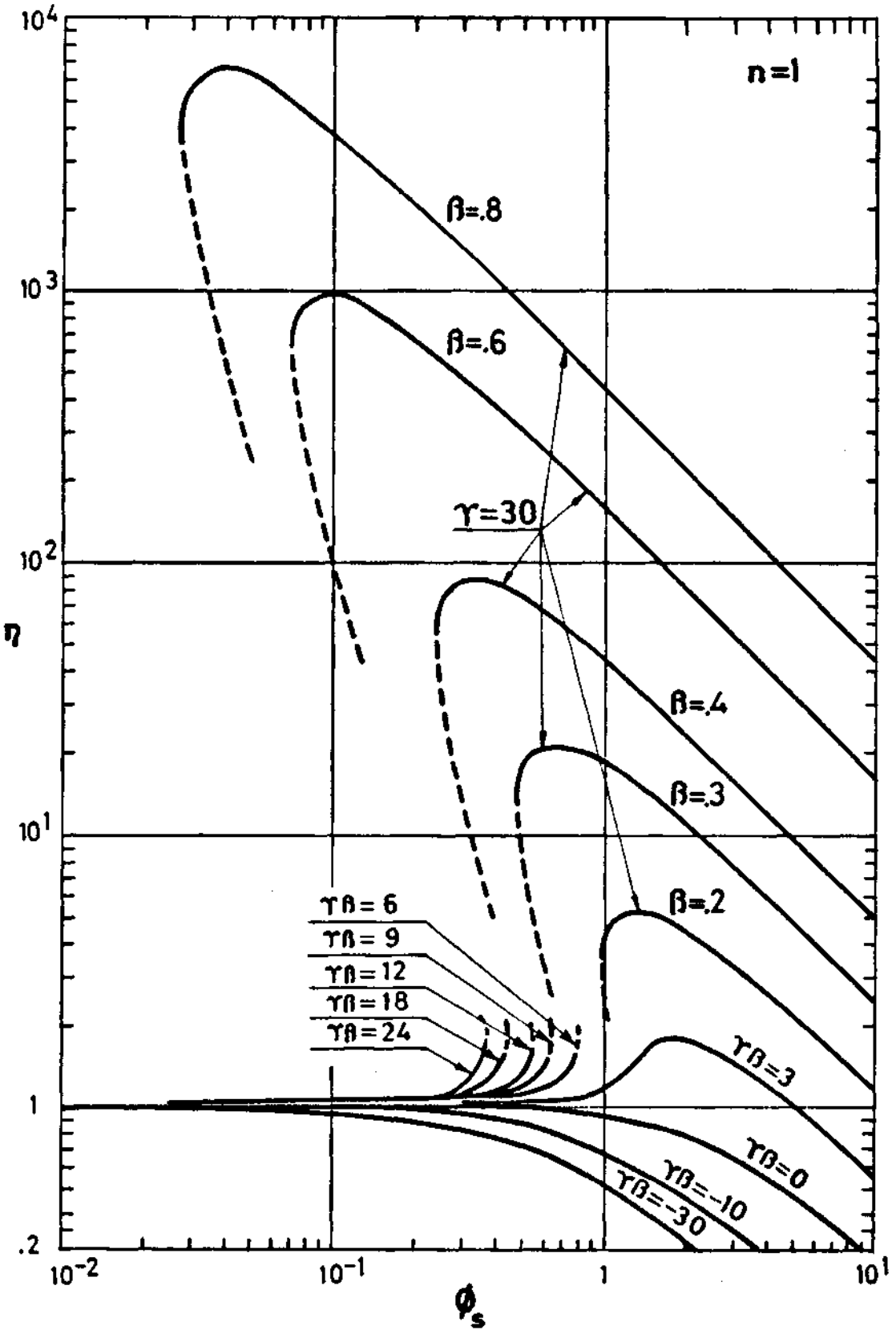
n=1
β=.8
β=.6
γ=30
β=.4
β=.3
β=.2
γβ=6
γβ=9
γβ=12
γβ=18
γβ=24
γβ=3
γβ=0
γβ=-10
γβ=-30
η
ϕ_s
10^4
10^3
10^2
10^1
1
.2
10^{-2}
10^{-1}
1
10^1

P A R T IV

STEADY STATE ANALYSIS OF HYDRAZINE MONOPROPELLANT THRUSTERS

Authors J.L. Urrutia
A. Liñán
A. Crespo
E. Fraga

LIST OF SYMBOLS

A - Parameter defined in (32).

A_p - External surface area of catalyst particle per unit volume.

a - Particle radius.

B - Constant defined in (46).

b_h - Frequency factor of hydrazine decomposition.

C - Constant defined in (20).

c_a - Defined in (31).

c_p - Specific heat of constant pressure.

D - Diffusion coefficient.

G - Mass flow rate per unit cross area of the chamber.

H_h - Heat of reaction for hydrazine decomposition.

h_c - Heat transfer coefficient.

I - Specific impulse.

J - Parameter defined in (51).

K_c^j - Mass transfer coefficient of species j.

k - Reaction rate.

L - Heat of vaporization of hydrazine.

l - Chamber length.

l^* - Length of the isothermal region.

M - Mach number.

m - Mean molecular weight.

m_h - Molecular weight of hydrazine.

p - Pressure.

p_{vr} - Reference vapour pressure.

R - Universal gas constant.

S - Area.

T - Temperature.

T_A - Activation temperature.

v - Velocity.

Y_j - Mass fraction of species j.

z - Coordinate along the catalytic chamber.

δ - Void fraction.

η - Utilization factor.

θ - Nondimensional temperature.

μ - Viscosity.

ν - Stoichiometric coefficient.

ξ - Nondimensional distance along the chamber.

ρ - Density.

τ - $T - T_o$.

ϕ - Thiele modulus.

Subscripts

a - ammonia

b - boiling

c - cross section

f - reference value, see formulae (41) and (42)

h - hydrazine

i - interstitial

ind - induction

o - initial

s - surface

t - throat

hom - homogeneous

STEADY STATE ANALYSIS OF HYDRAZINE MONOPROPELLANT THRUSTERS

- - - - - -

I. INTRODUCTION

The purpose of this work is the theoretical analysis of the steady state operation of hydrazine monopropellant thrusters.

In the operation of these thrusters, hydrazine enters in pure form in the catalytic chamber and flows through the interstices between the catalyst porous particles. Part of the hydrazine will leave the interstitial fluid to penetrate into the particles by diffusion and will decompose there catalytically to yield ammonia, hydrogen and nitrogen. The ammonia itself may also decompose catalytically within the particles to yield more hydrogen and nitrogen.

The products of these decomposition reactions, leaving the particles by diffusion, will be incorporated to the intersticial fluid which thus will change in composition when flowing along the chamber of the thruster. Because of the thermal energy release associated with these reactions - positive for hydrazine decomposition and negative for ammonia decomposition a certain amount of heat will leave the particles by heat conduction, resulting in changes in the temperature of the interstitial fluid along the catalytic chamber.

For sufficiently large temperatures of the interstitial fluid the homogeneous gas phase decomposition of hydrazine should also be taken into account.

At the end of the catalytic bed the fluid will then have a certain composition and temperature that will depend upon the operating parameters of the thrusters, i.e., bed loading, bed packing, size of the catalyst particles, length of the catalytic bed and, of course, of the initial state of the hydrazine injected. Knowledge of this state of the fluid, at the end of the catalytic bed, will lead to the determination of the performances of the thruster.

II. *GOVERNING EQUATIONS*

The description of the steady state evolution, along the reaction chamber, of the temperature, pressure and concentration of the interstitial fluid between the catalyst particles, can be obtained from the conservation equations of energy,momentum, and mass for each of the species, together with the equation of state for the mixture.

When writing the mass and energy conservation equations, it will be assumed that the temperature and concentrations are uniform across the chamber. Heat conduction and mass diffusion along the chamber will be neglected, the same that heat losses to the wall of the chamber.

The energy conservation equation states that the increment, per unit distance along the chamber, of the thermal enthalpy flux per unit cross sectional area of the chamber is due to the thermal energy release per unit volume and time associated with two reactions corresponding to the heterogeneous catalytic decompositions of hydrazine and ammonia. Each of these reactions contributes to the mass production rate per unit volume of the individual species, which results in a rate of change of the flux of each species along the chamber.

In the range of temperatures and pressures appropriate for the operation of hydrazine monopropellant thrusters, the overall heterogeneous decomposition reactions of hydrazine and ammonia can be represented by the expressions[1]

$$N_2H_4 \rightarrow NH_3 + 0.5N_2 + 0.5H_2 \qquad (1)$$

$$NH_3 \rightarrow 0.5N_2 + 1.5H_2 \qquad (2)$$

respectively. Reference 1 also gives the following expressions for the corresponding reaction constants per unit mass of reactant

$$k_h = 10^{10}\exp(-1389/T) \qquad (3)$$

$$k_a = 2.53 \times 10^{12}\rho_{H_2}^{-1.6}\exp(-27778/T) \qquad (4)$$

Subscripts h and a mean hydrazine and ammonia respectively. k_h

and k_a are given in sec^{-1} if T is in °K and ρ_{H_2} in gr/l. For the homogeneous decomposition of hydrazine in the interstitial phase, the reaction is also represented by expression (1) and the corresponding reaction rate is[1]:

$$k_h^{hom} = 2.19 \times 10^{10} \exp(-18333/T) \ \frac{1}{sec}$$

To calculate the rates, per unit volume and time, of the thermal energy release and mass production of each species, associated with these heterogeneous reactions, the mass and energy production rates, associated with each individual particle, will be multiplied by the number of particles per unit volume.

In order to write the appropriate governing equations we shall first give a description of the different regions that appear in the catalytic chamber.

There is a first region of the bed chamber, the induction region, in which the hydrazine is still in liquid form and the temperature is below the boiling temperature at the chamber pressure. The heterogeneous decomposition of ammonia will be frozen, and will not make any significant contribution to the decomposition mechanism. The only relevant decomposition reaction, in this region, will then be the catalytic decomposition of hydrazine. It will be shown later that this region ends up with a sudden increase of the temperature to

the boiling temperature of hydrazine. This induction region is followed by a region where the gaseous and liquid hydrazine coexist and when the temperature is approximately equal to the boiling temperature of hydrazine at the governing pressure. It can be shown that the thickness of this two-phase region is very small compared to the thickness of the induction region. At the end of the two-phase region the mixture is in gaseous form.

After this there is a postinduction region where the fluid is in gaseous form and both the heterogenous hydrazine and ammonia decomposition processes are of importance. The interstitial fluid temperature first increases because of the exothermic hydrazine decomposition processes, reaches a maximum and then decreases when the endothermic ammonia decomposition takes over.

The appropriate equations to be used in the postinduction region are:

$$(G/\rho_i)\ \frac{dY_{ji}}{dz} = -K_c^j(Y_{ji}-Y_{js})A_p \qquad (5)$$

$$G\ \frac{dc_p T_i}{dz} = -h_c(T_i - T_s)\ A_p \qquad (6)$$

The first equation expresses that the increase in the mass of the different species in the interstitial fluid is due to the

mass transfer between the catalyst particle and the interstitial fluid. This mass transfer is assumed to be proportional to the difference between the mass fraction of each specie in the particle surface, Y_{js}, and the corresponding value in the interstitial fluid, Y_{ji}. The heat transfer is supposed to be proportional to the difference between the temperatures of the particle surface and the interstitial fluid. j denotes the different species, hydrazine, ammonia, hydrogen and nitrogen. The heat and mass transfer coefficientes, h_c, and K_c^j, can be taken from the literature, for example, Kesten[1] gives:

$$K_c^j = \frac{0.61G}{\rho_i} \left(\frac{A_p \mu}{G}\right)^{0.41} \left(\frac{\rho_i D_{ji}}{\mu}\right)^{0.667} \qquad (7)$$

$$h_c = 0.74 \left(\frac{A_p \mu}{G}\right)^{0.41} c_p G \qquad (8)$$

G is the mass flow rate per unit cross area of the chamber. A_p is external surface area of the catalyst particles per unit volume. Both G and A_p are supposed to be data of the problem.

The contribution of the homogeneous decomposition of hydrazine should also be taken into account en equations (5) and (6), by adding in the right hand side of these equations a term that, for the case of hydrazine decomposition, would be of the form $\delta Y_{hi} k_h^{hom.}$, and that should be compared with $K_c^h Y_{h_i} A_p$. If the nondimensional parameter $K_c^h A_p / \delta k_h^{hom}$ is much larger than one

then the homogeneous hydrazine decomposition can be neglected. This happens for most cases of interest.

The density of the fluid, ρ , is given by the equation of state:

$$p = \rho T R \left[\frac{Y_{H_2}}{2} + \frac{Y_{N_2}}{28} + \frac{Y_a}{17} + \frac{Y_h}{32} \right] \qquad (9)$$

R is the universal gas constant. c_p and μ are known function of the state of the fluid.

The variation of pressure along the chamber can be taken into account by using the momentum equation for which ref.1 gives the following expression, known as Ergun formula.

$$\frac{dp}{dz} = - \frac{1-\delta}{\delta^3} \left[1.75 + \frac{150(1-\delta)}{2aG/\mu} \right] \frac{G^2}{2a\rho} \qquad (10)$$

δ being the void fraction, a the particle radius, and μ the fluid viscosity. However, in our analysis we suppose that the pressure variations are small compared to the pressure itself, and we will use a constant value for p when solving the above conservation equations. After the problem has been solved equation (10) can be used to calculate the pressure less through the chamber.

Equations (5) and (6) can then be considered as a system of five differential equations for the five unknowns: $T_i, Y_{ai}, Y_{hi}, Y_{N_2 i}, Y_{H_2 i}$. The corresponding values of the temperature and mass fractions at the particle surface that also appear in these equations have to be found by a detailed analysis of the processes within the particle. This calculation has been done in Appendix A of this part, where expressions have been found that relate these mass fractions and

temperatures at the particle surface and in the interstitial fluid.

The initial conditions for the system (5) and (6) are provided by the values of the temperature and mass fractions at the end of the vaporization region. Equations (5) and (6) are not appropriate to study the vaporization region. Instead of this,the equations in that region will be written in terms of the utilization factor that is the factor by which we should have to multiply the particle volume and the reaction rate that would be obtained considering that the conditions in the particle are identical to those in the interstitial fluid,to obtain the actual production rate. The appropriate form of this utilization factor has been obtained in Appendix A of this work. However, the detailed solution of the equations in the induction region is not really needed to obtain the initial conditions for the postinduction region. As it will be shown an overall conservation equation for the vaporization region is sufficient to calculate these initial conditions.

III. *INDUCTION REGION*

In the steady operation of hydrazine monopropellant thrusters, the temperature of the fluid in the region adjacent to the injector, - the induction region - although increasing along the chamber due to the heat release within the catalyst particles, is of the same order of magnitude of the temperature of the injected hydrazine.

Due to the large value of the heat of vaporization of hy-

drazine, the induction region is characterized by the fact that the temperature of the interstitial fluid keeps a value very close to the one corresponding to injection until a certain station in which there is a temperature runaway, or precipituous rise in temperature, and the hydrazine, after reaching the boiling temperature, is then rapidly vaporized.

The length of the induction region will be associated with the station where the precipituous rise in temperature occurs. We neglect the additional length required to obtain complete vaporization of hydrazine.

To calculate the evolution of the temperature of the fluid in this region we shall assume that because of the low value of the characteristic temperature in this region, the contribution of the heterogeneous decomposition of ammonia is irrelevant. In addition, it is also necessary to take into account, the heat of vaporization of hydrazine, L, that has to be substracted from the heat of reaction for hydrazine decomposition H_h. With these simplifications the energy conservation equation adopts, in this region, the following form

$$\frac{dT}{dz} = \frac{H_h - L}{Gc_p} \frac{a}{3} A_p k_h \eta \rho Y_h \qquad (11)$$

The functional form of the utilization factor, η, in this region can be obtained by assuming, following the work of

Kesten[1], that liquid hydrazine does not wet the surface of the catalyst particles, so that these particles are surrounded by a gaseous layer in which the hydrazine vapor is in equilibrium with the liquid phase. This assumption means that the concentration of hydrazine at the surface of the catalyst particles is a known function of the temperature and pressure, as given by the Clausius Clapeyron equation. Thus, we shall use in eq. (11) this equilibrium value for the density of hydrazine, and an utilization factor, η , corresponding to the case when a thermal or diffusional boundary layer external to the particle does not exist.

It can be seen that for the conditions appropriate to the operation of these thrusters, the asymptotic form of the utilization factor in this region is given, as shown in Appendix B , by

$$\eta = 3/\Phi_h \tag{12}$$

so that eq. (11) may be written as

$$\frac{dT}{dz} = \frac{H_h - L}{Gc_p \Phi_h} a A_p k_h \rho_{hs} \tag{13}$$

where ρ_{hs} is given by the following approximate form of the Clausius-Clapeyron equation, for constant L , namely

$$\frac{RT}{m_h} \rho_{hs} = p_{vr} \exp(-L/RT) \tag{14}$$

and p_{vr} is a constant. In these equations

$$\Phi_h^2 = a^2 k_h / D_h \quad , \tag{15}$$

where D_h is the diffusion coefficient of hydrazine in the particle, and

$$k_h = b_h \exp(-T_A/T) \tag{3a}$$

so that it is possible to write eq.(13) as

$$\frac{dT}{dz} = \frac{H_h - L}{Gc_p} A_p p_{vr} \frac{m_h}{RT} \sqrt{D_h b_h} \exp\left(- \frac{L/R + T_A/2}{T}\right) \tag{16}$$

to be solved with the initial condition

$$\text{at} \qquad z = 0 \quad , \quad T = T_o \tag{17}$$

It is worth to note that, because of the large value of L/R, the apparent activation temperature, $L/R + T_A/2$, in equation (16), is much larger than the characteristic temperature of the fluid in this region, so that small increments in temperature above the initial value T_o produce large changes in the reaction rate in Eq.(16), by changing the exponential factor without affecting the value of the preexponential factor.

If one is interested in the study of the region in which the temperature departure from its initial value $T - T_o$, is small but sufficient to produce relative increments of order unity in the reaction rate, then this exponential function may

be linearized in the manner of Frank-Kamanetskii[2], as follows,

$$\exp\left(-\frac{L/R + T_A/2}{T}\right) \simeq \exp\left(-\frac{L/R + T_A/2}{T_o}\right) \exp\left(\frac{L/R + T_A/2}{T_o^2}(T - T_o)\right) \quad (18)$$

Therefore by assuming that in this region $\frac{L/R + T_A/2}{T_o^2}(T-T_o)$ is at most of order one, the evolution of temperature is given, in the first approximation by the equation,

$$\frac{d\tau}{dz} = C \exp\left[(L/R + T_A/2)\tau/T_o^2\right] \quad (19)$$

with $\tau = T - T_o$ and the constant C given by the following expression:

$$C = \frac{H_h - L}{c_p} \frac{A_p}{G} p_{vr} \frac{m_h}{RT_o} \sqrt{D_{ho} b_h} \exp\left[-(L/R + T_A/2)/T_o\right] \quad (20)$$

where D_{ho} is the value of the diffusion coefficient for $T = T_o$, the value of the temperature of hydrazine at the injector site.

The effect of the chamber pressure in this equation is through the diffusion coefficient which depends upon the pressure as the inverse of its square root.

With the boundary condition, $T = T_o$ at $z = 0$, the solution of Eq (19) becomes,

$$\tau = -\frac{T_o^2}{L/R + T_A/2} \ln\left[1 - C \frac{L/R + T_A/2}{T_o^2} z\right] \quad (21)$$

It is interesting to note that, according to this equation, τ increases slowly along the axis of the catalytic bed. However, when z approaches a certain value given by

$$z_{ind} = \frac{1}{C} \frac{T_o^2}{L/R + T_A/2} \qquad (22)$$

τ grows very rapidly towards infinity.

By taking C from equation (20) into (22) and using the following values:

$$H_h = 1070 \frac{cal}{gr}$$

$$L = 10300 \frac{cal}{mol}$$

$$c_p = 0.7332 \frac{cal}{gr\ ^oK}$$

$$b_h = 10^{10}\ 1/seg.$$

$$D_h p = 4.487 \times 10^{-5} T^2 New/seg.$$

$$p_{vr} \frac{m_h}{R} = 2.4944 \times 10^8 \frac{Kg}{m^3}\ ^oK$$

$$T_A = 1389^oK$$

$$L/R = 5175^oK$$

equation (22) takes the form:

$$z_{ind} = 5.6381 \times 10^{-19} \frac{G\sqrt{p}}{A_p} T_o^2 \exp \frac{5869.5}{T_o}$$

which is plotted in Fig.1. z_{ind} is given in meters, G in $Kg/m^2seg.$, A_p in $1/m$, p in New/m^2, and T_o in ^oK.

At this section, $z = z_{ind}$, the temperature of the fluid will reach the value corresponding to the boiling temperature of liquid hydrazine at the existing local pressure*. The induction region will be followed by a two phase flow region in which the temperature of the fluid will keep a constant value, equal to the boiling temperature of the liquid; however, since the extent of this two phase flow region is small compared with that of the induction zone, we shall not carry out a detailed analysis of this thin region although we shall take into account its global effects; this is accomplished by considering that, at the end of the induction zone the hydrazine is completely vaporized and that the value of the temperature of the gaseous mixture coincides there with the boiling temperature of liquid hydrazine at the local pressure. In order to estimate the thickness of the two-phase flow region, we shall now make the following calculations. The global energy conservation equation, in the two phase flow isothermal region, simply states that the heat release due to the exothermic catalytic decomposition of hydrazine is entirely absorbed by the vaporization of the liquid hydrazine. Mathematically, if we denote

* The boiling temperature T_b is the temperature for which the partial pressure of the hydrazine given by (14) equals the local pressure or, within our approximation, the injection pressure

$$L/RT_b = \ln(p_{vr}/p)$$

by l^* the length of the isothermal region, then the energy conservation equation adopts the following form:

$$l^* H_h k_h \rho_h^n = LG$$

It is straitforward to see, using Eq (22), that the ratio between this length, l^*, and that of the induction region is

$$\frac{l^*}{z_{ind}} = \frac{L/R + T_A/2}{T_o} \frac{H_h - L}{c_p T_o} \frac{L}{H_h} \frac{A_p a}{3} \sqrt{\frac{D_{ho}}{D_{hb}}} \exp\left[- \frac{T_b - T_o}{T_b \; T_o} \left(\frac{L}{R} + \frac{T_A}{2} \right) \right]$$

which is indeed very small, since the value of the preexponential factor is of order unity while that of the exponential factor is small, of the order of exp(-8).

IV. *POST-INDUCTION REGION*

The post-induction region is the region where the fluid is in gaseous form after it has been vaporized in the previously analyzed induction region. In this region the heterogeneous decomposition processes of ammonia and hydrazine have to be taken into account. Both processes take place within the particle where the products are created and heat is generated or consumed according to whether the hydrazine or ammonia decomposition process is dominant. The products created and the heat generated or consumed diffuse from the particle to the interstitial fluid, as

expressed by equations (5) and (6). The production mechanisms are then dominated by the particle temperature that, as we shall see, is always fairly large and has its maximum value at the beginning of this region, whereas the interstitial temperature reaches its highest value later. The production and diffusion processes within the particle have been studied in the previous part of this work and the results obtained there will be used here.

The initial conditions for equations (5) and (6) state that at the beginning of this region the temperature T of the gaseous mixture takes the value T_b corresponding to the boiling temperature of the liquid hydrazine at the local chamber pressure. We have to determine now the initial values of the mass fractions of the species. In order to do this, we observe that in the previous region only hydrazine was decomposed, according then to the stoichiometry indicated in equation (1), the following relations held for the mass fractions of the different species at the end of the vaporization region

$$Y_{ab} = (17/32)(1 - Y_{hb}) \tag{23}$$

$$Y_{N_2b} = (14/32)(1 - Y_{hb}) \tag{24}$$

$$Y_{H_2b} = (1/32)(1 - Y_{hb}) \tag{25}$$

The mass fraction of hydrazine Y_{hb} is determined by ap-

plying the global energy conservation equation between the injection section and the section marking the end of the induction region; if we neglect the small contribution of the changes in kinetic energy, this energy equation states that the specific enthalpy of the fluid must be constant. Thus we obtain

$$h_{h_o} = \left[h_h Y_h + (17h_a + 14h_{N_2} + h_{H_2})(1 - Y_h)/32 \right]_b \qquad (26)$$

In this equation h_j is the specific enthalpy of species j and h_{ho} is the specific enthalpy of the liquid hydrazine at the temperature of injection. From equation (26) it is obtained the following correlation giving Y_{hb} as function of T_b

$$Y_{h_b} = 0.87 - 0.0006T_b \qquad (27)$$

deduced by substituting the values of the enthalpies[2] in equation (26) for the intervals

$$273 \leq T_o \leq 300°K$$

$$400 \leq T_b \leq 600°K$$

The dependence of Y_{hb} with T_o is very slight for the above interval and consequently has been neglected.

Our initial conditions for the equations (5) and (6) are given by equations (23), (24), (25) and (27) with

$$T_i = T_b \qquad (28)$$

The terms of the right hand side of equation (5) have been obtained in the Appendix A of this part, that gives for the species production:

$$Y_{ji} - Y_{js} = - \frac{\nu_{aj} c_a}{\rho_i K_c^j} - \nu_{hj} \frac{K_c^h}{K_c^j} Y_{hi} \qquad (29)$$

$$j = N_2 , H_2 , a \quad , \quad \nu_{aa} = -1 \ .$$

and

$$Y_{hs} = 0 \qquad (30)$$

The hydrazine mass fraction at the particle surface was found to be very small compared to the corresponding value in the interstitial fluid.

The last term of (29) expresses the contribution of hydrazine decomposition within the particle, ν_{hj} being the stoichiometric coefficients for hydrazine decomposition. The first term of the right hand side of (29) gives the contribution of ammonia decomposition and c_a is given by:

$$c_a = \rho_s D_{as} \frac{Y_{as}}{a} A \qquad (31)$$

where D_{as} is the diffusion coefficient for ammonia within the particle evaluated at the conditions of the particle surface, and

$$A = \phi \ \mathrm{cth} \ \phi - 1 \qquad (32)$$

$$\phi = \sqrt{\frac{k_{as} a^2}{D_{as}}} \qquad (33)$$

k_{as} is the reaction rate for ammonia decomposition (equation (4)) evaluated at the particle surface.

The right hand side term of equation (6) that gives the heat production within the particle is given by:

$$T_i - T_s = \frac{H_a c_a}{h_c} - \frac{H_h \rho_i K_c^h}{h_c} Y_{hi} \qquad (34)$$

where as before the first term of the right hand side expresses the heat consumed in the ammonia decomposition, and the second one the heat released in the hydrazine decomposition. With equations (29) to (34) the right hand side of equations (5) and (6) are expressed as implicit functions of the conditions in the interstitial fluid in the form:

$$\frac{G}{\rho_i} \frac{dY_{hi}}{dz} = -K_c^h A_p Y_{hi} \qquad (35)$$

$$G \frac{d}{dz} (Y_{ji} + \nu_{hj} Y_{hi}) = A_p \nu_{aj} c_a \qquad (36)$$

$$j = a \ , \ N_2 \ , \ H_2$$

$$G \frac{d}{dz} (c_p T_i + H_h Y_{hi}) = -H_a c_a A_p \qquad (37)$$

By combining linearly equation (36) corresponding to ammonia

conservation with the other two equations corresponding to hydrogen and nitrogen conservation and the energy equation (37) it is possible to cancel the effect of the ammonia decomposition expressed by the right hand side of these equations. In this way we can express that the following linear combinations of temperature and concentrations do not change with z

$$\nu_{aN_2}\,(Y_{ai} + \nu_{ha}Y_{hi}) + Y_{N_2 i} + \nu_{N_2 h}\,Y_{hi} = \nu_{aN_2}\nu_{ha} + \nu_{N_2 h} \qquad (38)$$

$$\nu_{aH_2}\,(Y_{ai} + \nu_{ha}Y_{hi}) + Y_{H_2 i} + \nu_{H_2 h}\,Y_{hi} = \nu_{aH_2}\nu_{ha} + \nu_{H_2 h} \qquad (39)$$

$$H_a\,(Y_{ai} + \nu_{ha}Y_{hi}) - c_p T_i - H_h\,Y_{hi} = H_a\nu_{ha} - c_p T_b - H_h Y_{hb} \qquad (40)$$

where the right hand sides of these equations have been calculated using the initial conditions (23) to (25) that can be alternatively written as

$$Y_{jb} + \nu_{hj}Y_{hb} = \nu_{hj} \qquad (23a)$$

$$j = a\,,\ N_2\,,\ H_2$$

and equation (28).

In analogous way it is possible to combine equations (29) and (34) to eliminate the term containing the ammonia production, and an algebraic combinations similar to those expressed by (38) to (40) can also be obtained. As a matter of fact, the only difference will consist in making the substitutions

$$Y_{ji} \rightarrow K_c^j (Y_{ji} - Y_{js}) \quad , \quad Y_{hs} = 0$$

$$c_p T_i \rightarrow \frac{h_c}{\rho_i} (T_i - T_s)$$

in the left hand side of these equations and equating them to zero. If we assume that the Schmidt numbers for the different species are approximately equal to one then

$$K_c^j = K_c = \frac{h_c}{\rho_i c_p} = \frac{0.74G}{\rho_i} \left(\frac{A_p \mu}{G}\right)^{0.41} \quad , \qquad (7a)$$

and equations (38) to (40) are valid for the mass fractions and temperature of the particle surface, taking into account that Y_{hs} is equal to zero. Using the stoichiometric coefficients corresponding to equations (1) and (2) we obtain the following relations equivalent (38) to (40)

$$\frac{14}{17} Y_{ai} + Y_{N_2 i} + \frac{7}{8} Y_{hi} = \frac{7}{8} \qquad (38a)$$

$$\frac{14}{17} Y_{as} + Y_{N_2 s} = \frac{7}{8} \qquad (38b)$$

$$\frac{3}{17} Y_{ai} + Y_{H_2 i} + \frac{1}{8} Y_{hi} = \frac{1}{8} \qquad (39a)$$

$$\frac{3}{17} Y_{as} + Y_{H_2 s} = \frac{1}{8} \qquad (38b)$$

$$\left(Y_{ai} + \frac{17}{32} Y_{hi}\right) - \frac{c_p}{H_a}\left(T_i + \frac{H_h}{c_p} Y_{hi}\right) = \frac{17}{32} - \frac{c_p}{H_a}\left(T_b + \frac{H_h}{c_p} Y_{hb}\right) \quad (40a)$$

$$Y_{as} - \frac{c_p}{H_a} T_s = \frac{17}{32} - \frac{c_p}{H_a}\left(T_b + \frac{H_h}{c_p} Y_{hb}\right) \quad (40b)$$

The values of Y_{ai} , Y_{hi} , and Y_{as} needed to complete the system (38a) to (40b) are obtained from the equations (35), (36) (for j = a), and (29) (for j = a).

In order to solve these equations the temperatures were made nondimensional with the value

$$T_f = T_b + \frac{H_h}{c_p} Y_{hb} \quad , \quad \theta = T/T_f \quad , \quad (41)$$

that can be interpreted as the maximum temperature that would be reached by the mixture is there would not be ammonia decomposition. In an analogous way we can define a reference value of the density, ρ_f , that would correspond to the temperature given in (41) and mass fractions of (17/32), (1/32), and (14/32) for the ammonia, hydrogen and nitrogen respectively, that would correspond to the same physical situation presented above:

$$\rho_f = 32\rho_{H_2 f} = (pm_f)/(2RT_f) \quad (42)$$

The distance along the chamber is made nondimensional with a length related to the external mass transfer to the particle

$$\xi = z\left(\frac{\rho_f}{G}\right) A_p K_{cf} = 0.74\, A_p \left(\frac{A_p \mu_f}{G}\right)^{0.41} z \quad (43)$$

with this, equation (35) becomes

$$\frac{dY_{hi}}{d\xi} = -Y_{hi}\left(\frac{\mu}{\mu_f}\right)^{0.41} = -Y_{hi}\theta_i^{0.41} \qquad (44)$$

if we assume that the viscosity varies linearly with the absolute temperature. Equation (36) for ammonia decomposition with the value of c_a taken from (31) can be written:

$$\frac{d}{d\xi}\left(Y_{ai} + \frac{17}{32}Y_{hi}\right) = -\left(\frac{D_{af}}{K_{cf}a}\right)\left(\frac{\rho_s}{\rho_f}\right)\left(\frac{D_{as}}{D_{af}}\right)Y_{as}A \qquad (45)$$

In this equation the factor $(\rho_s/\rho_f)(D_{as}/D_{af})$ can be expressed as function of the non-dimensional particle temperature θ_s, and the mass fractions of the particle if we assume that the ammonia diffusion coefficient within the particle can be expressed as a product of different powers of pressure and temperature. In our calculations we shall assume that

$$D_a = BT^2/p \qquad (46)$$

that would correspond to the case where diffusion in the particle is in the continuum limit. The parameter A is related to the Thiele modulus ϕ, by equation (32) and from equation (33), can be expressed as:

$$\phi = \phi_f\left(\frac{k_a}{k_{af}}\right)^{1/2}\left(\frac{D_{af}}{D_a}\right)^{1/2} \quad ; \quad \phi_f^2 = k_{af}a^2/D_{af} \qquad (47)$$

From equations (4) and (46) that give k_a and D_a and using (41)

and (42) it can be seen that the ratios k_a/k_{af} and D_{af}/D_a can be expressed as functions of θ_s , the mass fractions at the particle surface and the parameter T_a/T_f , where T_a is the activation temperature for ammonia decomposition (equation (4)) equal to 27778°K.

Equation (29) for j = a can be written as:

$$Y_{ai} - Y_{as} = \left(\frac{D_{af}}{aK_{cf}}\right) AY_{as} \left(\frac{\rho_s}{\rho_f}\right) \left(\frac{\rho_f}{\rho_i}\right) \left(\frac{D_{as}}{D_{af}}\right) \left(\frac{K_{cf}}{K_c}\right) - \frac{17}{32} Y_{hi} \qquad (48)$$

In an analogous way it can also be seen that the last four factors of this equation only depende on θ_s , θ_i and the mass fractions.

So far,if equations (35) (36) (for j = a) and (29) (for j = a), are written in non-dimensional form ((44), (45) and (48)) only the three non-dimensional parameters $(D_{af}/K_{cf}\,a)$, (T_a/T_f) and ϕ_f appear in our problem. In addition we shall also consider the parameters appearing in the algebraic system (38a) to (40b):

$$\nu_{ij} \;,\; \frac{c_p T_f}{H_a} \;,\; \frac{c_p T_f}{H_h}$$

and those related to the initial conditions for the postinduction region (equations (27) and (28)) that are

$$\theta_i(o) = \theta_b = T_b/T_f \quad , \quad Y_{hb} \qquad (49)$$

However, it turns out that the dimensional number $0.0006°K^{-1}$

appearing in (27) is very approximately equal to H_h/c_p. Then, on using equations (41) and (27) we obtain that

$$Y_{hb} = 0.87 - \frac{H_h}{c_p T_f}\,\theta_b \qquad (50)$$

and that T_f is constant equal to 1450°K. If we assume as we already have done that the stoichiometric ratios ν_{ij} are those corresponding to equations (1) and (2) and that the numbers $c_p T_f/H_a$, $c_p T_f/H_h$, T_a/T_f are constant, because T_f is also constant, the only parameters appearing in our problem will be:

$$D_{af}/(K_{cf}a) \quad , \quad \phi_f \quad , \quad \text{and} \quad \theta_b$$

However, it frequently happens that the Thiele modulus ϕ is a large quantity and then A (equation (32)) can be written as

$$A \simeq \phi \qquad (32,a)$$

Then in equations (48) and (45) only could appear as a parameter the product of $D_{af}/(K_{cf}a)$ and ϕ_f that we shall denominate J_1

$$J_1 = (k_{af}D_{af})^{1/2}/K_{cf} \qquad (51)$$

We observe that in this approximation the particle radius does not appear in our problem. This is due to the fact that both hydrazine and ammonia decomposition take place at the particle surface in the limit of large Thiele modulus. The parameter J_1 can be interpreted as giving the ratio between the characteristic velocity for diffusion of ammonia within the particle associated to its chemical production and the velocity of external

diffusion from the interstitial fluid to the particle. It may be more convenient to operate with the associated heat transfer processes, consequently we modify the definition of J_1, by multiplying it by the factor $(H_a/c_p T_f)$ and calling it J

$$J = H_a(k_{af}D_{af})^{1/2}/(c_p T_f K_{cf}) \qquad (52)$$

All our calculations will be presented for different values of J , ϕ_f , and θ_b . For large values of ϕ_f the results will only depend on J and θ_b . On the other hand θ_b only depends on the boiling temperature of hydrazine that in turn only varies with chamber pressure. If the chamber pressure changes from 7 to 70 atm the values of θ_b vary from 0.31 to 0.39, on the other hand, in practical cases J can vary by a factor of one hundred. Consequently we may conclude that in most practical cases the behaviour of the thruster can be characterized by the single parameter J.

Another way of writing the parameter, J , will be by substituting the values of k_{af} , D_{af} , and K_{cf} from equations (4), (46) and (7a) with the reference values of densities and temperatures given in equations (41) and (42), into equation (52):

$$J = \left[\frac{13.7H_a(Bb_a)^{1/2}\exp(T_a/2T_f)}{c_p(RT_f/m_h)^{0.2}}\right]\frac{1}{p^{0.3}G(A_p\mu/G)^{0.41}} \qquad (53)$$

where b_a is the preexponential factor $2.53\times10^{12}(gr/l.)^{1.6}/sec.$

appearing in equation (4). The first factor in equation (53) is constant, and for $B = 2 \times 10^{-8}$ $(dm^2/sec.)(atm/°K^2)$, its value is 200 $atm^{0.3}gr/dm^2sec$. J will then change proportionally to $G^{-0.59}$, $p^{-0.3}$, and $A_p^{-0.41}$, and its range of variation for typical thruster behaviours is between 0.1 and 10.

The results of the integration of a typical case with values of J = 0,56, $\phi_f = 90$, and $\theta_b = 0,31$ has been presented in figure 2.

The temperature at the surface of the particle, θ_s , has its maximum value at the beginning of this region, and decreases afterwards, whereas the interstitial temperature reaches a maximum, and then decreases. This maximum value occurs when the interstitial and particle temperatures are equal, then, there is no net heat transfer from the particle to the interstitial fluid and the heats evolved from the hydrazine decomposition and the ammonia decomposition are exactly equal and opposite. Before this moment, the heat evolved from the hydrazine decomposition is larger than that corresponding to the ammonia decomposition, and the net reaction is exothermic and the interstitial temperature increases, after that moment the opposite occurs and the interstitial temperature decreases. Consequently also before this maximum is reached the particle surface temperature has to be larger than the interstitial temperature, because heat is transferred from the particle to the fluid, and

the opposite occurs after the maximum is reached.

As we said before, the hydrazine decomposition is being governed by the rate at which the hydrazine is transferred to the particle, because as soon as it reaches the catalyst surface it is rapidly decomposed, consequently the distance in which hydrazine will be decomposed will be inversely proportional to the mass transfer coefficient multiplied by the specific catalyst particle divided by the specific flow rate, but this is exactly the variable with which the distance along the chamber has been made non-dimensional, consequently the hydrazine will disappear exponentially in non-dimensional distances of order unity.

The ammonia decomposition reaction is slow due to the high activation temperature of that reaction, and when the heats evolved from the hydrazine and ammonia reactions are equal, it is because the hydrazine concentration has become very small. So when the maximum interstitial temperature is reached the hydrazine concentration is already small. Consequently we can also say that after the maximum is reached, the only reaction will essentially be the ammonia decomposition. Since the ammonia concentration is decreasing, and the catalyst surface temperature is also decreasing, the heat evolved from the reaction will be decreasing and the difference between the interstitial and surface temperatures will become smaller along the chamber. All

the variations of the properties will be much slower in the ammonia decomposition region, and these variations will be decreasing along the chamber.

At the beginning the ammonia mass fraction increases because hydrazine decomposes, then, when the ammonia decomposition is more important, the ammonia mass fraction will start to decrease.

The hydrogen and nitrogen mass fractions will increase along the chamber because both reactions will contribute to that increase.

In figure 2 is also presented the value of the maximum specific impulse that would be obtained if the catalytic chamber would be terminated at the corresponding stage, and the gaseous mixture would be expanded to the vacuum. The maximum velocity obtained in this way is

$$v = \sqrt{2h}$$

where

$$h = \Sigma h_i Y_i \quad , \quad i = h,\ a,\ N_2,\ H_2$$

and the values of h_i have been taken from ref.2. The specific impulse is then

$$I = v/g \ .$$

In figure 2 it can be seen that the specific impulse first increases, then reaches a maximum and afterwards decreases very

slowly, this is associated to the variations of the interstitial temperature. However, the specific impulse decreases much more slowly than the interstitial temperature, this is due to the fact that hydrogen, whose molecular weight is very low, is being produced.

In figures 3 and 4 are presented the maximum values of the interstitial and catalyst surface temperatures, θ_i , θ_s , as functions of J for different values of ϕ_f and for the two pressures 7 atm, and 70 atm respectively that correspond to the initial values of the interstitial temperature, θ_b , 0.31 and 0.39 respectively.

In these figures it can be seen that as the parameter J increases (mass flow rate, specific catalyst surface, and operating pressure decreasing) both temperatures decrease. The reference value of the Thiele modulus for ammonia decomposition ϕ_f is usually large, its minimum value for practical applications is around 50. However, it should be noticed that the actual Thiele modulus appearing in equation (32) is smaller because ϕ_f has been evaluated for $\theta_f = 1$ that is always larger than θ_s. Nevertheless, it can be seen in figures 3 and 4 that the influence of the Thiele modulus is still small, and that the curves giving the maximum values of θ_i and θ_s for a finite value of ϕ_f do not differ significantly from those corresponding to an infinite value of ϕ_f that would correspond to taking the value of A equal

to ϕ as expressed in formula (32a). It should be noticed that ϕ_f is proportional to $a/p^{0.3}$ so that, for the same particle radius, as the pressure increases the Thiele modulus is smaller, this is the reason why we have put different values of ϕ_f in figures 3 and 4.

In figure 5 are presented the maximum values of θ_s and θ_i as functions of J for ϕ_f equal to infinity and the two values of θ_b, 0.31 and 0.39 that correspond to pressures of 7 and 70 atm respectively. It should be noticed that although the operating pressure changes by a factor of 10, the corresponding values of the boiling temperature do not differ significantly and its influence in the variation of θ_s and θ_i is small.

The dependence of the maximum values of θ_s and θ_i with ϕ_f and θ_b is very small for small values J (large values of the flow rate). The following interpretation can be given for this lack of dependence with ϕ_f . As it was seen before as J decreases θ_i and θ_s increase, and the corresponding actual value of ϕ to be used in (32) will be larger.

In figures 6 and 7 are presented the maximum values reached by the specific impulse along the chamber as a function of J for different values of the reference Thiele modulus ϕ_f and for θ_b = 0.31 and 0.39 respectively. As J, ϕ_f , and θ_b increase the specific impulse decrease, however, these last two parameters

have a smaller influence as it happened with the interstitial and particle surface temperatures.

So far it has been assumed that the mass flow rate, $S_c G$, and the chamber pressure, p , are indepent quantities. However, if we have a given thruster and type of catalyst, those two parameters are no larger independent and are related by

$$\frac{GS_c}{S_t} = \frac{p}{\sqrt{RT_c/m}} \left(2/(\gamma+1)\right)^{(\gamma+1)/2(\gamma-1)} \sqrt{\gamma}$$

where S_c and S_t are the cross sectional areas of the chamber and of the nozzle, T_c is the chamber temperature where the catalytic region ends, that is assumed to be the stagnation temperature for the nozzle flow, m is the mean molecular weight, and γ is the ratio of the specific heats of the mixture. γ and m can be calculated if the composition of the mixture is known, this and the value of T_c can be obtained by integrations similar to those whose results appear in figure 2. However, from this figure 2 and figures 3, 4, and 5 it can be seen that the temperature does not change much neither with chamber length (once we are in the ammonia decomposition region) nor with operating conditions. On the other hand it can also be seen that γ and m do not vary much. Then G will be proportional to p and the parameter J will vary like $p^{0.89}$ for a given thruster.

V. *PRESSURE DROP*

As it was stated in paragraph II, the pressure along the chamber decreases in an amount that is small compared with the absolute value of the pressure itself. By using the results obtained previously we shall be able to calculate this pressure drop along the catalytic chamber.

To integrate Ergun formula {equation (10)} it is necessary to know the variations of μ and ρ_i along the chamber. This can be done by using the results of the previous paragraph. On using the equation of state (9) the non-dimensional distance along the chamber given by equation (43) and the non-dimensional temperature given by equation (41), Ergun formula (10) can be integrated in the form:

$$p^2 - p_b^2 = \frac{1}{0.74}\left(\frac{G}{A_p\mu_f}\right)^{0.41}\frac{1-\delta}{\delta^3}(A_p a)\frac{RT_f}{G^2}\times$$

$$\times\int_o^{\xi}\left[1.75+\frac{75(1-\delta)}{2(A_p a)(G/A_p\mu_f)}\theta_i\right]\theta_i\left[\frac{Y_{H_2}}{2}+\frac{Y_{N_2}}{28}+\frac{Y_a}{17}+\frac{Y_h}{32}\right]^{-1}d\xi \qquad (54)$$

where p_b is the pressure at the end of the vaporization region, approximately equal to the injection pressure if we neglect the small pressure drop in the vaporization region that on one hand is short, and on the other hand has a much smaller pressure drop per unit length because of the low liquid velocity. This can be easily seen from Ergun formula (10) if we neglect the influence

of viscosity; dp/dz is proportional to G^2/ρ, G is the same in the liquid and gas regions, however, ρ is much larger in the liquid region. The integral in the right hand side of equation (54) can be evaluated with the results of the previous integrations that give the values of θ_i and Y_j as function of ξ.

Catalytic chamber lengths are chosen according to stability reasons and ignition criteria and are usually much larger than the length of the initial hydrazine decomposition region where the interstitial temperature increases (figure 2). Most of the pressure drop contribution will come from the ammonia decomposition region where the interstitial temperature and the concentrations will vary very slowly. On the other hand if also our earlier assumption of considering that the pressure decrease is small compared to the pressure itself is valid, the right hand side of equation (10) will be independent of z and can be integrated readily giving a linear variation of the pressure decrease with z. With this, the total pressure drop can be written in the form:

$$\frac{\Delta p}{p} = 1.75 \left(\frac{1-\delta}{2\delta^2}\right)\gamma M^2 \left(\frac{l}{a}\right)$$

if we assume that the Reynolds number (aG/μ), as it usually happens, is large and we can neglect the second term in the right hand side of equation (10). Although the chamber length, l, is much larger than the particle radius, a, the Mach number at the

end of the catalytic chamber is very small and our earlier assumption of considering Δp much smaller than p usually holds. For example if S_c/S_t is 30 and $\gamma = 1.4$ the corresponding Mach number is 0.02.

V. *CONCLUSIONS AND COMPARISON WITH EXPERIMENTS*

The theoretical analysis of the steady state operation of hydrazine monopropellant thrusters has been made by dividing the length of the chamber in three regions:

a) *Induction region*: goes from the injector until the point where the boiling temperature is reached. The hydrazine is in liquid form. The length of this region is given analytically in (22), and its value multiplied by $A_p/G\sqrt{p}$ turns out to be a function of only the injection temperature that is presented in Fig.1. The temperature distribution in this region is given by equation (21).

b) *Two-phase flow region*: its length is short compared to the induction length and the temperature remains constant equal to the boiling temperature.

c) *Post-induction region*: in this region the fluid is in gaseous form and both hydrazine and ammonia decompose simultaneously. The temperatures of the interstitial temperature and the surface of the catalyst particle are different. This difference

is more important at the beginning when the exothermic hydrazine decomposition process dominates over the endothermic ammonia decomposition process. This fact has also been noticed in reference 4. In figure 2 is given a plot of the variations of all the relevant properties of the mixture along the catalyst chamber for a particular case. In figures 3 to 7 are presented the variations of the most important overall properties of the thruster in steady state behaviour as functions of three nondimensional parameters, namely, nondimensional boiling temperature, reference value of the Thiele modulus, and a parameter called J that is the ratio of the velocities of the heat generated within the particle and that corresponding to the external heat transfer to it. However, it looks as though, for practical cases, the most relevant parameter is J and the dependence with the other two parameters is not significant, particularly for low values of J. The parameter J decreases as the specific mass flow rate, the operating pressure, and the specific particle surface area increase, and for a a particular geometry and granulometry of the thruster is inversely proportional to the operating pressure raised to the power 0.9. The maximum value of the catalyst surface temperature, that is reached at the beginning of the postinduction region, decreases as J increases. The same behaviour exhibit the maximum interstitial temperature, that is reached at the stage of the chamber where the heats evolved from the endothermic reactions are equal, and the maxi-

mum value of the specific impulse that is also attained approximately at that location. It is found (see figure 2) that if the catalyst chamber would be larger than the stage corresponding to the maximum specific impulse, no significant decrease of this quantity will be noticed; this is due to the production of hydrogen, whose molecular weight is low, that somewhat compensates the decrease of interstitial temperature. Because of this reason it has not been considered of interest to calculate any characteristic chamber length associated to this region, on the other hand the lengths of these chambers are usually much larger than those needed to reach maximum specific impulse, and they are imposed by reasons related to the stability and ignition characteristics of the thruster that lie outside the scope of this work.

A series of experiments have been carried out at INTA to measure the fluid temperature along a catalytic chamber for hydrazine decomposition. The chamber is 20.5 mm. long and has an internal diameter of 16 mm., the fluid discharges to ambient pressure through a convergent divergent nozzle whose throat area is 1/64 of the catalyst chamber cross sectional area. The temperature is measured at three points in the axis of the chamber located at 3 mm., 9.5 mm., and 16 mm. from the entrance by means of Pt Rh-Pt thermocouples and a recorder. Sufficient time was allowed to elapse during each firing so that the signal in the

recorder will show that a steady state has been reached. The operating pressures ranged from 3.5 to 14 atm. and the bed packing was taken to consist of 8-12 mesh size catalyst particles of Shell 405 in some cases, and 20-25 in others. A comparison has been carried out of these results with our theoretical predictions, although this comparison shows a good qualitative agreement, the predicted temperatures seem to be lower than the ones that have been measured. A much better agreement is obtained by comparing our theory with the temperature measurements made at the Rocket Research Corporation.[7]

In figure 5 the maximum measured temperatures have been plotted as function of the parameter J. It can be seen that the maximum temperature decreases as the parameter J increases. Most of the measured temperatures are between the maximum values of the particle and interstitial temperatures, this may be due to the fact that there is an uncertainty in which temperature has been really measured. In figure 8 are plotted the calculated values of T_i and T_s as functions of axial distance and the temperatures obtained experimentally for an operating pressure of 3.5 atm. and a granulametry corresponding to a 20-25 mesh size. The vaporization length of the induction region has been disregarded because the above calculations give that is of the order 10^{-2} mm. in this case.

REFERENCES

1. KESTEN, A. : "Analytical Study of Catalytic Reactors for Hydrazine Decomposition" NASA, UACRL F910461-12, May 1967.

2. FRANK-KAMANETSKII, D.A. : "Diffusion and Heat Transfer in Chemical Kinetics" Chapter VI, Pergamon Press, 1969.

3. JANAF Thermochemical Tables 2nd edition. National Bureau of Standards. June 1971.

4. KESTEN, A. : "Analytical Study of Catalytic Reactors for Hydrazine Decomposition" NASA, UARL G910461-24, May 1968.

5. E. E. PETERSEN : "Chemical Reaction Analysis" Prentice-Hall (1965).

6. R. ARIS : "Introduction to the Analysis of Chemical Reactors" Prentice-Hall. 1965.

7. Rocket Research Corporation: Development of Design and Scaling Criteria for Monopropellant Hydrazine Reactors Employing Shell 405 Spontaneous Catalyst. RRC-66-R-76. January 1967.

A P P E N D I X A

ANALYSIS OF CATALYTIC DECOMPOSITION OF HYDRAZINE WITHIN A CATALYTIC PARTICLE WITH A TWO STEP REACTION MECHANISM AND EXTERNAL TRANSPORT RESISTENCE

- - - - - - - -

When studying the catalytic decomposition of hydrazine in vapor form, it is found that this decomposition process should not be described by an overall reaction as it was assumed in the analysis carried out in part III of this work. Because of this reason it is necessary to readapt the analysis of that part so that it can be used in the present part IV for the analysis of hydrazine thrusters.

A theoretical analysis is presented for the catalytic decomposition of hydrazine within a porous particle, when the reaction is modelled by means of a two step reaction mechanism. In the first step the hydrazine decomposes exothermically to generate ammonia, hydrogen and nitrogen. In the second step the ammonia decomposes endothermically generating hydrogen and nitrogen.

The first reaction is very fast and, as a result, the hydrazine is found to decompose very close to the surface of the

particles. The ammonia generated in the thin hydrazine reaction region is lost to the interstitial fluid or diffuses inward to the interior of the particle, where it decomposes in a region adjacent to the thinner hydrazine decomposition region.

The thickness of the ammonia decomposition region is small compared with the particle radius for high temperatures at the particle surface; the interior of the particle is then free from ammonia. For small surface temperatures the ammonia decomposition is found to be kinetically controlled; with small temperature and concentration differences within the particles.

The analysis provides analytical expressions for the rate of consumption, per particle, of hydrazine and ammonia, in terms of the temperature and composition of the gaseous mixture bathing the particle and the physical properties of the porous particle.

The chemical reactions occurring within the catalytic particles are modelled, according to Kesten[1], by a reaction mechanism involving two reactions of overall stoichiometry

$$N_2H_4 \rightarrow NH_3 + 0.5N_2 + 0.5H_2 \qquad (A1)$$

$$NH_3 \rightarrow 0.5N_2 + 1.5H_2 \qquad (A2)$$

and reaction rates, per unit particle volume

$$k_h = 10^{10}\, e^{-1389/T} \qquad (A3)$$

$$k_a = 2.53 \times 10^{12} \rho_{H_2}^{-1.6} e^{27778/T} \qquad (A4)$$

where k_h and k_a are the consumption rates of hydrazine and ammonia respectively per unit mass of reactant.

Because of the coexistence of the two reactions within the catalytic particle, the results of the analysis presented previously in this part for a single reaction, see also Petersen[5] and Aris[6] are not directly applicable. However the Thiele modulus ϕ_h^2 for hydrazine decomposition is so large, for particle sizes of interest, that the hydrazine decomposition occurs within a very thin layer adjacent to the particle surface (see figure A-1). In this thin layer the amount of ammonia decomposition, of much lower Thiele modulus ϕ_a^2 , can be neglected in first approximation. The hydrazine reaction layer is so thin that conservation equation take, there, the one-dimensional form

$$\frac{\partial^2 Y_h}{\partial r^2} = \frac{k_h Y_h \rho_p}{\rho_p D_{hp}} \qquad (A5)$$

$$\frac{\partial^2 Y_j}{\partial r^2} = - \frac{\nu_{hj} k_h Y_h \rho_p}{\rho_p D_{jp}} \qquad (A6)$$

$$\frac{\partial^2 T}{\partial r^2} = - \frac{H_h k_h}{K_p} \rho_p Y_h \qquad (A7)$$

for the mass conservation of hydrazine, Eq(A5), all other species Eq(A6), and energy Eq(A7). Here ν_{hj} are stoichiometric coeffi-

cients, equal to $\frac{17}{32}$, $\frac{1}{32}$ and $\frac{14}{32}$ for ammonia, hydrogen and nitrogen respectively. H_h is the energy released per unit mass of hydrazine decomposed according reaction (A1).

The heat conduction coefficient K_p and the product $\rho_p D_{hp}$ and $\rho_p D_{jp}$ of the density and diffusion coefficients within the particles are considered as constant when writing Eqs.(A5) to (A6). However this assumption is substantiated by the results of the analysis. Consequently we shall use instead the corresponding values of these coefficients at the particle surface $\rho_s D_{js}$ and K_s.

The boundary conditions for these equations are derived from the mass and energy conservation principles at the interface between the particles and the interstitial fluid. Thus

$$\rho_s D_{js} \left.\frac{\partial Y_j}{\partial r}\right|_{r=a} = \rho_i K_c^j (Y_{ji} - Y_{js}) \qquad (A8)$$

$$K_s \left.\frac{\partial T}{\partial r}\right|_{r=a} = h_c (T_i - T_s) \qquad (A9)$$

where the subscript s and i refers to the conditions at the particle surface and mean conditions of the interstitial fluid. The coefficients K_c^j and h_c account for the mass and heat transfer from the interstitial fluid to the particle. They can be written in terms of the diffusion and heat conduction coeffi-

cients D_{ji} and K_i of the interstitial fluid, the particle radius a, as

$$K_c^j = \sigma^j D_i^j / a \tag{A10}$$

$$h_c = \nu K_i / a \tag{A11}$$

where σ^j and ν are the Sherwood and Nusselt numbers, which are functions of the Reynolds number based on the interstitial mean velocity and particle radius. See for example the book by Aris[6].

The boundary conditions at the interior of the reaction zone will be given below, as obtained from the matching conditions with the solution for the thicker interior region of ammonia decomposition.

From (A5)-(A7) we obtain

$$\rho_s D_{js}(Y_j - Y_{js}) + (Y_h - Y_{hs})\nu_{hj} D_{hs} \rho_s = c_j (r-a) \tag{A12}$$

$$K_s(T - T_s) + (Y_h - Y_{hs}) H_h \rho_s D_{hs} = c_T (r-a) \tag{A13}$$

where, if we take into account the boundary conditions (A8) and (A9) in the particle surface, the constant c_j and c_T, can be written in terms of the gradients of the concentrations and temperature just inside the hydrazine reaction zone,

$$c_j = \rho_i (Y_{ji} - Y_{js}) K_c^j + \rho_i (Y_{hi} - Y_{hs}) \nu_{hj} K_c^h \tag{A14}$$

$$c_T = (T_i - T_s) h_c + (Y_{hi} - Y_{hs}) \rho_i H_h K_c^h \tag{A15}$$

The stoichiometric coefficients ν_{hj} , according to (A1), have the values 17/32, 14/32 and 1/32 for ammonia, nitrogen and hydrogen, respectively. The conservation equation (A5) for hydrazine can be integrated formally, once, to give

$$\frac{1}{2}\left(\frac{\partial Y_h}{\partial r}\right)^2 = \int_o^{Y_h} (k_h \rho_p Y_h / \rho_s D_{hs}) dY_h \qquad (A16)$$

if we use the boundary condition $Y_h \to 0$, and therefore $\partial Y_h/\partial r \to 0$, for large values of (a-r), inside the hydrazine decomposition zone. At the particle surface, r = a , the concentration gradient is given by (A8), and $Y_h = Y_{hs}$, so that from (A16) we obtain

$$\frac{1}{2}\left\{\rho_i K_c^h (Y_{hi} - Y_{hs})/\rho_s D_{hs}\right\}^2 = \int_o^{Y_{hs}} (k_h \rho_p Y_h / \rho_s D_{hs}) dY_h \qquad (A17)$$

We can use (17) to obtain an order of magnitude estimate of Y_h and Y_{hs}

$$Y_h \sim Y_{hs} \sim Y_{hi} \sigma^h \frac{D_{hi}}{D_{hp}} \sqrt{\frac{D_{hs}}{a^2 k_{hs}}} \qquad (A18)$$

and for typical values of the right hand side of relation (A18) we obtain

$$Y_{hs} << Y_{hi} \qquad (A19)$$

That is, the rate constant of the catalytic decomposition of hydrazine is so large that the mass fraction of hydrazine in the reaction zone takes a small value compared with Y_{hi} , dictated

by the amount of hydrazine reaching the particle surface from the interstitial fluid. The ammount of hydrazine decomposition is thus controlled by the external diffusion to the catalytic particles. It is equal, per unit particle surface, to $\rho_i K_c^h Y_{hi}$ if we use the approximate result

$$Y_{hs} = 0 \tag{A20}$$

in Eq (A4) (see figure A-1). This approximation allows us to simplify (A14) and (A15) to

$$\rho_i K_c^j (Y_{ji} - Y_{js}) + \rho_i Y_{hi} \nu_{hj} K_c^h = c_j \tag{A21}$$

$$h_c (T_i - T_s) + Y_{hi} \rho_i H_h K_c^h = c_T \tag{A22}$$

From Eq.(A5) we can obtain the following estimate for the thickness of the hydrazine reaction zone δ_h

$$\delta_h / a \sim \sqrt{D_{hs}/a^2 k_{hs}} \tag{A23}$$

For typical values of the right hand side of this relation it can be shown that δ_h is much smaller than the particle radius, a . From equations (A21) and (A22), the estimates (A18), (A19) and (A23), and equation (A10) for σ_h it can be shown that for typical values of the parameters of the problem.

$$c_j \delta_h / \rho_s D_{js} \sim Y_{hs}/Y_{hi} << 1 \tag{A24}$$

$$C_T \delta_h / K_s T_s << 1$$

Taking this result into equations (A12) and (A13) it shows that the relative changes of Y_j and T_s through the hydrazine reaction zone are very small. Even though no significant changes in the temperature and mass fractions occur in the thin hydrazine decomposition zone (see figure A-1), this layer acts as a source of energy and ammonia, nitrogen and hydrogen which is added to the energy and mass of the species reaching the particle from the interstitial fluid.

The equations to be solved to obtain the temperature and concentrations of ammonia, nitrogen and hydrogen in the interior of the particle which is free from hydrazine, are

$$\Delta Y_a = - \Delta(Y_j D_{js}/D_{as}\nu_{aj}) = \Delta(TK_s/\rho_s D_{as} H_a) \qquad (A25)$$

with

$$\Delta Y_a = \frac{1}{r^2} \frac{\partial}{\partial r}\left(r^2 \frac{\partial Y_a}{\partial r}\right) = k_a Y_a \rho/\rho_s D_{as} \qquad (A26)$$

where the stoichiometric coefficients ν_{aj} are 14/17 and 3/17 for nitrogen and hydrogen respectively. H_a is the energy absorbed per unit mass of ammonia decomposed, according to reaction (A2).

The boundary conditions are imposed at r = a where, neglecting the small changes in concentration and temperature through the thin hydrazine reaction zone, we can write

$$r = a : \quad T = T_s \quad , \quad Y_a = Y_{as} \quad Y_j = Y_{js} \qquad (A27)$$

The gradients of temperature and concentration at r = a are obtained by matching with the solution (A12) and (A13) for the thin reaction zone (see figure A-1). At the interior edge of this zone the mass fraction of hydrazine, and its gradient, has dropped to zero. So that we obtain

$$K_s \left.\frac{\partial T}{\partial r}\right|_{r=a} = c_T \ , \ \rho_s D_{js} \left.\frac{\partial Y_j}{\partial r}\right|_{r=a} = c_j \qquad (A28)$$

where c_T and c_j are given by (A21) and (A22).

From Eqs (A25), the boundary conditions (A27) and (A28), and the condition that the concentrations and temperature are continuous in the interior of the particle we obtain

$$Y_j D_{js}/D_{as}\nu_{aj} + Y_a = Y_{js} D_{js}/D_{as}\nu_{aj} + Y_{as} \qquad (A29)$$

and

$$TK_s/\rho_s D_{as} H_a - Y_a = T_s K_s/\rho_s D_{as} H_a - Y_{as} \qquad (A30)$$

and

$$c_j = -\nu_{aj} c_a \quad , \quad c_T = H_a c_a \qquad (A31)$$

In the interior of the particle the ammonia decomposition is then described by the single equation (A26), where the production term ρk_a , given by (A4), can now be written in terms of Y_a by means of Eq. (A29) and (A30).

The boundary conditions, at r = a , are

$$Y_a = Y_{as} \qquad (A32)$$

and

$$\rho_s D_{as} \left.\frac{\partial Y_a}{\partial r}\right|_{r=a} = c_a = \rho_i (Y_{ai} - Y_{as}) K_c^a + \rho_i Y_{\varpi i} \nu_{ha} K_c^2 \qquad (A33)$$

If the weaker dependence of k_a on ρ_{H_2} is approximated using the value $\rho_{H_2 s}$ for ρ_{H_2} we can use the results of the analysis of the chapter III based on the fact that the activation temperature $T_a = 27778$ is very large compared with the temperature of the particle to obtain a relation between $\Phi/3 = ac_a/\rho_s D_{as} Y_{as}$ and $\gamma_s = 27778/T_s$,

$$\beta_s = \frac{\rho_s D_{as} H_a Y_{as}}{K_s T_s} \text{ and } \phi_s^2 = \frac{a_s k_{as}}{D_{as}} = \frac{2.53 \times 10^{12} \rho_{H_{2s}}^{-1.6} a^2}{D_{as}} e^{-\gamma_s}$$

this relation can be simplified in first approximation, because $\gamma_s \beta_s$ is moderately small, to

$$ac_a/\rho_s D_{as} Y_{as} = \Phi/3 = \phi_s \text{cth} \phi_s - 1 = A \quad * \qquad (A34)$$

This relation with equations(A21), (A22) and (A31) enable us to calculate the interstice particle mass and heat transfer rates

$$Y_{ji} - Y_{js} = - \frac{\nu_{aj} c_a}{\rho_i K_c^j} - \nu_{hj} \frac{K_c^h}{K_c^j} Y_{hi} \qquad (A35)$$

$$T_i - T_s = \frac{H_a c_a}{h_c} - \frac{H_h K_c^h \rho_i}{h_c} Y_{hi} \qquad (A36)$$

the first term in the right hand side of those equations gives the contribution of the ammonia decomposition and the second term that of the hydrazine decomposition.

- - - - - -

* In this part IV A is used. In the previous one (part III) Φ was used instead.

A P P E N D I X B

As it is mentioned in the text, this is a case of no external resistance and the concentration at the surface of the catalyst particle is a known function of temperature and pressure.

For the conditions appropriate to this region, the heat effect parameter β that has been defined in paragraph II of part III of this work is of the order

$$\beta \approx 10^{-3}$$

The ratio between the activation temperature for hydrazine decomposition and the temperature at the surface of the catalyst particle[1] γ is at most of order 5, so that $\gamma\beta \approx 0.005$. Consequently this corresponds to the case of an exothermic reaction with null heat effects (paragraph V, of part III) and the appropriate form of the utilization factor is

$$\eta = \frac{3}{\phi_h^2} \left[\phi_h \operatorname{cth} \phi_h - 1 \right]$$

On the other hand ϕ_h^2 is large, or order 10^5, and

$$\eta = 3/\phi_h$$

LIST OF FIGURE CAPTIONS

Fig.1.- Induction distance as function of injection temperature.

Fig.2.- Nondimensional temperature and concentrations as function of non-dimensional distance along the chamber in the post-induction region.

Fig.3 and 4.- Maximum non-dimensional interstitial and particle temperatures versus parameters ϕ_f and J for different operating pressures.

Fig.5.- Idem for $\phi_f = \infty$ and comparison with experimental results.

Fig.6 and 7.- Maximum specific impulse for different values of J , ϕ_f , and operating pressures.

Fig.8.- Temperature distribution along the chamber and comparison with experimental results.

Fig.A1.- Schematic showing temperature and concentration profiles.

FIG. Nº 1

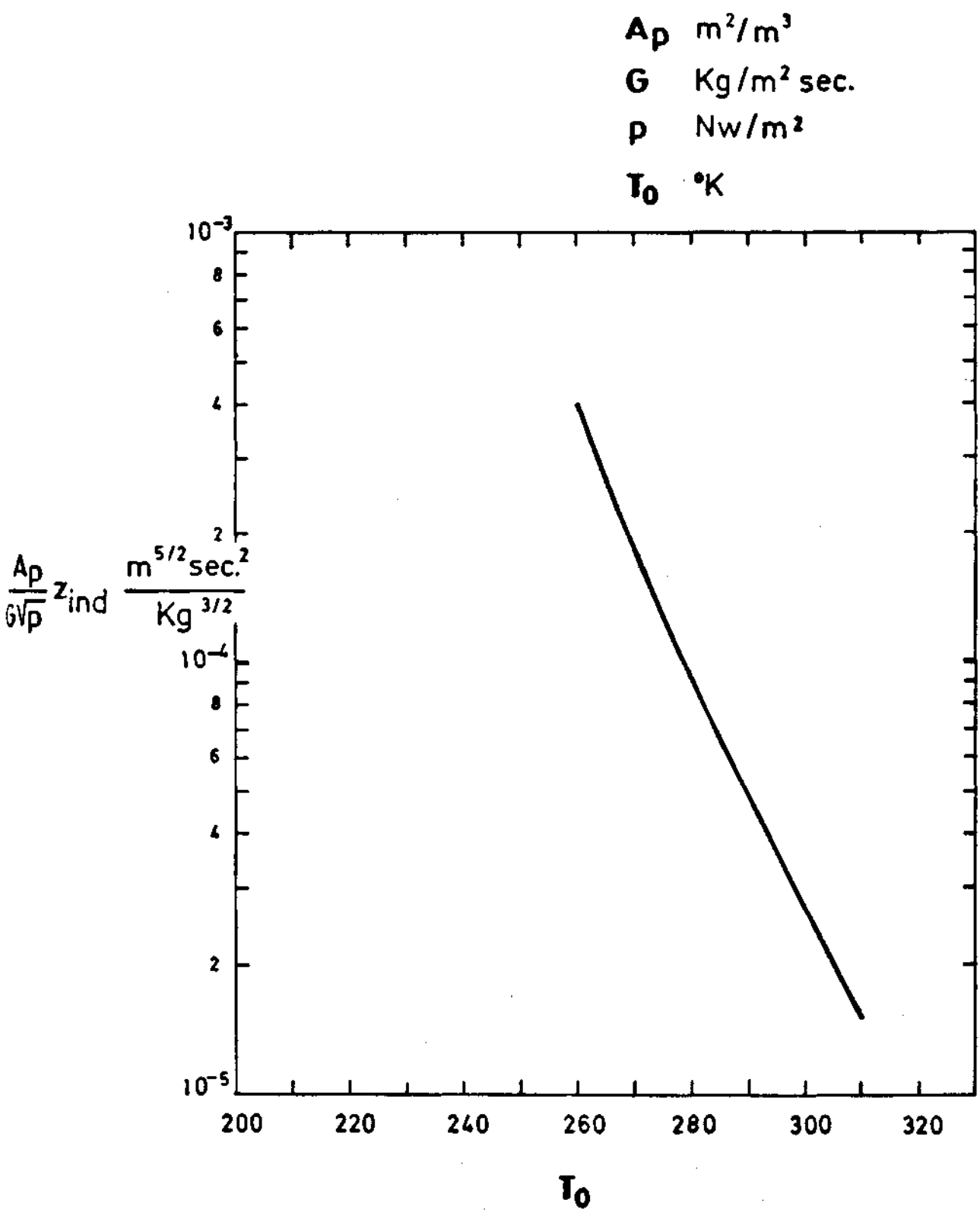
Ap m²/m³
G Kg/m² sec.
p Nw/m²
T0 °K
Ap/G√p z ind m^5/2 sec.²/Kg^3/2
10⁻³
8
6
4
2
10⁻⁴
8
6
4
2
10⁻⁵
200
220
240
260
280
300
320
T0

FIG. Nº 2

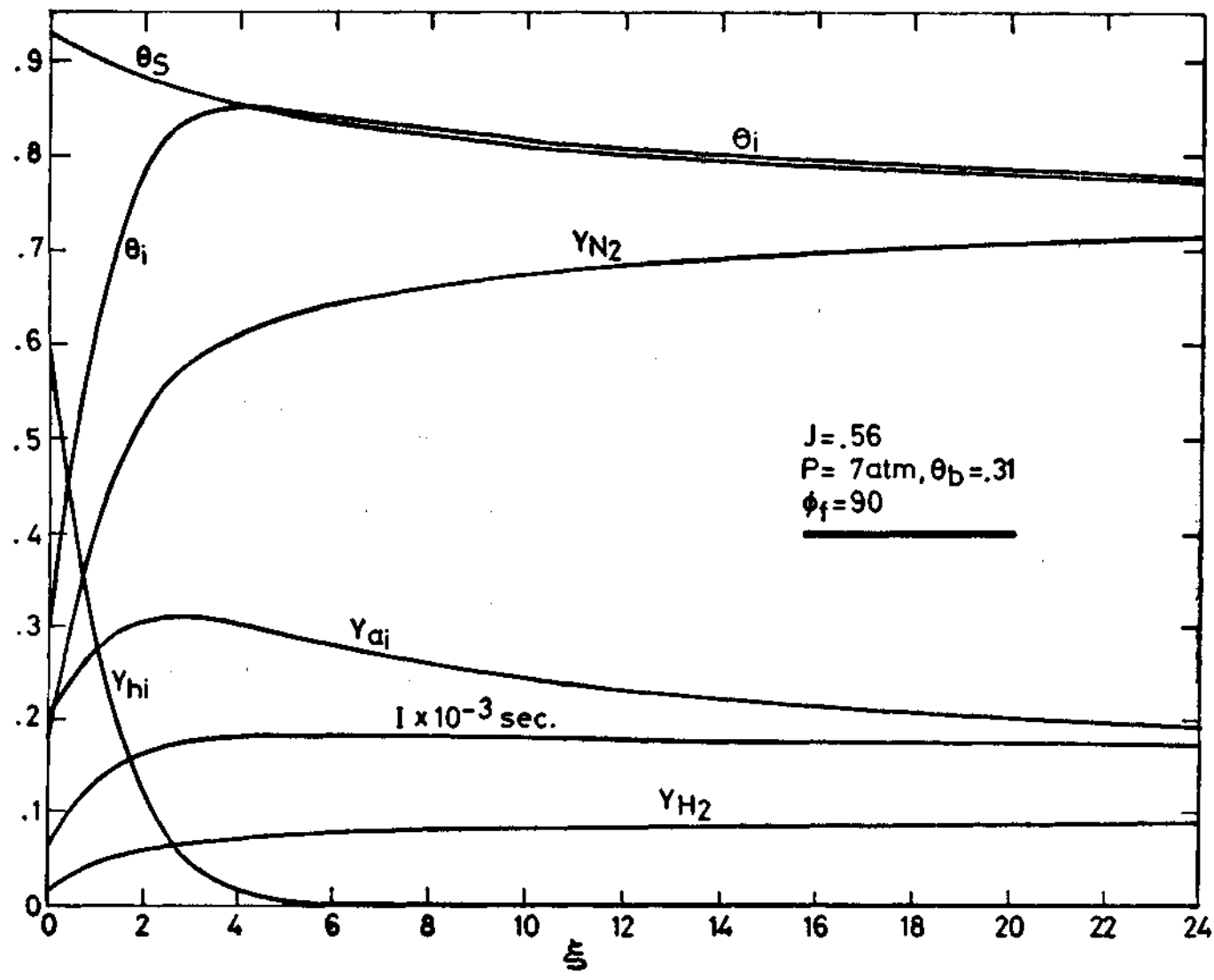
θS
θi
θi
YN2
J=.56
P= 7atm, θb=.31
φf=90
Yai
Yhi
I x10⁻³ sec.
YH2
0
.1
.2
.3
.4
.5
.6
.7
.8
.9
0
2
4
6
8
10
12
14
16
18
20
22
24
ξ

FIG. Nº3

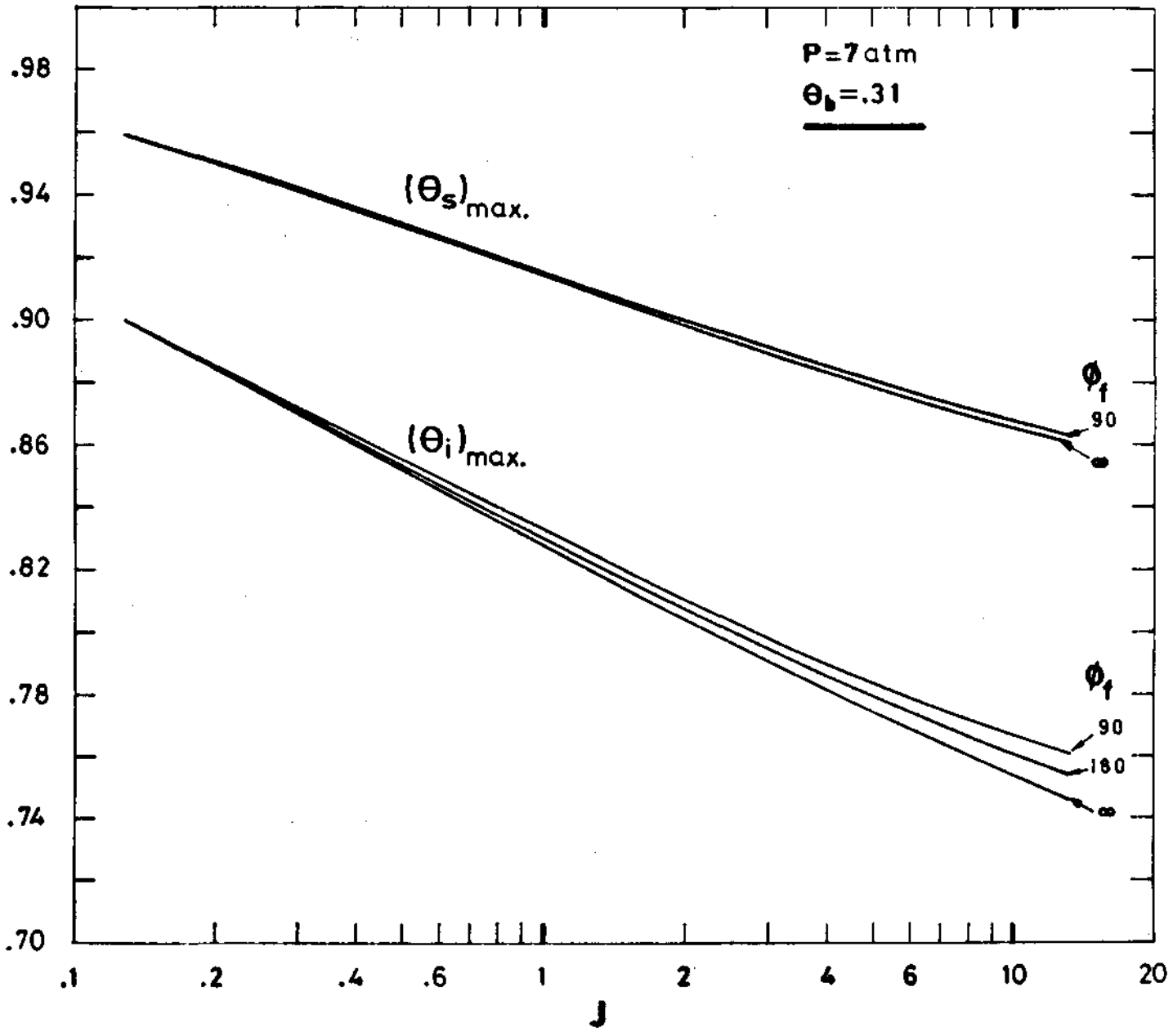
P=7 atm
θ_b=.31
$(\theta_s)_{max.}$
$(\theta_i)_{max.}$
ϕ_f
90
∞
ϕ_f
90
180
∞
.98
.94
.90
.86
.82
.78
.74
.70
.1
.2
.4
.6
1
2
4
6
10
20
J

FIG. Nº 4

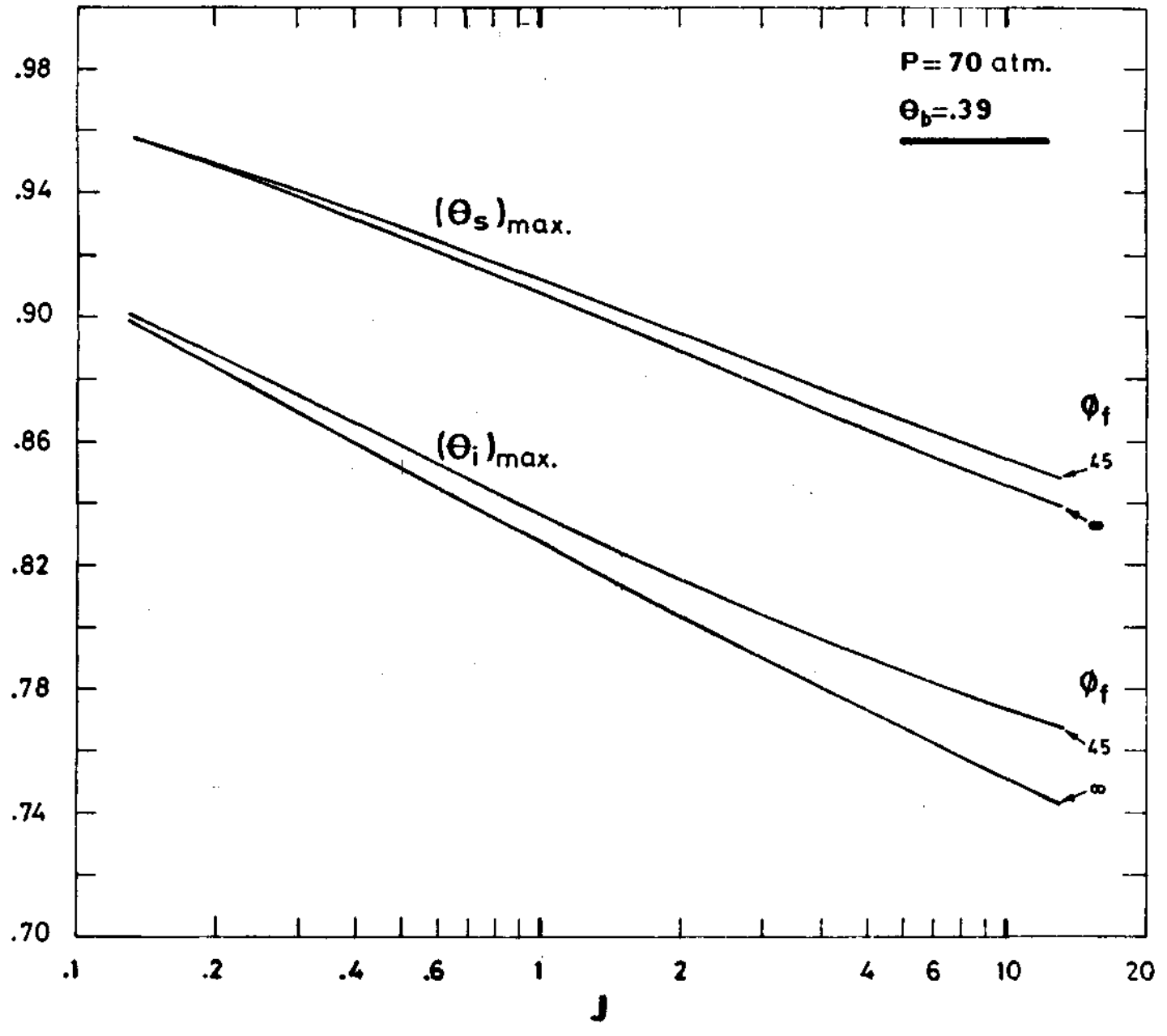
P= 70 atm.
θ_b=.39
$(\theta_s)_{max.}$
$(\theta_i)_{max.}$
ϕ_f
45
∞
ϕ_f
45
∞
.98
.94
.90
.86
.82
.78
.74
.70
.1
.2
.4
.6
1
2
4
6
10
20
J

FIG. Nº 5

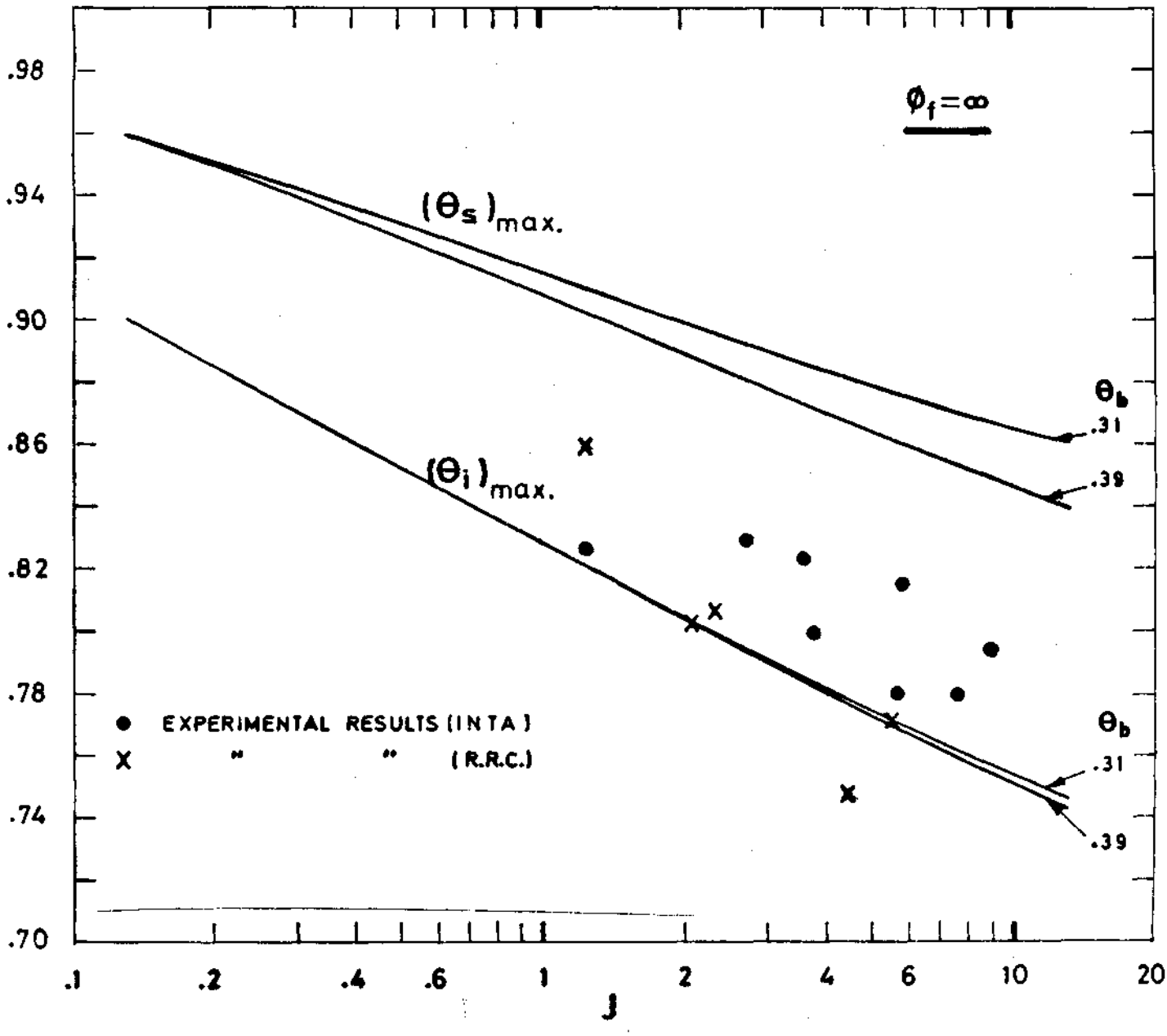
.98
.94
.90
.86
.82
.78
.74
.70
.1
.2
.4
.6
1
2
4
6
10
20
J
$\phi_f = \infty$
$(\theta_s)_{max.}$
$(\theta_i)_{max.}$
θ_b
.31
.39
θ_b
.31
.39
● EXPERIMENTAL RESULTS (INTA)
X " " (R.R.C.)

FIG. N° 6

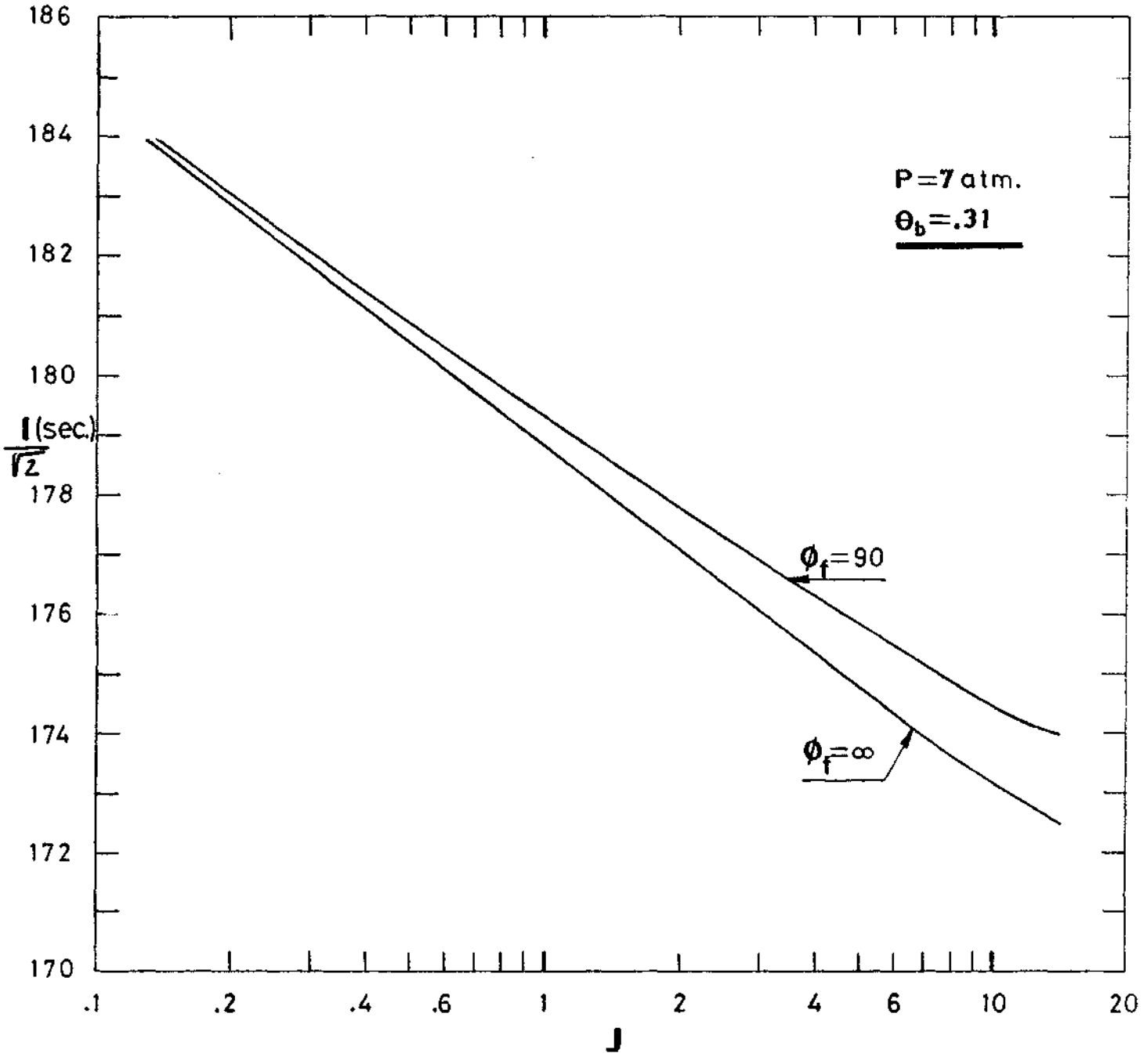
186
184
182
180
I (sec.)
√Z
178
176
174
172
170
P=7 atm.
θb=.31
φf=90
φf=∞
.1
.2
.4
.6
1
2
4
6
10
20
J

FIG. Nº 7

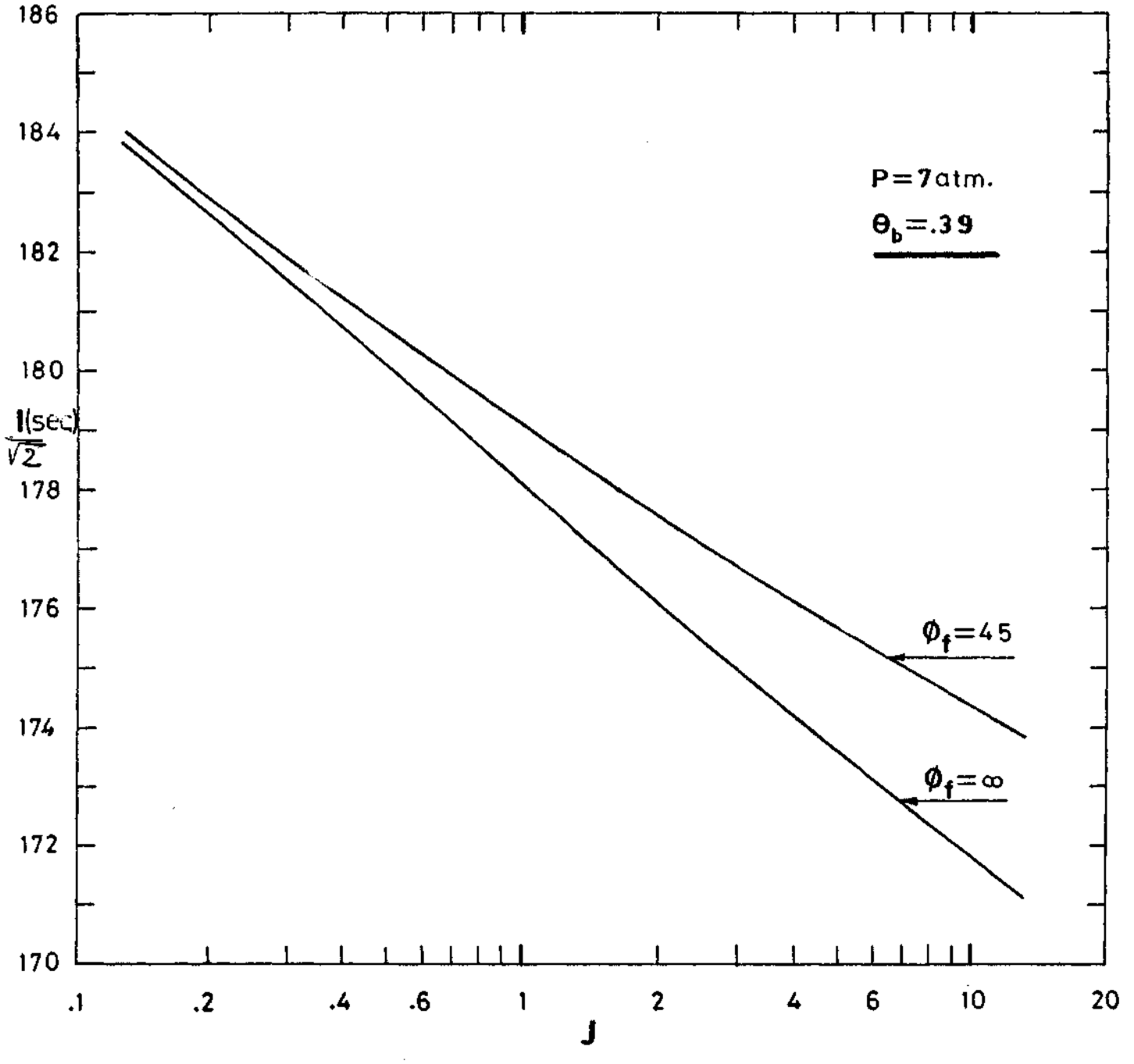
186
184
182
180
178
176
174
172
170
I(sec)/√2
P=7atm.
θb=.39
φf=45
φf=∞
.1
.2
.4
.6
1
2
4
6
10
20
J

FIG. Nº 8

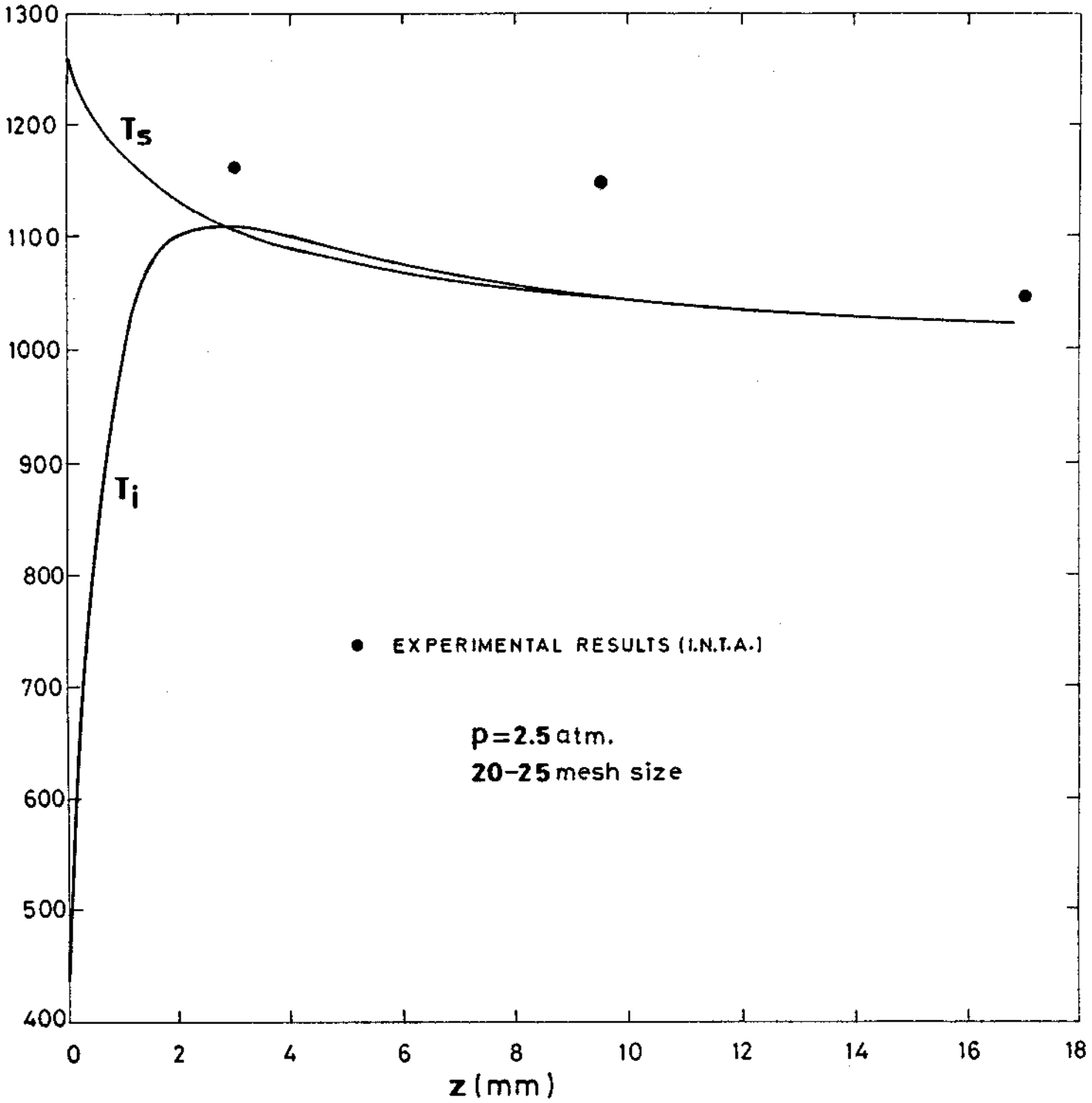
1300
1200
1100
1000
900
800
700
600
500
400
T_s
T_i
EXPERIMENTAL RESULTS (I.N.T.A.)
p=2.5 atm.
20-25 mesh size
0
2
4
6
8
10
12
14
16
18
z (mm)

FIG. Nº A-1

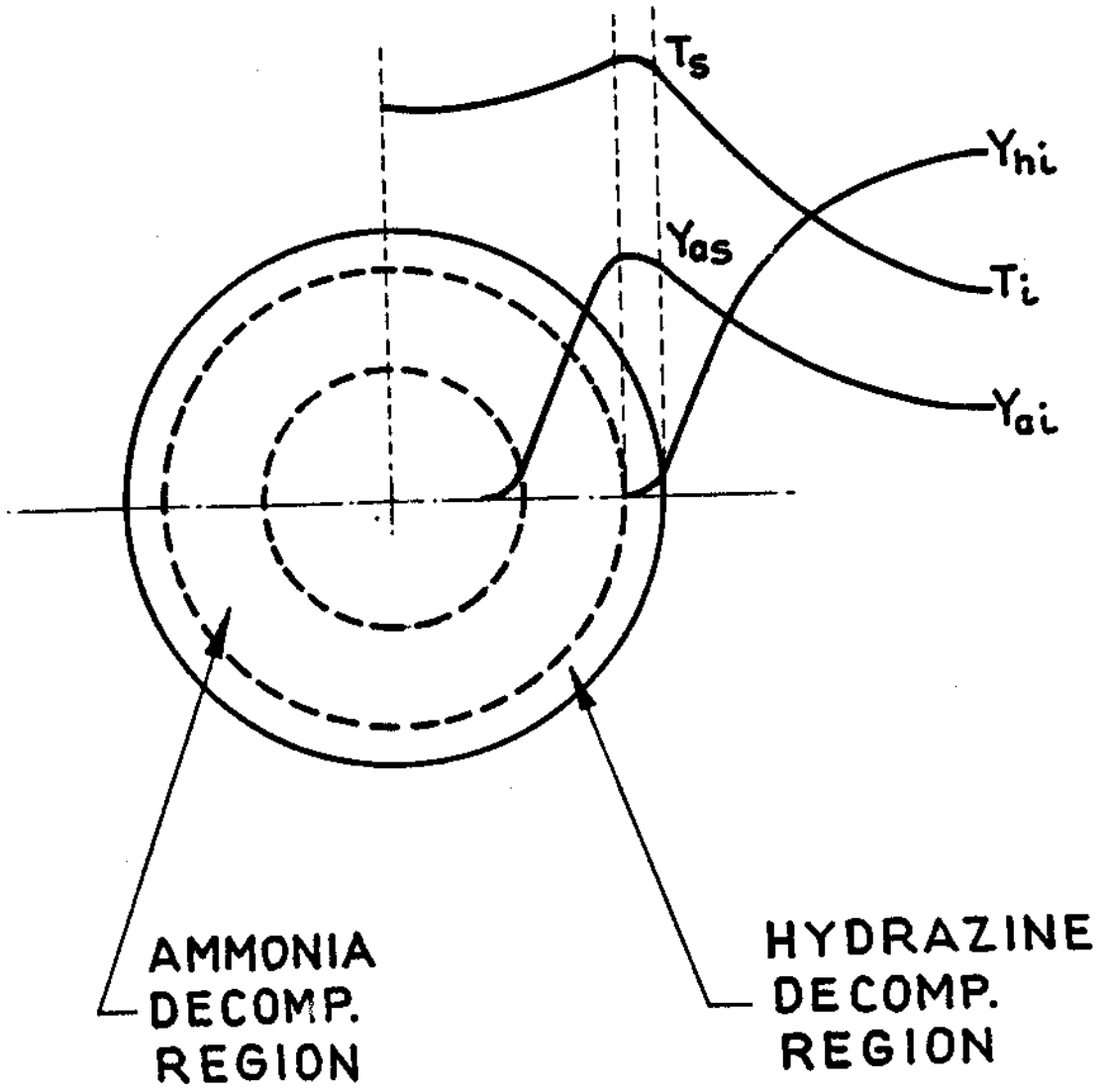
T_s
Y_{hi}
Y_{as}
T_i
Y_{ai}
AMMONIA
DECOMP.
REGION
HYDRAZINE
DECOMP.
REGION